

Emulsification with microstructured devices

Abid Aslam Maan

Thesis committee**Promotors**

Prof. dr. ir. C.G.P.H. Schroën

Personal chair at the Laboratory of Food Process Engineering, Wageningen University

Prof. dr. ir. R.M. Boom

Professor of Food Process Engineering, Wageningen University

Other members

Dr. M.C. Guell, Universitat Rovira i Virgili, Tarragona, Spain

Prof. dr. ir. M.T. Kreutzer, Delft University of Technology

Prof. dr. A.C.M. van Hooydonk, Wageningen University

Prof. dr. E. van der Linden, Wageningen University

This research was conducted under the auspices of the Graduate School VLAG (Advanced studies in Food Technology, Agrobiotechnology, Nutrition and Health Sciences).

Emulsification with microstructured devices

Abid Aslam Maan

Thesis

submitted in fulfilment of the requirements for the degree of doctor

at Wageningen University

by the authority of the Rector Magnificus

prof. dr. M.J. Kropff,

in the presence of the

Thesis Committee appointed by the Academic Board

to be defended in public

on Monday 11 March 2013

at 11 a.m. in the Aula.

Abid Aslam Maan

Emulsification with microstructured devices

163 pages

Thesis, Wageningen University, Wageningen, The Netherlands (2013)

With propositions, references and summary in English

ISBN: 978-94-6173-463-1

Contents

Chapter 1	Introduction – emulsions and emulsification	9
Chapter 2	Spontaneous emulsification systems <i>- perspectives for food applications -</i>	21
Chapter 3	Preparation of water-in-oil emulsions through semi-metal EDGE systems	55
Chapter 4	Preparation of oil-in-water emulsions through semi-metal EDGE systems	77
Chapter 5	Effect of surface wettability on microfluidic emulsification	99
Chapter 6	Preparation and analysis of w/o/w double emulsions	111
Chapter 7	General discussion	141
Summary		153
Acknowledgements		157
Curriculum vitae		159
Publications		161
Training activities		163

Chapter 1

Introduction
(Emulsions and emulsification)

Many processed foods consist of a dispersion of two or more components. Emulsions, dispersions of two immiscible liquids, are the most common type. This chapter gives an introduction to emulsions and their importance in our daily life with some examples of emulsion based products. After that some emulsification techniques which are in use at commercial scale or under investigation in laboratories are discussed. At the end, main objectives of the thesis and an outline of the subsequent chapters are given.

1. Emulsions

Emulsions consist of suspension of droplets of one liquid (e.g. oil) into another immiscible liquid (e.g. water) and may be complex in structure and composition. Emulsions can be oil-in-water (o/w, oil droplets dispersed in aqueous phase) or water-in-oil (w/o, water droplets distributed in oil phase), but also more complex compositions exist such as double emulsions, which consist of an emulsion in an emulsion. Figure 1.1 shows a chart of some commonly available emulsion based products.

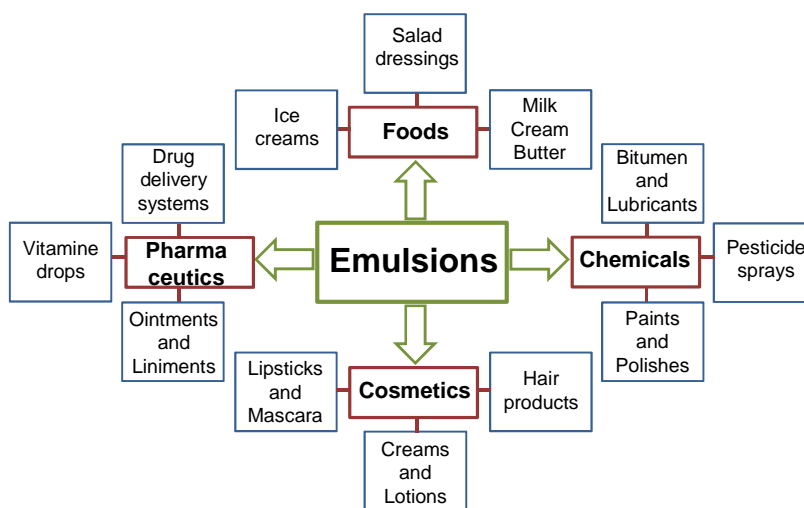


Figure 1.1: Some commonly available emulsion based products.

Emulsions are generally meta or even unstable (except micro-emulsions¹) and can separate into their constituent oil and aqueous phases either due to coalescence of the droplets or due to creaming/sedimentation resulting from density differences between the two phases. Coalescence can be prevented by adding a surfactant or emulsifier

(possibly in combination with a stabiliser), which reduce coalescence by adsorbing at the interface. Creaming or flocculation can be reduced by decreasing the droplet size, increasing continuous phase viscosity, or matching the densities of the phases.

2. Emulsification techniques

The size and size distribution of the dispersed droplets influence the stability and properties of emulsion based products. For example, fine emulsions were reported to have higher viscosities as compared to coarse emulsions due to their (comparatively) narrower size distribution, decreased droplet deformability and stronger colloidal interactions^{2,3}. The visual appearance of an emulsion depends on the droplet size as well; for example an emulsion with droplets >10 µm appears turbid, and the turbidity increases with decreasing droplet size⁴, until the droplet size is less than the wavelength of visible light; the emulsion then becomes transparent⁵. Further, a wide size distribution in polydispersed emulsions promotes coalescence⁶ and Ostwald ripening.

The emulsification process should therefore be such that the droplet size and uniformity is controlled; however, this is not always the case in the industrial methods that are briefly discussed below.

2.1. Traditional methods

Emulsions are commercially prepared through mechanical shearing using instruments like high pressure homogenisers, rotor-stator systems and ultrasound homogenisers⁷⁻⁹. Generally a coarse emulsion is first prepared by gently mixing oil and water phases before starting the main emulsification process. This coarse pre-mix, consisting of large and polydispersed droplets that may be present at high volume fraction, is then passed, in general several times, through the emulsification device to break large droplets into smaller ones until the required droplet size and size distribution are achieved. The resulting droplets are stabilised against coalescence by surfactants and stabilisers present in the pre-mix; however, there is limited control on the droplet size, resulting in polydispersity⁶. A generalised scheme of an emulsification process can be seen in figure 1.2.

A high energy input is required for 'classic' emulsification technology of which >90% is wasted in the form of heat^{10, 11}. The high energy input and resulting heat may influence shear sensitive ingredients (starch, proteins etc.) that may lose their functional properties¹². Similarly, double emulsions cannot appreciably be produced by traditional methods due to the fragility of the droplet-in-droplet arrangement that results in break-up of the primary droplets during the second emulsification step and coalescence of the inner with the outer phase.

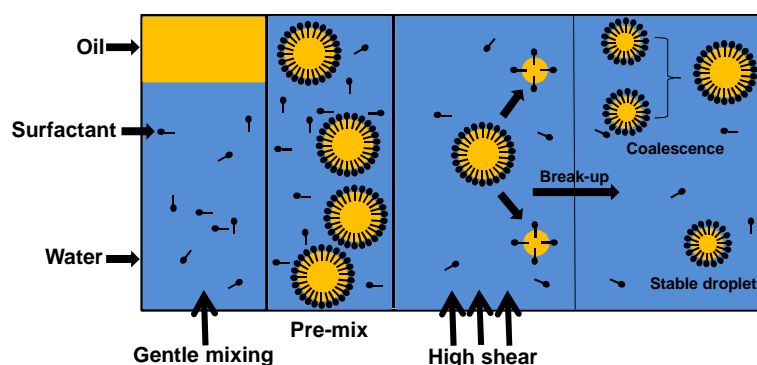


Figure 1.2: Schematic illustration of the pre-mix emulsification process of an o/w emulsion (modified from Eisner¹³)

It is clear that for all emulsions there is a need to develop systems which are mild in operation, ensure uniform droplets and consume less energy.

2.2. Membrane emulsification

Membranes are porous structures used most commonly for separation but can also be employed for emulsification¹⁴. The advantages of membrane emulsification are milder operation, high energy efficiency as compared to traditional methods (figure 2.10) and better control over droplet sizes. Membrane emulsification can be operated in cross-flow or pre-mix mode. In cross-flow emulsification, the dispersed phase is pressed through the membrane and the droplets formed at the membrane surface are sheared off by a cross-flowing continuous phase (figure 2.2)¹⁵. Narrowly dispersed emulsions (with a coefficient of variation (CV) of around 10%) can be produced by this method at dilute concentrations (typically <10 volume%)⁹. In pre-mix membrane emulsification a coarse

pre-mix emulsion is broken up into smaller droplets when pressed through the pores of a membrane¹⁶. This later method is suitable for preparing concentrated emulsions (even >50%); however, the uniformity of the droplet sizes is not as good as reported for cross-flow emulsification (typical span values of around 1)^{17,18}.

2.3. Microfluidic emulsification

Microfluidic devices containing micrometre sized channels have been extensively studied in science and some have even found application in industry, for example in the field of labs-on-a-chip¹⁹. An emerging area is in the preparation of emulsions. Through the well-defined dimensions and geometry of pores and channels prepared with micro-engineering methods, very uniform droplets can be formed (with a typical coefficient of variation of $CV < 5\%$,^{7, 20-22}) compared to membrane emulsification. As is the case for membranes, depending on the properties of the surface of the channels in the microfluidic device, both oil-in-water (hydrophilic surface) and water-in-oil (hydrophobic surface) emulsions can be prepared^{8, 23, 24}. Apart from single emulsions, double emulsions can be successfully produced due to the mild operation conditions in microfluidics and well controlled droplet formation process^{21, 25, 26}.

Microfluidic systems with several geometries have been reported in literature^{24, 27-31}. Depending upon the mechanism of droplet formation they can be classified into two different categories: (1) the spontaneous emulsification systems in which droplet formation takes place spontaneously through Laplace pressure differences (figure 1.3a) and (2) shear based systems in which droplet generation occurs through shear flow, similar to cross-flow membrane emulsification (figure 1.3b). In spontaneous emulsification the dispersed phase flows from a shallow and wide area into a deeper channel and changes its shape from a flattened disc to a spherical droplet. Laplace pressure differences between the disc and droplet cause the oil to flow from the shallow area to the deeper channel, which causes the droplet to suddenly detach. Most common examples of spontaneous emulsification devices are so-called microchannel systems in which single droplets are formed in a single droplet formation unit²⁹ (figure 2.3) and EDGE (Edge based Droplet GEneration) (figure 1.3a) systems²⁷ that are able to generate multiple droplets from a single droplet formation unit.

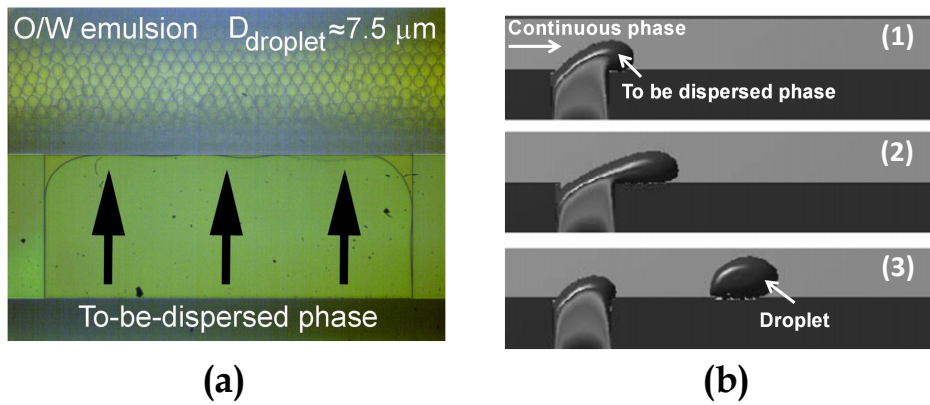


Figure 1.3: Typical examples of (a) spontaneous emulsification (an EDGE device) with arrows indicating the droplet formation locations, and (b) shear driven emulsification (a T-shaped microchannel junction, modified from van der Graaf et. al.,²⁴) showing the flow of the dispersed phase in continuous phase channel (1), deformation of dispersed phase into droplet (2) and its detachment (3).

Spontaneous emulsification is mostly employed for the preparation of single emulsions, since for double emulsions the droplets in the primary emulsion need to be small enough to pass through the shallow part of the system, which may be $1 \mu\text{m}$ or even less in height; as is the case for the EDGE systems investigated in this thesis (chapters 3, 4 and 5).

In shear based emulsification systems a shear flow is responsible for detachment of the dispersed phase droplets into a cross-flowing or co-flowing continuous phase. Most common examples are T -, Y - junctions, flow focussing geometries and co-flow systems (figure 2.3)^{26, 28, 31, 32}. With co-flow and flow focussing systems, highly monodispersed double emulsions and even triple and high order emulsions (with co-flow systems) can be produced with controlled size and number of inner droplets^{26, 33}, although it should be mentioned that the dimensions of these emulsions are rather large, mostly just below millimetre size, while scaling up by having very many of these nozzles working reliably, and all producing the same droplet sizes in parallel, is nontrivial.

Microfluidic devices have potential for the production of emulsions: however, in order to make larger amounts of emulsions, the microfluidic chips need to be scaled up. In

this thesis, we investigate various aspects of EDGE technology that are related to this up-scaling, such as the surface roughness and the wettability of the channel walls (see chapters 3, 4 and 5). The glass or silicon chips that are generally used in research and in analytical applications are rather expensive, and since silicon is brittle, they may contaminate the products without being able to trace the shards in the final food product. The production costs of polymeric systems are much lower; however, materials as PDMS which are mostly the polymers of choice, swell in the presence of oil, and cannot be used for the production of emulsions. When considering a practical application, a metal surface is the most logical choice, because of its high mechanical strength, ease of cleaning and resistance to chemicals, while their use in food production is accepted³⁴. A stainless steel based microchannel was investigated by Tong et al.,³⁴ for o/w emulsification, which yielded monodispersed droplets with individual channels, however, the precise fabrication of many channels on the same chip was not possible and the monodispersity of droplets coming from different channels on the system was questionable.

This implies that insight is lacking for metal based microfluidic devices for emulsification. Some of the most important differences of metal systems compared to silicon based systems, is the roughness of the surfaces obtained with metals (those with silicon are usually extremely smooth), while the properties of metal surfaces are fundamentally different from those of silicon or glass surfaces. Thus, in the work reported here, focus was on these aspects. We intended to obtain more insight in the nature and influence of these properties on the emulsification behaviour, and with that insight bring microfluidic emulsification in general and specifically EDGE emulsification a step closer to up-scaling to preparative volumes, and industrial application.

In EDGE emulsification, the dispersed phase is confined onto a narrow flat area (the plateau) before it makes droplets into the continuous phase channel. This plateau can be very shallow; plateaus as shallow as 1 μm have been reported. The plateau height is the most important parameter in determining the droplet size; while the wettability by the continuous phase is the most important parameter for the spontaneous droplet detachment. It is therefore expected that the surface roughness and wettability of the

(metal) surfaces of this plateau will be of considerable influence on the emulsification behaviour.

3. Aim of the thesis

The aim of this research project was to understand the influence of the most important parameters in EDGE emulsification, which are related to the translation of the EDGE method to the preparation of monodispersed emulsions with metal based systems. We focus on the production of small droplets (typically $\leq 5 \mu\text{m}$). On the basis of this insight, we aim to contribute to the realisation of metal-based EDGE systems on industrial scale.

Semi metal EDGE systems with different surface roughness and wettability were investigated for the preparation of o/w and w/o emulsions. From the insight obtained, criteria for better process stability and improved efficiency of the system are recommended. To already put the findings in perspective towards the preparation of more complex emulsions, we prepared w/o/w double emulsions, albeit with different flow focussing designs, and investigated the inner droplet size and stability of these double emulsions.

4. Thesis outline

In **chapter 2**, an overview is given of the potential of spontaneous droplet formation microfluidics for application in foods. Amongst others, the influences of design and process parameters are discussed in relation to droplet size and size distribution.

In **chapter 3**, metal coated EDGE systems having different surface roughnesses are investigated for w/o emulsification, and in **chapter 4** we investigate the same aspect, but now combined with the surface wettability for oil-in-water emulsions. This shows the potential of these systems for practical applications. The results obtained on roughness and wettability are further interpreted by using silicon based EDGE systems with flat surfaces, with which we can vary the surface wettability by surface modification, while not changing the surface roughness. The resulting effects on emulsification are presented and discussed in **chapter 5**.

Chapter 6 reports on the preparation and characterisation of monodispersed w/o/w double emulsions with single or multiple monodispersed inner droplets using flow-focussing systems having different geometries.

Finally, in **chapter 7** a comparison of various microfluidic emulsification systems is given together with an outlook on the scale up of microfluidic emulsification for large scale food applications.

References

1. J. R. Milton, *Surfactants and interfacial phenomena* Wiley, New York, 1989.
2. R. Pal, *AIChE Journal*, 1996, **42**, 3181-3190.
3. H. A. Barnes, *Colloid Surface A*, 1994, **91**, 89-95.
4. W. Chantrapornchai, F. Clydesdale and D. J. McClements, *Journal of Agricultural and Food Chemistry*, 1998, **46**, 2914-2920.
5. T. J. Wooster, M. Golding and P. Sanguansri, *Langmuir*, 2008, **24**, 12758-12765.
6. M. Saito, L. J. Yin, I. Kobayashi and M. Nakajima, *Food Hydrocolloid*, 2006, **20**, 1020-1028.
7. S. Sugiura, M. Nakajima and M. Seki, *Langmuir*, 2002, **18**, 5708-5712.
8. H. Liu, M. Nakajima and T. Kimura, *J. Am. Oil Chem. Soc.*, 2004, **81**, 705-711.
9. A. A. Maan, K. Schroën and R. Boom, *J Food Eng*, 2011, **107**, 334-346.
10. K. C. van Dijke, K. Schroën, A. van der Padt and R. M. Boom, *J Food Eng*, 2010, **97**, 348-354.
11. D. J. McClements, *Food Emulsions: Principles, Practice, and Techniques*, 1999.
12. C. Charcosset, I. Limayem and H. Fessi, *J Chem Technol Biot*, 2004, **79**, 209-218.
13. V. Eisner, PhD, Swiss Federal Institute of Technology, 2007.
14. A. R. Linnemann, C. G. P. H. Schroen and M. A. J. S. Boekel, *Food product design-An integrated approach*, Wageningen Academic Publishers, Wageningen, 2011.
15. T. Nakashima, M. Shimizu and M. Kukizaki, *Key Eng. Mater.*, 1992, **61-62**, 513-516.
16. A. Nazir, K. Schroën and R. Boom, *J. Membr. Sci.*, 2010, **362**, 1-11.
17. G. T. Vladislavljević, M. Shimizu and T. Nakashima, *J. Membr. Sci.*, 2004, **244**, 97-106.
18. A. Nazir, K. Schroën and R. Boom, *J. Membr. Sci.*, 2011, **383**, 116-123.
19. Z. T. Cygan, J. T. Cabral, K. L. Beers and E. J. Amis, *Langmuir*, 2005, **21**, 3629-3634.
20. I. Kobayashi, K. Uemura and M. Nakajima, *Food Biophys*, 2008, **3**, 132-139.
21. I. Kobayashi, X. Lou, S. Mukataka and M. Nakajima, *J. Am. Oil Chem. Soc.*, 2005, **82**, 65-71.
22. S. Sugiura, M. Nakajima and M. Seki, *J. Am. Oil Chem. Soc.*, 2002, **79**, 515-519.
23. S. Sugiura, M. Nakajima, S. Iwamoto and M. Seki, *Langmuir*, 2001, **17**, 5562-5566.
24. S. van der Graaf, T. Nisisako, C. G. P. H. Schroën, R. G. M. van der Sman and R. M. Boom, *Langmuir*, 2006, **22**, 4144-4152.
25. S. Sugiura, M. Nakajima, K. Yamamoto, S. Iwamoto, T. Oda, M. Satake and M. Seki, *J. Colloid Interface Sci.*, 2004, **270**, 221-228.
26. M. Seo, C. Paquet, Z. Nie, S. Xu and E. Kumacheva, *Soft Matter*, 2007, **3**, 986-992.
27. K. C. van Dijke, G. Veldhuis, K. Schroën and R. M. Boom, *AIChE Journal*, 2010, **56**, 833-836.
28. M. L. J. Steegmans, K. C. G. P. H. Schroën and R. M. Boom, *Langmuir*, 2009, **25**, 3396-3401.
29. S. Sugiura, M. Nakajima, N. Kumazawa, S. Iwamoto and M. Seki, *J. Phys. Chem. B*, 2002, **106**, 9405-9409.
30. I. Kobayashi, S. Mukataka and M. Nakajima, *Ind. Eng. Chem. Res.*, 2005, **44**, 5852-5856.
31. A. S. Utada, L. Y. Chu, A. Fernandez-Nieves, D. R. Link and D. A. Weitz, *MRS Bull*, 2007, **32**, 702-708.
32. S. van der Graaf, M. L. J. Steegmans, R. G. M. van der Sman, C. G. P. H. Schroën and R. M. Boom, *Colloid Surface A*, 2005, **266**, 106-116.

33. R. K. Shah, H. C. Shum, A. C. Rowat, D. Lee, J. J. Agresti, A. S. Utada, L.-Y. Chu, J.-W. Kim, A. Fernandez-Nieves, C. J. Martinez and D. A. Weitz, *Materials Today*, 2008, **11**, 18-27.
34. J. Tong, M. Nakajima, H. Nabetani, Y. Kikuchi and Y. Maruta, *J. Colloid Interface Sci.*, 2001, **237**, 239-248.

Chapter 2

Spontaneous Droplet Formation Techniques for Monodispersed Emulsions Preparation

- *perspectives for food applications* -

This chapter has been published as: Maan, A. A., Schroën, K., Boom, R., 2011. Spontaneous droplet formation techniques for monodispersed emulsions preparation-perspectives for food applications. Journal of food engineering 107, 334-346.

Abstract

Spontaneous droplet formation through Laplace pressure differences is a simple method for making monodisperse emulsions and is claimed to be suited for shear and temperature sensitive products, and those requiring high monodispersity. Techniques belonging to this category include (grooved) microchannel emulsification, straight-through microchannel emulsification, and EDGE (Edge-based Droplet Generation).

In this paper, an overview is given of the process, and design parameters that play a role in microchannel emulsification including their effect on droplet size and distribution. Besides, various products made by microchannel emulsification are discussed.

Industrial microchannel emulsification is still not possible due to the low production rates. The new EDGE mechanism seems an interesting development, since it promises larger throughputs per droplet formation unit, better scalability, and shows robust operation with practical, food-grade components. However, for spontaneous emulsification techniques to be used on large scale, improvements in construction materials (including surface modification) are expected to be of essence.

1. Introduction

Emulsions play an important role not only in foods, but also in cosmetics, pharmaceuticals and petrochemicals. Characteristics of emulsions including rheology, appearance, chemical reactivity, and physical stability are all affected by the size of the droplets and distribution of droplet sizes^{1,2}; coefficient of variation (CV) is mostly used as an index to characterize the size distribution. An emulsion having CV less than 25% is considered as a monodispersed emulsion while the one having CV above this value is considered as a polydispersed emulsion³. Monodispersed emulsions have several applications in science and industry⁴. Traditional equipments used for emulsions preparation include high pressure homogenizers, ultrasound homogenizers and rotor-stator systems (stirred vessels, colloid mills or toothed disc dispersing machines) (figure 2.1)⁵.

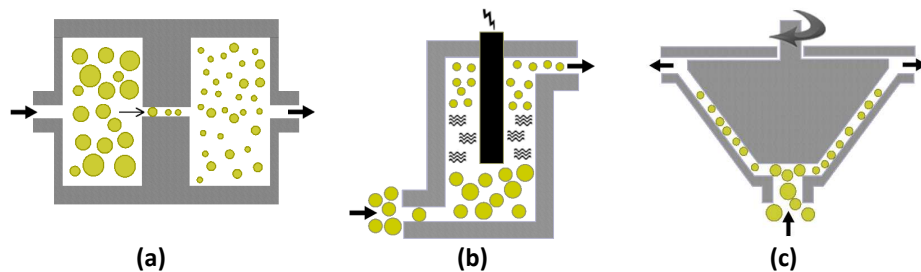


Figure 2.1: Schematic illustration of traditional emulsification equipment. High pressure homogenizer (a) ultrasound homogenizer (b) and rotor stator system (c).

These instruments apply a high shear stress to deform and disrupt the large droplets into smaller ones. Only 1-5% of the applied energy is used for droplet formation and remaining is lost as heat⁶ which can cause temperature and shear sensitive ingredients (starch, proteins etc.) to lose their functional properties⁷. In addition, prepared emulsions are polydispersed with coefficient of variation (CV) of around 40%⁸, which makes these emulsions intrinsically unstable.

In the last two decades, alternative emulsification techniques have been proposed, which can provide better control over droplet size while consuming less energy. Nakashima et al.⁹ proposed the cross-flow membrane emulsification technique to produce

monodisperse emulsions at much lower mechanical stress which results in low energy requirements. A schematic diagram of the process of cross-flow membrane emulsification is shown in Figure 2.2. The dispersed phase is pressed through the pores of a membrane and droplets are formed at the pore openings, where the droplets are sheared off and carried away by the cross-flowing continuous phase. This technique is useful for producing monodisperse emulsions with a coefficient of variation of about 10%¹⁰, but it is feasible only for dilute emulsions (<10%) that can be produced in one step; recirculation that may be used to increase the dispersed phase fraction, induces wider droplet size distributions.

Within the field of microtechnology, new emulsification techniques have emerged. One class of devices is similar to cross-flow membrane emulsification and uses shear forces to form droplets. Some examples are T-, Y- shaped microchannel junctions (see figures 2.3a & b respectively), in which a cross-flow is used, and flow-focusing devices (figures 2.3c & d) in which co-flow of phases exerts extensional shear. Another class of devices uses so-called spontaneous droplet formation, of which the most studied form is microchannel emulsification (figures 2.3e & f). Spontaneous emulsification is an interesting technique to develop further because it renders emulsions that can be high in dispersed phase fraction while still having a sharp droplet size distribution ($CV \approx 5\%$)¹; the processing time is proportional to the dispersed phase fraction.

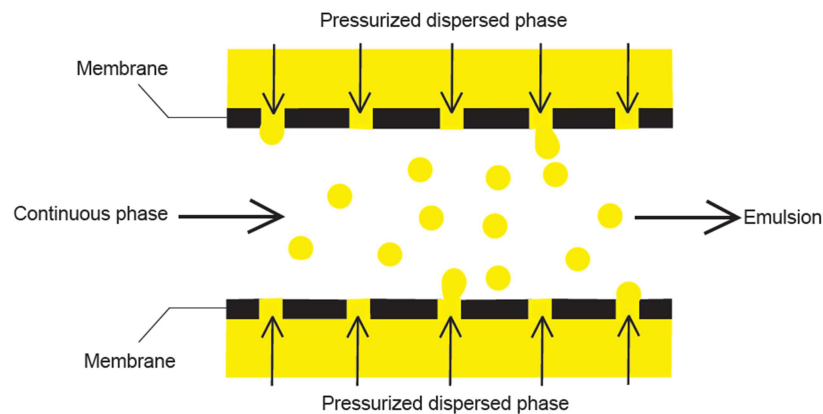


Figure 2.2: Schematic illustration of cross flow membrane emulsification.

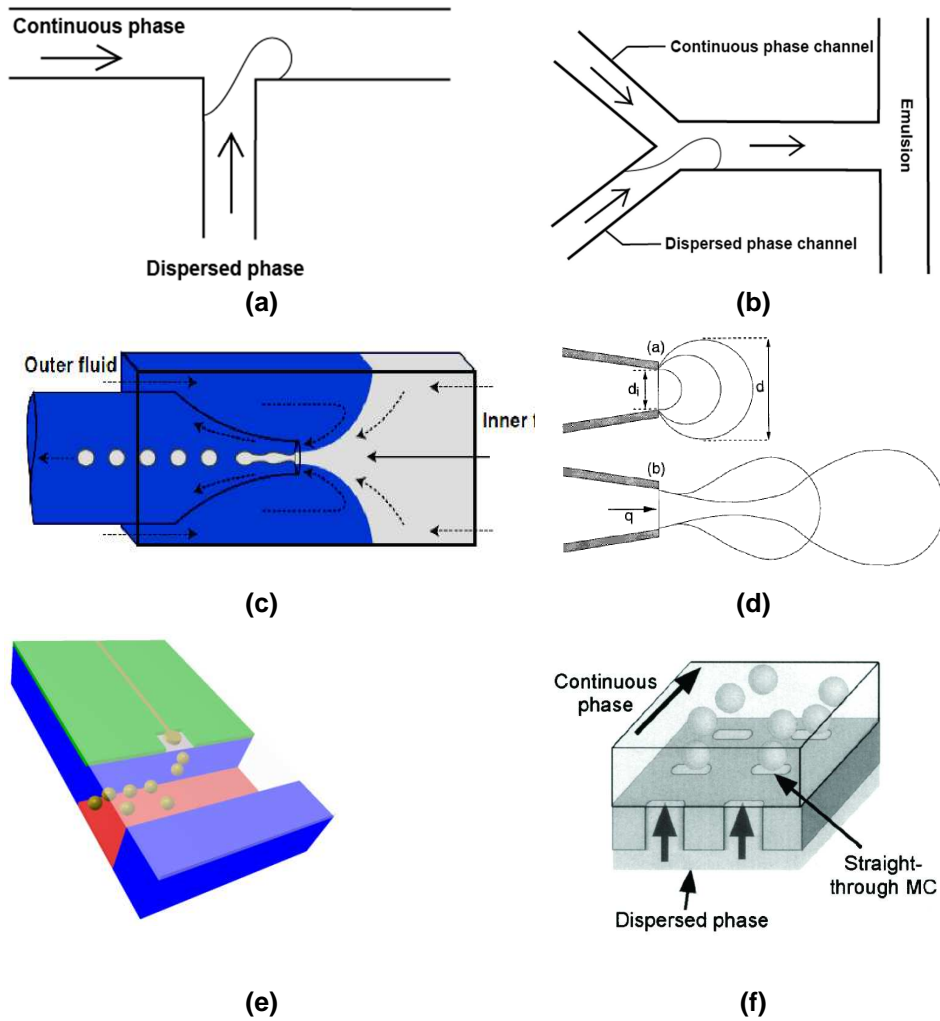


Figure 2.3: Some examples of microfluidic devices which are capable of producing monodisperse droplets. (a) T-Junctions (b) Y-Junctions (c) Flow-focusing microcapillary device (Reprinted with permission from Utada et al.¹²) (d) Co-flow system (droplet growth (a) and separation (b)) (Reprinted from Umbanhowar et al.¹³) (e) Grooved microchannel (Reprinted from van Dijke et al.¹⁴) (f) Straight-through microchannel device (Reprinted from Kobayashi et al.¹⁵)

Microchannel emulsification is a relatively new technique for preparation of monodisperse emulsions. Both, terrace-shaped structures (grooved)¹⁰ and straight-through microchannel arrays¹¹ (figures 2.3e & f respectively) have been extensively

reported in literature. As mentioned, the distinguishing feature of this technique is that no shear forces are needed to form droplets, and further, the size of droplets is mostly determined by the microchannel geometry (see also figure 2.4), and to a lesser extent by the to-be-disperse-phase flow. Interfacial tension is used as a driving force for droplet formation; and less energy (a factor of 10-100 less) as compared to the conventional techniques is needed¹⁰, for the production of various products such as o/w emulsions, w/o emulsions, lipid microparticles, polymer microparticles or microcapsules¹⁶.

This chapter aims to provide an overview of microchannel emulsification including, process principles, process parameters, applications, and an outlook on new emulsification technology based on spontaneous droplet formation that can be used in the production of food (related) products.

2. Microchannel emulsification

A (grooved) microchannel consists of a narrow channel fabricated in a microchip (made of silicon or a polymer) covered tightly with a (glass) plate. The channel ends into a slit like structure, the terrace, which leads to a deep continuous phase/emulsion channel. A schematic diagram of the process of droplet formation through a typical microchannel design is shown in figure 2.4.

On applying enough pressure, the dispersed phase flows through the narrow channel and spreads over the terrace in the form of a flattened disk-like shape (figures 2.4a-c). Curvature of the interface produces a pressure difference between the two phases called Laplace pressure which is defined as⁴.

$$\Delta P_L = \gamma_{ow} \left(\frac{1}{R_1} + \frac{1}{R_2} \right) \cos\theta \quad 2.1$$

Where ΔP_L is the Laplace pressure (Pa), γ_{ow} is the interfacial tension between the oil and water phases ($\text{N}\cdot\text{m}^{-1}$), R_1 and R_2 are the two radii of curvature of the interface (m) and ϑ is the contact angle (-). On reaching the end of the terrace (figure 2.4d) the tip of the dispersed phase leaps over into the continuous phase channel, and assumes a spherical shape which is energetically favorable (figure 2.4e), and detaches spontaneously (figure 2.4f) when the droplet has become large enough. (Laplace) pressure differences

are the driving force behind microchannel emulsification¹⁰, as is indicated by the curvatures in figure 2.4g-i, and as could also be derived from CFD simulations reported by Kobayashi and colleagues¹⁷ and van Dijke and co-workers¹⁴. In the later publication, design rules are shown that are based on an analytical model that uses local (Laplace) pressure differences.

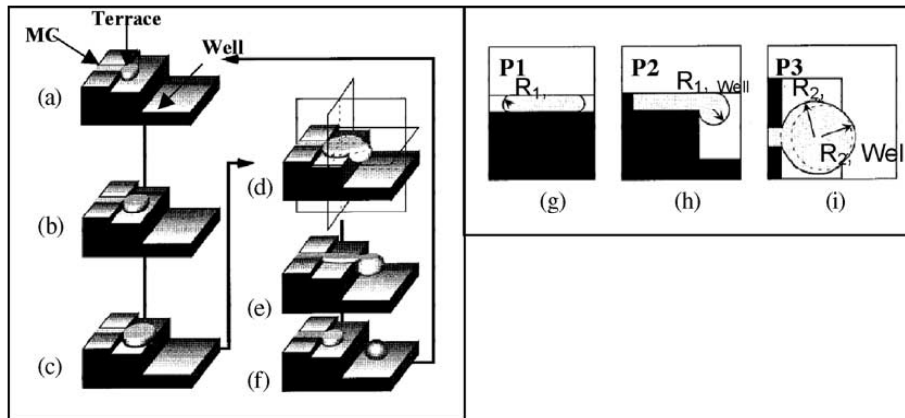


Figure 2.4: Droplet formation process in microchannel emulsification (a-f), together with cross sections in various positions in the microchannel (g-i) (Reprinted from Sugiura et al.¹⁰)

A straight-through microchannel device¹¹ consists of a large number of through holes fabricated on a single microchip (figure 2.3f), that works according to the same mechanism described for grooved microchannels. The dispersed phase is pressurized from one side of the device, pressed through the holes, and forms droplets on other side. The channels are constructed such that the continuous phase can intrude into the holes, to help in the formation and shrinkage of the neck inside the channel, and ultimately, formation of a droplet¹⁷.

3. Process parameters

As mentioned previously, two distinct geometries are used for microchannel emulsification, grooved systems, and straight-through systems. Here we first describe the geometry of both systems together with the typical dimensions that are related to both. After that, the properties related to the process operation such as applied pressure will be discussed, followed by liquid (viscosity) and ingredient properties (surfactants etc.) that

will be discussed in the light of the emulsification process, and finally surface properties will be touched upon.

3.1. Geometry

3.1.1. Grooved microchannels: The grooved microchannels consist of a channel and a terrace part (see figure 2.5a).

Terrace: Terrace geometry is defined with its length (L_T), width (W_T) and height (H_T). The terrace causes formation of a neck and promotes droplet formation. Kobayashi et al.¹⁸ showed that an array of microchannels with terraces gave monodisperse microspheres, while without terrace polydispersed microspheres were obtained. In general, droplet size increases with increasing available volume on the terrace without affecting the monodispersity of droplets^{19,20}; basically, the entire terrace empties to form the droplet.

Channel: The channel geometry is defined with its length (L_{ch}), width (W_{ch}) and depth (D_{ch}), and especially the length influences the pressure range within which monodisperse emulsions can be obtained, but not the droplet size^{5, 21}. This was also concluded from the analytical model presented by van Dijke and co-workers¹⁴; the pressure needed for flow through a longer channel is higher, while the Laplace pressure on the terrace and in the droplet will be unaffected, and this leads to higher monodispersity for longer channels because the system is less pressure sensitive.

Sugiura et al.⁵ reported that the droplet size is not affected by channel width, but Kawakatsu et al.¹⁹ and Kobayashi et al.¹⁸ found an increase in droplet diameter by increasing channel width. Similar results have been reported by Sugiura et al.². In general, an increase in the equivalent hydrodynamic diameter of the channel leads to a narrower pressure range for stable droplet formation and monodispersity decreases as a result thereof. This is also true for other variations in channel dimensions as studied by Liu et al.²¹ for convexes and Kawakatsu et al.¹⁹ for triangular channels.

3.1.2. Straight-through microchannels: The geometry of straight-through channels is identified as shorter length (S), longer length (L) and the depth (D) as shown in figure 2.5b.

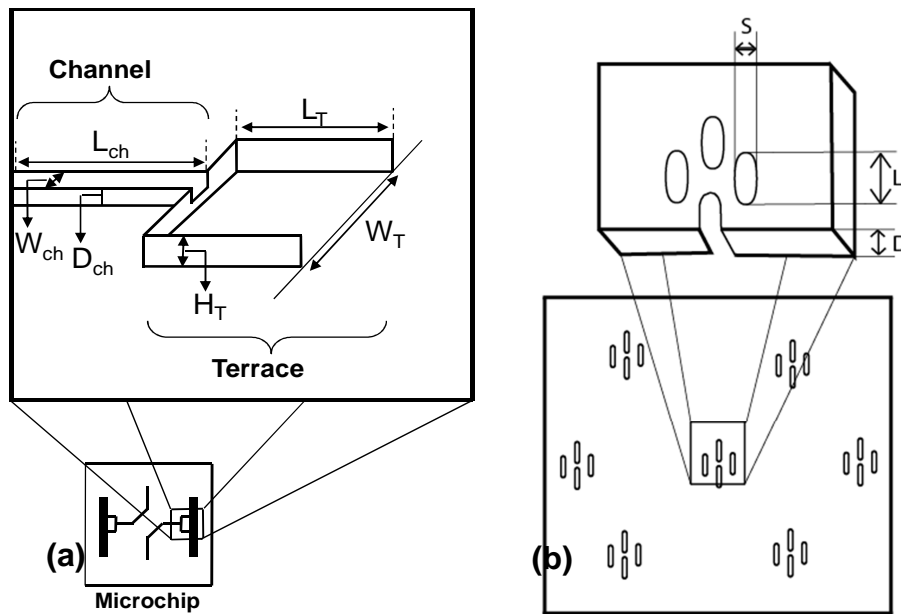


Figure 2.5: Schematic illustration of microchannel geometries. (a) grooved microchannel (b) straight through microchannel.

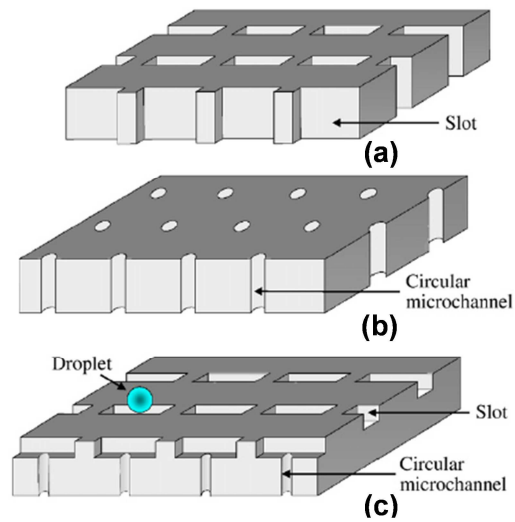


Figure 2.6: Schematic representation of symmetric (a and b) and asymmetric microchannels (c) (Reprinted from Vladisavljevic et al.²²).

Two distinct designs have been reported in literature, one with equal dimension all through the structure (symmetric), and one in which a narrow channel ends into an area with these dimension (asymmetric, and similar to the terrace system) (figure 2.6)²².

Monodispersed droplets are produced from channels with a slot aspect ratio (length/width ratio) above 3-3.5. At lower aspect ratios, cross section of the channel is completely occupied by the growing droplet, which prevents the inflow of the continuous phase, and therewith, droplet formation^{17, 23}, again indicating the importance of the 'terrace' that induces instability in the to-be-dispersed phase. Monodispersed emulsions were reported for asymmetric and oblong symmetric channels; only if the resistance of the supply channel became too high, polydisperse emulsions were observed and even continuous outflow.

3.2. Pressure and dispersed phase flow rate

Microchannel emulsification requires a pressure to be exerted on the dispersed phase to cause it to flow through the channel, and subsequently on the terrace. When the applied pressure reaches a certain value, (which is very low compared to pressures applied in e.g. high pressure homogenizers); the droplets begin to form from the terrace end. This pressure at which the droplet formation starts is called breakthrough pressure and can be estimated with¹:

$$\Delta P_{BT} = \frac{4\gamma_{ow}\cos(\theta)}{H} \quad 2.2$$

Where, ΔP_{BT} is the breakthrough pressure (Pa), γ_{ow} is the interfacial tension (Nm^{-1}), and θ is the contact angle of the interface with the channel surface (-) and H is the terrace height (m:smallest dimension of the terrace).

Upon increasing the pressure (liquid flow velocity), the droplet frequency will increase and the size of the droplets (and distribution) will also increase slightly as shown in figure 2.7. Please note that flow velocity data need to be interpreted with care, because the applied pump rate that is normally used on the x-axis may be quite different from the actual flow rate due to pressure build-up inside the microchips.

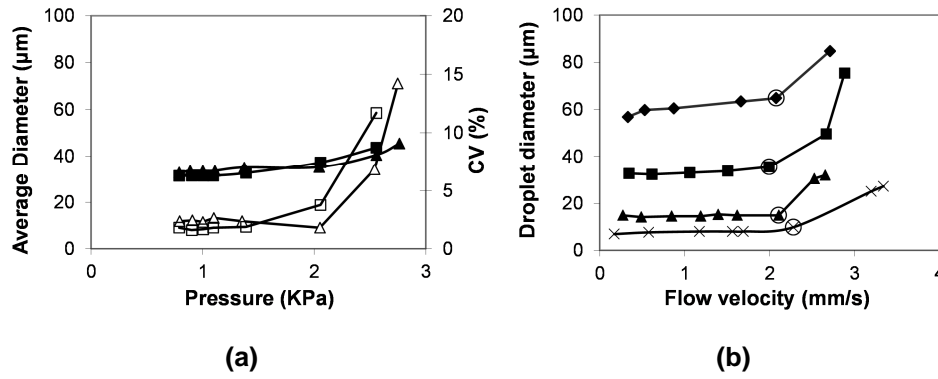


Figure 2.7: Effect of pressure and flow velocity on droplet formation: (a) Average droplet diameters (▲, ■) and coefficient of variation (CV) (Δ, □) of water/decane emulsions, containing surfactants CR310 (▲, Δ) & PO500 (■, □), as a function of applied pressure (data taken from Liu et al.²⁴) (b) Average droplet diameters as a function of flow velocity of dispersed phase using different microchannels (MC-2 (×) $D_{ch}=2\ \mu\text{m}$, $W_{ch}=3.3\ \mu\text{m}$, $L_{ch}=7.7\ \mu\text{m}$, $L_T=15\ \mu\text{m}$; MC-4 (▲) $D_{ch}=4\ \mu\text{m}$, $W_{ch}=4.7\ \mu\text{m}$, $L_{ch}=14\ \mu\text{m}$, $L_T=28\ \mu\text{m}$; MC-8 (■) $D_{ch}=8\ \mu\text{m}$, $W_{ch}=8.3\ \mu\text{m}$, $L_{ch}=32\ \mu\text{m}$, $L_T=57\ \mu\text{m}$; MC-16 (▪) $D_{ch}=16\ \mu\text{m}$, $W_{ch}=16\ \mu\text{m}$, $L_{ch}=68\ \mu\text{m}$, $L_T=113\ \mu\text{m}$) (data taken from Sugiura et al.²⁵). Experimental system: 1% SDS solution in Milli Q water as continuous phase and triolein as dispersed phase.

With increasing pressure, up to a certain critical velocity (encircled points in figure 2.7b) the droplets stay monodisperse, but above this critical pressure/flow velocity, the droplet diameter increases more rapidly (as can be seen in the figure) and monodispersity decreases, and eventually blow-up occurs (i.e. the phase flows out continuously). At these pressures, the flux from the supply channel, across the terrace to the droplet is so large that it does not allow the neck, that keeps the droplet connected to the terrace, to collapse, as described by the flux criterion defined by van Dijke and co-workers¹⁴, as summarized in Appendix B.

The effect of the applied pressure (and flow velocity) on droplet size depends on various parameters such as microchannel geometry¹⁴, viscosity ratio of dispersed and continuous phase²⁶ and the type and concentration of surfactants^{5, 16}. More details are given in the respective sections.

3.3. Liquid and ingredient properties

3.3.1. Viscosity: The viscosities of dispersed and continuous phases have important effect on the performance of microchannel emulsification processes. The average droplet diameter of w/o emulsions was reported to increase with increasing continuous phase viscosity^{24, 27} and for o/w emulsions, the average droplet diameter was reported to decrease with increasing dispersed phase viscosity^{22, 27}. All these effects may be covered by the observations by van Dijke and coworkers²⁶, who linked the viscosity ratio (viscosity of dispersed phase/viscosity of continuous phase) to the droplet size. In general, the droplet size scales with the viscosity ratio; at high viscosity ratio, the droplet size is constant, and at low viscosity ratio, the droplet size increases (figure 2.8). This can be interpreted as follows: as long as the continuous phase can flow onto the terrace freely (compared to the to-be-dispersed phase flow), the neck will break rapidly, and the droplet size will not be influenced. If the continuous phase is very viscous, this will prevent the neck from collapsing rapidly; keep the droplet connected to the feed channel for a longer time, and lead to larger droplets.

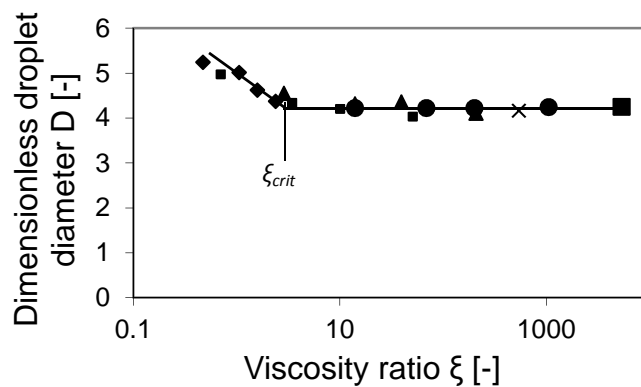


Figure 2.8: Effect of viscosity ratio (η_d/η_c) on dimensionless droplet diameter D (resultant droplet diameter D_{drop} /height of the terrace H) using (■) silicon oil 5000, (●) silicon oil 1000, (×) silicon oil 500, (▲) silicon oil 200, (▪) soybean oil and (◆) hexadecane, (data taken from van Dijke et al.²⁶).

Temperature has a direct effect on the viscosities of dispersed and continuous phases but the viscosity ratio will not be greatly affected. Decrease in viscosity of phases increased the droplet formation frequency, but as long as the values for viscosity ratio

(η_d/η_c) remained above the critical viscosity ratio (and the interfacial tension is not too much influenced), the droplet size remains unaffected. Hence, the temperature can be used as a tool to tune the droplet diameters and droplet productivity. On the other hand, it makes the emulsification process more complex since it also influences e.g. interfacial tension; and temperature sensitive components should not be affected.

3.3.2. Surfactants and interfacial tension: Surfactants play two important roles in the emulsification process; firstly, they lower the interfacial tension and stabilize the droplets after formation, i.e. prevent coalescence and/or aggregation of emulsions. As a side effect, surfactants may influence the wettability of the emulsification device, therewith indirectly influencing local pressures, and through this, the droplet size. While in classic emulsification methods a low interfacial tension facilitates droplet formation, in microchannel emulsification, this is not the case. At high interfacial tension, the pressure differences between the feed channel and droplet are higher, and already at small size, the flux criterion of van Dijke et al.¹⁴ will be met. At low interfacial tension, the droplet needs to become bigger to result in a similar pressure difference. In general, it is expected that for microchannels the droplet formation process is thus slow that the surface will be saturated, i.e. at equilibrium interfacial tension⁶.

Whether the interfacial tension is lowered during the time of droplet formation, depends on the type of surfactant and its concentration²⁸. Vladislavljević et al.²² studied the effect of SDS (sodium dodecyl sulphate) concentration, on the preparation of oil-in-water emulsions using soybean oil as dispersed phase, with straight-through microchannels. Monodisperse droplets were formed in the range of 0.2-0.5 wt%; at lower concentration, the droplets coalesced, while at higher concentrations, satellite droplets were formed, therewith reducing monodispersity. Satellite droplets are generated as a result of imbalance of capillary forces during break-off of primary droplets²⁹ and has been reported in many droplet generation devices^{30,31}.

Kobayashi et al.³² investigated the effect of differently charged emulsifiers on the preparation of o/w emulsions with straight-through microchannels. Anionic surfactant SDS, nonionic surfactant Tween 20 (polyoxyethylene (20) sorbitan monolaurate) and a cationic

surfactant CTAB (cetyltrimethylammonium bromide) were dissolved in continuous phase while a cationic surfactant TOMAC (Tri-*n*-octylmethylammonium chloride) was dissolved in dispersed phase (soybean oil). Monodisperse emulsions were successfully produced by using anionic and nonionic surfactants, while cationic surfactants resulted in polydisperse emulsions and complete wetting of the channel surface by the dispersed phase, indicating that surface properties need to be considered in combination with surfactant properties.

Several investigations with food grade emulsifiers have been reported. Saito et al.³³ made oil-in-water emulsions using bovine serum albumin (BSA), β -lactoglobulin, γ -globulin, lysozyme, soybean flour, whey protein, and egg white protein. Stable monodispersed emulsions could only be prepared using BSA, β -lactoglobulin, soybean flour and whey protein.

Besides, the ingredients of the emulsion influence derived parameters such as the surface tension and emulsion stability. Fujii et al.³⁴ recently investigated the effect of temperature (10-70 °C) on microchannel emulsification. At higher temperature, the breakthrough pressure (ΔP_{BT}) increased because of higher interfacial tension (see equation 2.2), and smaller droplets were formed, albeit at higher frequency due to the lower viscosity of the to-be-dispersed phase.

3.4. Surface properties

For stable production of monodisperse emulsion droplets through microchannels, the continuous phase should wet the channel surface; hence the surface should be hydrophilic for o/w emulsification and hydrophobic for w/o emulsification³⁷. That also explains why Liu and coworkers²⁴ using a hydrophobic acrylic microchannel for the preparation of o/w emulsion found continuous out-flow of oil without any droplet formation. For the production of microchannels, mostly silicon-based materials are used, and various researchers investigated chemical modification of the surfaces. For example, silicon is hydrophobic but can be made hydrophilic by depositing a silicon-oxide layer through plasma treatment³⁷. Silicon can also be made more hydrophobic through silane coupler reagents, such as octadecyltrichlorosilane, and subsequent heating at 110 °C for 1h²⁴. However, silanization is not a permanent surface modification method, and may not be used for

food and pharmaceutical applications³⁸. For permanent modification, the covalent methods developed by Arafat and co-workers^{39, 40} and Rosso and colleagues⁴¹ seem more appropriate, although these methods have only been applied on flat surfaces until now.

Table 2.1: Effect of type and concentration of surfactants on microchannel emulsification.

Type of Emulsion	Surfactant type and concentration			Emulsification behavior	Ref.
	Surfactant	Type	Conc. (Wt %)		
Oil-in-water	SDS (w_c) ^a	anionic	0.01-0.02	Coalescence	22
	SDS (w_c)	anionic	>0.5	Satellite droplet formation	
	SDS (w_c)	anionic	0.2-0.5	Monodispersed emulsion	
Oil-in-water	γ -globulin (w_c)	-	0.5	Wetting of dispersed phase on channel surface	33
	Lysozyme	-	0.5	-	
	Egg white	-	0.5	-	
	BSA	-	0.5	Monodispersed emulsion	
Oil-in-water	CTAB (w_c)	cationic	1.0	Wetting of dispersed phase on channel surface and satellite droplet formation	32
	TOMAC (O_d) ^b	cationic	2.0	Wetting of dispersed phase on channel surface	
	Tween 20 (w_c)	nonionic		Monodisperse emulsion	
Polymeric microspheres	SDS (w_c)	anionic	<0.2	Wetting of dispersed phase on channel surface	35
Oil-in-water microspheres	Soybean and egg yolk lecithin	-	0.3	Wetting of dispersed phase on channel surface and coalescence	36

a = Dissolved in continuous water phase

b = Dissolved in dispersed oil phase

Also acrylic microchannels, which are originally hydrophobic and suitable for w/o emulsification, can be modified in order to make them suitable for o/w emulsification by a procedure described by Liu et al.⁴². Monodisperse emulsions were produced when using

an Exceval coating and SiO₂ vacuum deposition while Lipidure-PMB coating produced polydisperse emulsions. Clearly, surface properties need to be chosen carefully, and the durability of the modified layer needs to be evaluated carefully.

As mentioned in the previous section, the surface of the microchannels may also be affected by the surfactants. Various examples are summarized in table 2.1, and they clearly illustrate the dual effect of surfactants which are needed to stabilize the oil/water interface, but affect the (wettability of the) microchannel surface mostly negatively, but also sometime positively. Saito et al.³³ could not prepare oil-in-water emulsions with γ -globulin, lysozyme and egg white proteins because they influenced surface wettability, resulting in high water contact angles that prevent water intrusion on the terrace. In some other investigations, polydisperse o/w emulsions with large droplet sizes were obtained when surfactants adsorbed to the channel surface resulting in non-uniform wettability or even making it hydrophobic^{32,43}. Tong et al.³⁶ investigated the effect of soybean and egg yolk lecithin (dissolved in the oil phase), and found that the oil droplets coalesced and the microchannel surface lost its hydrophilicity due to lecithin adsorption, resulting in the continuous outflow of the oil phase. Similar behavior for lecithin has been reported by Sugiura et al.⁴³. For the preparation of lipid microspheres and polymeric microspheres, the same authors³⁵ found that the microstructure was not wetted uniformly below 0.2 wt% SDS; in this case, a certain amount of surfactant is needed to maintain appropriate surface wetting properties.

Changes in wettability will be especially important in the production of foods that contain many different surface active components. Which combination works best is hard to predict beforehand, given the multitude of interactions that play a role. e.g. the pH can influence the properties of the surface and those of the components, as reported by Huisman et al.⁴⁴ and Nakagawa et al.⁴⁵. Huisman et al.⁴⁴ used different ceramic membranes, and the charge of the membranes determines which surfactants can adsorb. Nakagawa et al.⁴⁵ investigated the influence of pH on the preparation of gelatin/acacia complex coacervate microcapsules, and regular sized microcapsules could not be obtained at pH 4.0, because gelatin molecules (isoelectric point 5.1) were positively charged and interacted with the negatively charged surface of microchannel, rendering it hydrophobic.

At a pH above the isoelectric point of gelatin, it was possible to produce monodisperse droplets due to the negative charge of the gelatin. Saito et al.³³ observed similar behavior for BSA at low pH (3 and 4), where the microchannel surface was wetted by the dispersed phase; clearly not only basic adsorption is important but also charge interactions (mostly with the microchannel) are crucial for maintaining emulsification. For this, surface modification methods, as suggested by Rosso and co-workers⁴¹ which prevent protein adsorption could be of great relevance.

For industrial applications, the use of polymer microchannels has an advantage over silicon in the sense that it is stronger and tougher than silicon. In addition, polymer is less expensive and can be processed more easily^{21,24}. However, the material from which the microstructures are made also has to satisfy other needs (appropriate surface properties, and it should allow preparation of small channels). Materials with high mechanical stability, especially metals which are expected to be of great industrial relevance, still need to be investigated. This is probably because the precise fabrication needed for microstructures is currently not possible. To get information on how metal surfaces will behave, EDGE devices coated with different metals have been investigated and are reported in chapters 3 and 4. However, given the opportunities that arise from emulsification with microchannels, it can be expected that metal fabrication will grow into a viable concept in near future.

4. Products produced by microchannel emulsification

Microchannel emulsification technique has been successfully applied for the preparation of simple emulsions, multiple emulsions, microspheres, and microcapsules. Here we shortly discuss these products and where possible we compare with similar products obtained by more traditional emulsification technology.

Oil-in-water emulsions were reported by many different authors, while water-in-oil emulsions are more sparingly reported e.g.^{21,24,27}. A complete overview of the data available in literature at the time of writing can be found in Table A1 for grooved microchannel systems, and in Table A2 for straight through systems. Saito et al.⁸ found that o/w emulsions prepared by microchannel technology showed higher stability than

those obtained by homogenization, which was attributed to the monodispersity of the emulsions.

A multiple emulsion is an emulsion in an emulsion⁴⁶, and they cannot or hardly be prepared by classic emulsification methods, because the second emulsification step is prone to destroy the primary emulsion. Literature is available on the preparation of w/o/w emulsions⁴⁷⁻⁴⁹ but no literature has been reported until now on the preparation of o/w/o emulsions by microchannel emulsification probably because they are less interesting from an application point of view. Typically, microchannel emulsification is used as a second step for dispersion of the primary emulsion into the continuous phase. Monodisperse emulsions were successfully prepared with little or no leakage of internal water phase⁴⁷, which makes this technology a very interesting preparation method for such products, which may be used as low-calorie products or as controlled release vehicles.

Microspheres are solid particles which can be utilized in food, cosmetics and pharmaceuticals^{50, 51}; microchannel emulsification was reported to successfully prepare monodisperse microspheres of sizes ranging from several to 100 μm ³⁵. Sugiura et al,²⁰ prepared divinylbenzene microspheres by combining microchannel emulsification of the monomer with polymerization, and the resultant microspheres had a narrow size distribution similar to those of polymeric microspheres prepared by seed polymerization. Other examples of microspheres prepared through microchannel emulsification can be found in Tong et al.^{52, 36} and Sugiura et al.⁴³.

Microcapsules are hollow microspheres that consist of a polymer wall or coat that covers a core that may contain an active ingredient⁵³⁻⁵⁵, being e.g. a food additive, a biocide, or an adhesive⁵⁶. Owing to its low energy input, microchannel emulsification can be used for shear sensitive substances like peptides and proteins. Some examples: Gelatin capsules with narrow size distribution were prepared by Iwamoto et al.⁵⁷ using iso-octane containing TGCR (Tetraglycerin condensed ricinoleic acid ester) as a continuous phase. Neves et al.⁵⁸ encapsulated β -carotene dissolved in soybean oil in sugar ester or gelatin, and obtained micrometer sized monodisperse loaded capsules, which were physically stable after 4 months of storage at 5 °C. Simple emulsions can be used for capsules built

by layer-by-layer adsorption as reported by Sagis et al.⁵⁹. When starting from monodisperse droplets obtained from microchannels, exact dosage in these capsules is within reach (please note, that this was not the case in⁵⁹).

5. Recent developments and comparison of emulsification techniques

The microchannel emulsification technique is claimed to be suitable for the production of 'supermonodisperse' emulsions¹⁰, however the low throughput of the disperse phase (less than 0.1 ml/h) from grooved microchannels²² limit the range of its practical applications. Development of straight-through devices was an effort to increase the productivity of the system and monodisperse emulsions at a rate of 65 L/(m²h) were successfully produced with average droplet diameter of 30 µm¹¹. However, for narrower microchannels that produce, i.e. droplets below 10 µm which is the size range required in most food applications, the maximum oil flow was only 0.708 L/(m²h)³⁷ because of a low percentage of active channels. In some cases, this percentage was below 1%, and upon slight increase of the pressure, the system became unstable. Most probably this is caused by pressure gradients just below the straight-through plate as was reported by Abrahamse et al.⁶⁰ for microsieve systems.

For small droplets (<10 µm) the new EDGE (Edge based Droplet Generation) mechanism⁴ which results in multiple simultaneously formed monodispersed droplets from a single droplet formation unit, can be of great interest. Droplet formation in an EDGE device is shown in figure 2.9a; the dispersed phase is pressurized through the oil channel which spreads over a large flattened area called plateau and on reaching the edge of the plateau, it spontaneously forms monodispersed droplets at several locations. In microchannel emulsification, the terrace would almost completely empty into one droplet, but that is obviously not the case for EDGE where the droplet volume is only a small fraction of the total volume of oil available on the plateau, and droplet formation takes place along the entire length of the edge.

The droplet size produced by EDGE is determined by the height of the plateau and a scaling factor of 6-8 has been observed. The EDGE technique has only very recently

been introduced (2009-2010); therefore, not a lot of information is available; Table A3 summarizes the investigations made with EDGE systems, and it is clear that the technique gives monodisperse emulsions with coefficients of variation generally around 5-6%. It is worth mentioning that initial studies have shown that the system is robust, more stable under pressure changes than the microchannels are, and it has been operated continuously for 3 consecutive days without the droplet size and monodispersity being affected. Besides it can be parallelized^{6, 61} (figure 2.9b) with all the plateaus completely filled with oil phase at breakthrough pressure and regular sized droplet formation from all plateaus as soon as the oil reaches the edge of the plateaus.

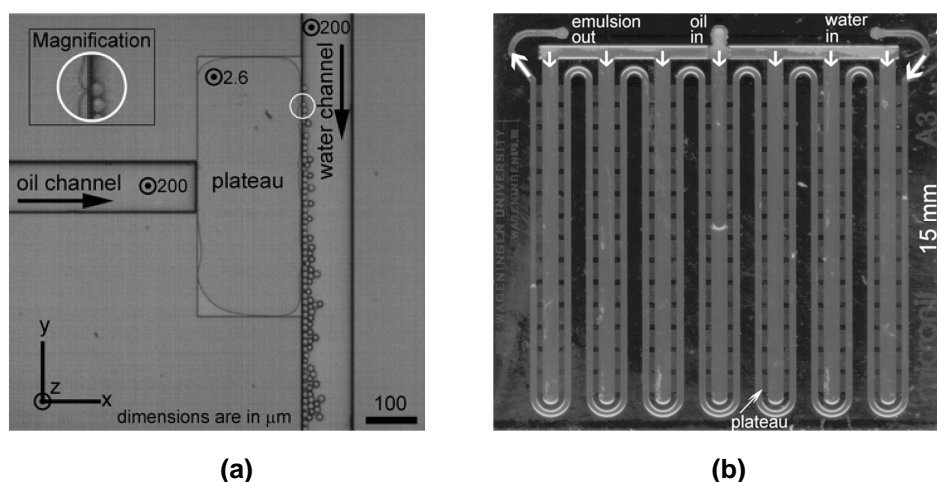


Figure 2.9: (a) Droplet formation through a typical EDGE device (Reprinted from van Dijke et al.⁴)
(b) A typical parallelized EDGE system (reprinted from van Dijke et al.⁶¹).

Emulsification efficiency of emulsification systems can be compared on energy density which is defined as energy input per unit volume of emulsion. Figure 2.10 compares spontaneous emulsification techniques (microchannels and EDGE) with shear based micro-systems (membranes and Y-junctions), and traditional emulsification systems (homogenizers and microfluidizers). The energy required for EDGE emulsification is comparable to the grooved and straight-through microchannels, and membrane emulsification, but seems less than needed for shear based and classic emulsification systems although the picture is obscured because the droplet sizes are not the same and

also the droplet size increases by increasing pressure in spontaneous emulsification (also see pressure and dispersed phase flow rate section). The pressure needed for spontaneous droplet formation is very low (mbar range) compared to that used in classic emulsification devices, and it can be expected that the supplied energy is mostly used for the formation of surfaces, and not dissipated as heat as is the case in homogenizers.

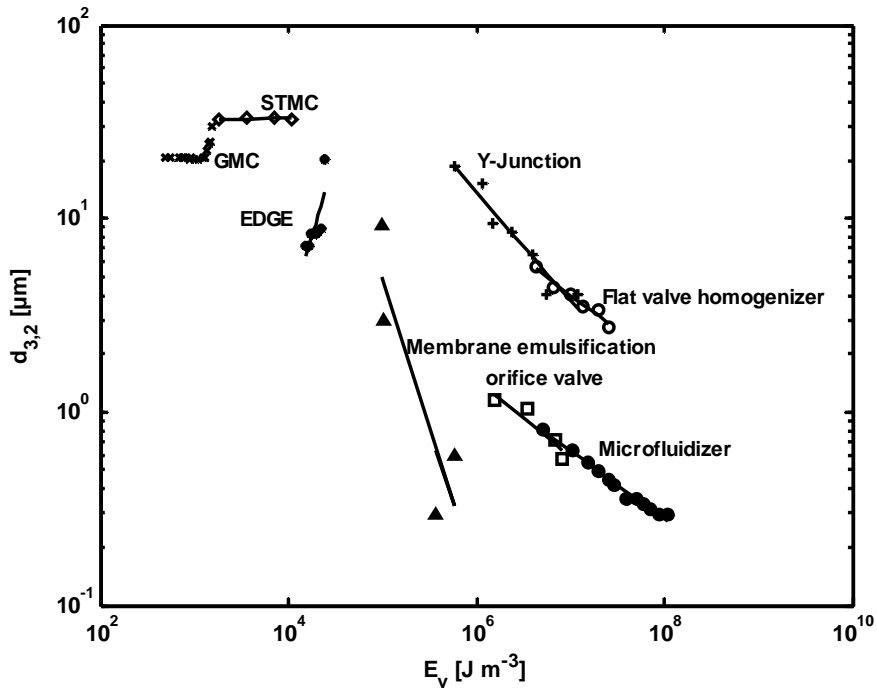


Figure 2.10: Energy efficiencies of various emulsification systems: (\times) grooved microchannels (GMC)⁴³, (\diamond) straight-through microchannels (STMC)¹¹, ($*$) EDGE systems⁶¹, ($+$) Y-junctions⁶², (\blacktriangle) membrane emulsification, (\circ) flat valve homogenizer, (\square) orifice valve and (\bullet) microfluidizer⁶³.

Away from monodispersity and energy density, also the microchip area (or volume) required to produce a unit volume of emulsion is an important parameter to evaluate the scalability of a technique. Figure 2.11 compares the area required of different spontaneous emulsification systems to obtain dispersed phase flux of $1 \text{ m}^3/\text{h}$. The values are calculated for systems that produce droplets of sizes $<10 \text{ }\mu\text{m}$ (GMC, STMC and EDGE) (see tables, A1, A2 and A3). The area required for EDGE systems is less as compared to the grooved and straight-through microchannels. GMCs require much larger area which is due

to the limited number of channels (100-1500) in most of the investigated systems²². Recently, Kobayashi and co-workers⁶⁴ investigated scale up of grooved microchannels through integration of microchannel arrays on a single microchip (60 × 60mm) consisting of 14 arrays and 1.2×10^4 channels. With this system, they were able to obtain dispersed phase flux of 1.5 mL/h ($d_{avg} \approx 10 \mu\text{m}$) which is a promising development and can effectively reduce the required area as can be seen in figure 2.11 (GMC-A). Whether any of these approaches can be successfully scaled-up is not clear; however we find that stable operation, and relatively easy fabrication (only one dimension i.e. height of the plateau needs to be precisely defined and maintained) makes EDGE unique among spontaneous emulsification systems and the most likely candidate for scale-up.

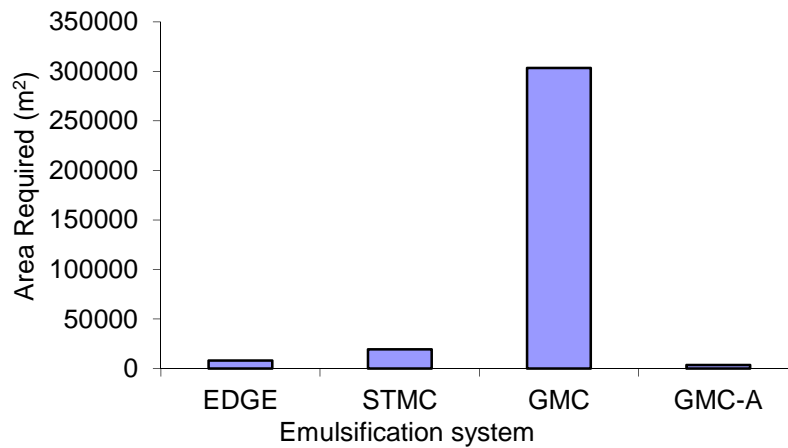


Figure 2.11: Area required of different spontaneous emulsification systems (EDGE^{6, 61}, STMC³⁷, GMC¹⁸ and GMC-A⁶⁴) to obtain dispersed phase flux of $1\text{m}^3/\text{h}$.

6. Conclusion and outlook

Spontaneous emulsification with microchannels is a popular method in literature, and the technique is suited for monodisperse emulsion production (CV \approx 5%), and for products containing shear and temperature sensitive ingredients (e.g. food). Industrial application is not yet possible, because of scaling issues. The production rates per channel are low, and for the production of small droplets (<10 μm), activation of all channels in straight-through emulsification is a technical challenge.

The new development called EDGE may be the solution to some of the scaling issues related to microchannel emulsification. Its wide plateau allows multiple monodisperse droplets to form from one droplet formation unit, with the size of the droplets only determined by the height of the plateau. Besides, some proof of principle on up-scaling is available, and food ingredients have been successfully applied.

Away from the choice of the spontaneous emulsification technique, it is of utmost importance to control the surface properties and maintain appropriate wettability all through emulsification and for this surface modification will be needed. Also, for industrial application, the material to be used for the construction of the devices needs to be (re-) considered, and it is expected that the current Si-based microchips will not be suitable for this. Most probably, polymer-based microchips, or even metal ones (as investigated in chapters 3 and 4) if they allow structure formation at the scale needed in microstructures, will be preferred.

Which of these factors will be the determining one for industrial application is still not clear. But it is sure that there is still sufficient room for optimization and maturation of spontaneous emulsification technology to make it an attractive alternative for classic emulsification techniques.

Appendix A

Table A1: Microchannel geometry, and resulting droplet diameters under various experimental conditions for grooved microchannels.

Microchannel Geometry					Dispersed phase (a) Continuous phase (b)	Pressure (KPa)	Drop size (μm)	CV (%)	Ref.
L_{ch}^a μm	W_{ch}^b μm	D_{ch}^c μm	L_T^d μm	W_T^e μm					
-	12	2.0	25	32	a. Divinyl benzene with 2wt.-% benzyl peroxide	8.8	10.0	4.4	35
-	3.2	1.0	5.0	7.3	b. 0.2 wt.-% SDS aqueous solution	16.6	4.2	9.1	
-	30	16	98	-	a. Divinyl benzene with 2wt.-% benzyl peroxide	1.1	74.9	2.8	20
-	30	16	240	-	b. 0.2 % SDS aqueous solution	1.0	90.2	2.3	
-	4.7	1.2	6.9	-	a. Soybean oil with 1.5wt.-% Tween 80 b. Physiological saline	5.4	5.0	7-9	18
199	27.2	5.0	-	-	a. Refined soybean oil	3.6	21.4	2.3	65
39.8	10.2	1.9	-	-	b. 1.0 wt.-% Tween 20 in Milli-Q water	7.2	9.0	3.1	
120	20 \pm 0.9	10	30	-		0.8-1.0	52-60	< 8.0	24
120	40 \pm 1.0	20	30	-	a. Water b. 3 wt.-% CR310 dissolved in triolein	0.3-0.6	62-98	< 8.0	
70	16 \pm 0.3	11	30	-		0.8-1.0	53-66	< 8.0	
-	14.4	4	29.6	-	a. Triolein b. 0.3 % SDS aqueous solution	3.5	17.8	2.8	10
50	10	5	15	-		-	24-37	5.6-7.7	21
150	10	5	15	-	a. Milli-Q water with 3wt.-% CR310 b. Decane/Triolein (20:80 wt/wt)	-	25-42	5.1-6.7	
500	10	5	15	-		-	27-54	4.6-5.5	

-	16	4	-	-	a. Air b. 0.3wt.-% SDS aqueous solution	-	33.6	1.8	66
-	30	16	98	-		1.16	64.4	3.4	
-	30	16	138	-	a. Triolein b. Milli-Q water with 1% SDS	1.12	74.6	2.1	1
-	30	16	240	-		1.43	98.1	2.5	
70	10	2	30	-	a. Soybean oil with 3.2 g/L of β - carotene b. Milli-Q water with 1 wt.-% sucrose monolaurate	-	9.1	6.2	58
250	10	10	50	10	a. Hexadecane b. Milli-Q with 1% SDS	20	30	-	14
25.3	-	8	51.7	-	a. Hexadecane b. Milli-Q water with 1 wt% SDS	-	34.8	2.5	26

a = Channel length, b = Channel width, c = Channel depth, d = Terrace length, e = Terrace width

Table A2: Channel geometry and resulting droplet diameters under various experimental conditions for straight-through microchannels.

L_{st}^a μm	Channel Geometry		Type	Dispersed phase (a) Continuous phase (b)	Pressure (KPa)	Drop size (μm)	CV (%)	Ref.
	S_{st}^b μm	D_{st}^c μm						
40	10	200	Symmetric	a. Refined Soybean oil b. 25mM NaCl solution containing 0.45% w/w BSA.	-	44.1	5.4	33
4.6	1.0	30.0	Symmetric	a. Refined soybean oil b. 1 wt.% SDS in Milli-Q	13.1	4.4	5.5	37
10.0	2.3	30.0			6.7	6.7	3.9	
15.0	3.3	30.0			4.6	9.8	2.7	
48.7	9.6	200	Symmetric	a. Refined soybean oil b. Demineralized water with 1.0 wt.% SDS	-	39.1	2.5	32
52.5	14.0	200	Symmetric	a. Refined soybean oil b. De-ionized water with 1.0 wt.% Tween-20.	-	48.9	2.1	67
48.7	9.6	200			-	38.1	1.9	
22.9	7.3	-	Symmetric	a. Milli-Q water solution of NaCl (5.0 wt.%) and glycerol with a weight ratio of 1:3 b. Decane solution of CR-310 (3.0 wt.%)	1.8	25.6	3.2	38
43.4	12.7	200	Symmetric	a. Silicon oil (KF96-50) b. Milli-Q water (1.0 wt.% SDS)	-	49.8	1.7	15
26.7	6.6	100	Symmetric	a. Soybean oil b. Milli-Q water with 1.0 wt.% SDS	-	31-32	9-10	68
40.8	10.8	200	Symmetric	a. Soybean oil b. Demineralized water with 1.0 wt.% SDS	-	41.9	1.9	69
50	10	30 ^e	Asymmetric	a. MCT (medium-chain fatty acid triglyceride) b. Milli-Q water with 2.0 wt.% Tween20	-	27.1-27.6	-	23
$D^d = 10$		70 ^f						

50	10	30 ^e	Asymmetric	a. Soybean oil b. Milli-Q water with 0.5 wt.% SDS	-	26.5	3-4	70
D = 10		70 ^f						

a = Longer length of straight-through channel (symmetric)/microslot (asymmetric)

b = Shorter length of straight-through channel (symmetric)/microslot (asymmetric)

c = Depth of straight-through channel (symmetric)/microslot (asymmetric)

d = Diameter of cylindrical channel (asymmetric), e = Microslots, f = Channels

Table A3: Plateau dimensions and resulting droplet diameters under various experimental conditions for EDGE systems.

L_p^a μm	Plateau dimensions			Dispersed phase (a) Continuous phase (b)	Pressure (mbar)	Drop size (μm)	CV (%)	Ref.
	W_p^b μm	H_p^c μm	N_p^d (-)					
200	500	1.2	1		175	7.1	5	
200	500	2.6	1	a. Hexadecane b. MilliQ (1% SDS)	80	14.6	5	4
200	500	1.2	196		180	7.0	4-5	
200	9500	1.2	14	a. Hexadecane b. MilliQ (1% SDS)	160	7.0	5	61
200	200-1200 ^e	1.2	112		160	7.0	5	
200	500	1.2	196	a. Sunflower oil b. WPC solution(6% w/v) or skim milk	310	7.2	11.8	
200	500	1.2	-	a. water-in-sunflower oil (10% w/w PGPR) b. WPC solution(6% w/v) or skim milk	400	7.4	6	6
200	500	1.2	-	a. air b. WPC solution(6% w/v) or skim milk	1000	30		

a = length of the plateau, b = Width of the plateau, c = Height of the plateau,

d = Total number of plateaus, e = Triangular shaped plateaus

Appendix B:

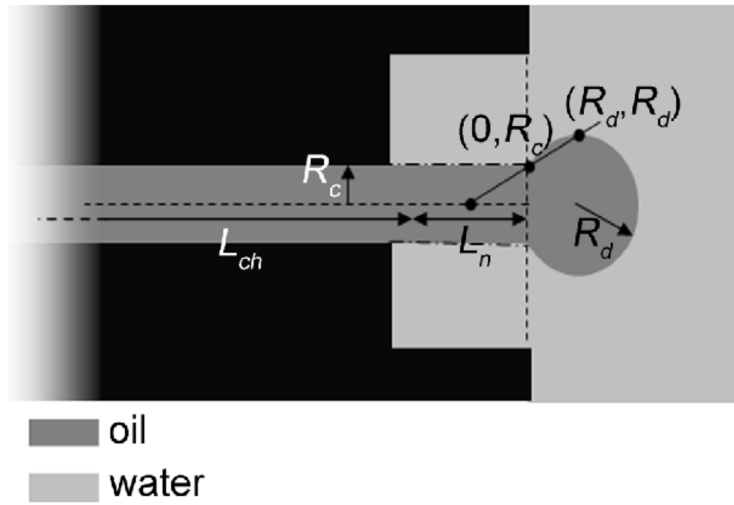


Figure B1: Schematic cross section of a microchannel showing length of neck (L_n) and length of channel (L_{ch}) (van Dijke et al., 2008).

Flux through the entire system is calculated with the Hagen-Poiseuille equation, given as

$$\left[\Phi_t = \frac{dV}{dt} = \pi \frac{R_c^4}{8\eta L_{ch}} \left[P_{app} - \frac{2\sigma}{R_{d,t}} \right] \right]$$

Where, Φ_t is the total flux, R_c is the radius of channel, L_{ch} is the length of channel η is the fluid viscosity, P_{app} is the applied pressure, σ is the interfacial tension and R_d is the droplet radius.

Flux through the channel to the neck is calculated as

$$\Phi_{ch,t} = \frac{dV}{dt} = \pi \frac{R_c^4}{8\eta L_{ch}} \left[P_{app} - \frac{\sigma \cos \theta}{R_c} \right]$$

And the flux through neck to the droplet is calculated as

$$\Phi_{n,t} = \frac{dV}{dt} = \pi \frac{R_c^4}{8\eta L_n} \left[\frac{\delta \cos \theta}{R_c} - \frac{2\delta}{R_{ct,d}} \right]$$

The droplet breakup criterion is defined as

$$\Phi_{n,t} > \Phi_{ch,t}$$

References

1. S. Sugiura, M. Nakajima and M. Seki, *J. Am. Oil Chem. Soc.*, 2002, **79**, 515-519.
2. S. Sugiura, M. Nakajima and M. Seki, *Langmuir*, 2002, **18**, 3854-3859.
3. A. I. Romoscanu, A. Fenollosa, S. Acquistapace, D. Gunes, T. Martins-Deuchande, P. Clausen, R. Mezzenga, M. Nydén, K. Zick and E. Hughes, *Langmuir*, 2010, **26**, 6184-6192.
4. K. C. van Dijke, G. Veldhuis, K. Schroën and R. M. Boom, *AIChE Journal*, 2010, **56**, 833-836.
5. S. Sugiura, M. Nakajima and M. Seki, *Langmuir*, 2002, **18**, 5708-5712.
6. K. C. van Dijke, K. Schroën, A. van der Padt and R. M. Boom, *J Food Eng*, 2010, **97**, 348-354.
7. C. Charcosset, I. Limayem and H. Fessi, *J Chem Technol Biot*, 2004, **79**, 209-218.
8. M. Saito, L. J. Yin, I. Kobayashi and M. Nakajima, *Food Hydrocolloid*, 2006, **20**, 1020-1028.
9. T. Nakashima, M. Shimizu and M. Kukizaki, *Key Eng. Mater.*, 1991, **61/62**, 513.
10. S. Sugiura, M. Nakajima, S. Iwamoto and M. Seki, *Langmuir*, 2001, **17**, 5562-5566.
11. I. Kobayashi, M. nakajima, K. Chun, Y. kikuchi and H. Fujita, *AIChE J*, 2002, **48**, 1639-1644.
12. A. S. Utada, L. Y. Chu, A. Fernandez-Nieves, D. R. Link and D. A. Weitz, *MRS Bull*, 2007, **32**, 702-708.
13. P. B. Umbanhowar, V. Prasad and D. A. Weitz, *Langmuir*, 2000, **16**, 347-351.
14. K. C. van Dijke, K. C. G. P. H. Schroën and R. M. Boom, *Langmuir*, 2008, **24**, 10107-10115.
15. I. Kobayashi, S. Mukataka and M. Nakajima, *Langmuir*, 2005, **21**, 5722-5730.
16. S. Sugiura, M. Nakajima, T. Oda, M. Satake and M. Seki, *J. Colloid Interface Sci.*, 2004, **269**, 178-185.
17. I. Kobayashi, S. Mukataka and M. Nakajima, *Langmuir*, 2004, **20**, 9868-9877.
18. I. Kobayashi, M. Nakajima, H. Nabetani, Y. Kikuchi, A. Shohnno and K. Satoh, *J. Am. Oil Chem. Soc.*, 2001, **78**, 797-802.
19. T. Kawakatsu, G. Trägårdh, Y. Kikuchi, M. Nakajima, H. Komori and T. Yonemoto, *J. Surfactants Deterg.*, 2000, **3**, 295-302.
20. S. Sugiura, M. Nakajima and M. Seki, *Ind. Eng. Chem. Res.*, 2002, **41**, 4043-4047.
21. H. Liu, M. Nakajima, T. Nishi and T. Kimura, *Eur. J. Lipid Sci. Technol.*, 2005, **107**, 481-487.
22. G. T. Vladislavljević, I. Kobayashi and M. Nakajima, *Powder Technol*, 2008, **183**, 37-45.
23. G. T. Vladislavljević, I. Kobayashi and M. Nakajima, *Microfluid Nanofluid*, 2010, DOI 10.1007/s10404-010-0750-9.
24. H. Liu, M. Nakajima and T. Kimura, *J. Am. Oil Chem. Soc.*, 2004, **81**, 705-711.
25. S. Sugiura, M. Nakajima, N. Kumazawa, S. Iwamoto and M. Seki, *J. Phys. Chem. B*, 2002, **106**, 9405-9409.
26. K. C. van Dijke, I. Kobayashi, K. Schroën, K. Uemura, M. Nakajima and R. M. Boom, *Microfluid Nanofluid*, 2010, **9**, 77-85.
27. T. Kawakatsu, G. Trägårdh, C. Trägårdh, M. Nakajima, N. Oda and T. Yonemoto, *Colloid Surface A*, 2001, **179**, 29-37.
28. S. M. Joscelyne and G. Trägårdh, *J. Membr. Sci.*, 2000, **169**, 107-117.

29. Y. C. Tan, V. Cristini and A. P. Lee, *Sensor Actuat B-Chem*, 2006, **114**, 350-356.
30. S. L. Anna, N. Bontoux and H. A. Stone, *Appl. Phys. Lett.*, 2003, **82**, 364-366.
31. Y. C. Tan, J. S. Fisher, A. I. Lee, V. Cristini and A. P. Lee, *Lab Chip*, 2004, **4**, 292-298.
32. I. Kobayashi, M. Nakajima and S. Mukataka, *Colloid Surface A*, 2003, **229**, 33-41.
33. M. Saito, L. J. Yin, I. Kobayashi and M. Nakajima, *Food Hydrocolloid*, 2005, **19**, 745-751.
34. K. B. Fujiu, I. Kobayashi, K. Uemura and M. Nakajima, *Microfluid Nanofluid*, 2010, DOI 10.1007/s10404-010-0708-y.
35. S. Sugiura, M. Nakajima, H. Itou and M. Seki, *Macromolecular Rapid Communications*, 2001, **22**, 773-778.
36. J. Tong, M. Nakajima and H. Nabetani, *Eur. J. Lipid Sci. Technol.*, 2002, **104**, 216-221.
37. I. Kobayashi, T. Takano, R. Maeda, Y. Wada, K. Uemura and M. Nakajima, *Microfluid Nanofluid*, 2008, **4**, 167-177.
38. I. Kobayashi, S. Hirose, T. Katoh, Y. Zhang, K. Uemura and M. Nakajima, *Microsyst Technol*, 2008, **14**, 1349-1357.
39. A. Arafat, M. Giesbers, M. Rosso, E. J. R. Sudholter, K. Schroën, R. G. White, L. Yang, M. R. Linford and H. Zuilhof, *Langmuir*, 2007, **23**, 6233-6244.
40. A. Arafat, K. Schroën, L. C. P. M. de Smet, E. J. R. Sudholter and H. Zuilhof, *J. Am. Chem. Soc.*, 2004, **126**, 8600-8601.
41. M. Rosso, M. Giesbers, A. Arafat, K. Schroën and H. Zuilhof, *Langmuir*, 2009, **25**, 2172-2180.
42. H. Liu, M. Nakajima, T. Nishi and T. Kimura, *Nippon Shokuhin Kagaku Kogaku Kaishi*, 2005, **52**, 599-604.
43. S. Sugiura, M. Nakajima, J. Tong, H. Nabetani and M. Seki, *J. Colloid Interface Sci.*, 2000, **227**, 95-103.
44. I. H. Huisman, G. Trägårdh, C. Trägårdh and A. Pihlajamäki, *J. Membr. Sci.*, 1998, **147**, 187-194.
45. K. Nakagawa, S. Iwamoto, M. Nakajima, A. Shono and K. Satoh, *J. Colloid Interface Sci.*, 2004, **278**, 198-205.
46. S. van der Graaf, C. G. P. H. Schroën and R. M. Boom, *J. Membr. Sci.*, 2005, **251**, 7-15.
47. I. Kobayashi, X. Lou, S. Mukataka and M. Nakajima, *J. Am. Oil Chem. Soc.*, 2005, **82**, 65-71.
48. S. Sugiura, M. Nakajima, K. Yamamoto, S. Iwamoto, T. Oda, M. Satake and M. Seki, *J. Colloid Interface Sci.*, 2004, **270**, 221-228.
49. T. Kawakatsu, G. Trägårdh and C. Trägårdh, *Colloid Surface A*, 2001, **189**, 257-264.
50. S. E. Friberg and K. Larsson, *Food Emulsions*, Marcel Dekker, Inc (USA), 1997.
51. F. C. Bor and G. J. Calvin, *J Microcolumn Sep*, 1997, **9**, 205-211.
52. J. Tong, M. Nakajima, H. Nabetani and Y. Kikuchi, *J. Surfactants Deterg.*, 2000, **3**, 285-293.
53. R. Arshady, *J. Microencapsulation*, 1993, **10**, 413-435.
54. P. Forssell, R. Partanen and K. Poutanen, *Food Sci. and Tech.*, 2006, **20**, 18-20.
55. P. Vilstrup, *Microencapsulation of food ingredients*, Leatherhead publishing, 2001.

-
56. C. Charcosset, *J Food Eng*, 2009, **92**, 241-249.
 57. S. Iwamoto, K. Nakagawa, S. Sugiura and M. Nakajima, *AAPS PharmSciTech*, 2002, **3(3)**.
 58. M. Neves, H. Ribeiro, I. Kobayashi and M. Nakajima, *Food Biophys*, 2008, **3**, 126-131.
 59. L. M. C. Sagis, R. de Ruiter, F. J. R. Miranda, J. de Ruiter, K. Schroën, A. C. van Aelst, H. Kieft, R. Boom and E. van der Linden, *Langmuir*, 2008, **24**, 1608-1612.
 60. A. J. Abrahamse, R. van Lierop, R. G. M. van der Sman, A. van der Padt and R. M. Boom, *J. Membr. Sci.*, 2002, **204**, 125-137.
 61. K. C. van Dijke, G. Veldhuis, K. Schroen and R. M. Boom, *Lab Chip*, 2009, **9**, 2824-2830.
 62. M. L. J. Steegmans, *Ph.D thesis, Wageningen Uivresity (WUR)* 2009.
 63. I. Lambrich and H. Schubert, *J. Membr. Sci.*, 2005, **257**, 76-84.
 64. I. Kobayashi, Y. Wada, K. Uemura and M. Nakajima, *Microfluid Nanofluid*, 2010, **8**, 255-262.
 65. I. Kobayashi, K. Uemura and M. Nakajima, *Food Biophys*, 2008, **3**, 132-139.
 66. M. Yasuno, S. Sugiura, S. Iwamoto, M. Nakajima, A. Shono and K. Satoh, *AIChE J*, 2004, **50**, 3227-3233.
 67. I. Kobayashi and M. Nakajima, *Eur. J. Lipid Sci. Technol.*, 2002, **104**, 720-727.
 68. I. Kobayashi, S. Mukataka and M. Nakajima, *Ind. Eng. Chem. Res.*, 2005, **44**, 5852-5856.
 69. I. Kobayashi, S. Mukataka and M. Nakajima, *J. Colloid Interface Sci.*, 2004, **279**, 277-280.
 70. G. T. Vladislavljevic, I. Kobayashi and M. Nakajima, *Powder Technol*, 2008, **183**, 37-45.

Chapter 3

Monodispersed Water-in-Oil Emulsions Prepared with Semi-Metal Microfluidic EDGE Systems

This chapter has been published as: Maan, A. A., Schroën, K., Boom, R., 2012. Monodispersed water-in-oil emulsions prepared with semi-metal microfluidic EDGE systems. *Microfluid Nanofluid*, DOI 10.1007/s10404-012-1037-0.

Abstract

Monodispersed water-in-oil emulsions were prepared with EDGE (Edge based Droplet Generation) systems, which generate many droplets simultaneously from one junction. The devices (with plateau height of $1.0\ \mu\text{m}$) were coated with Cu and CuNi having the same hydrophobicity but different surface roughness. Emulsification was performed by using water as dispersed phase and oils with different viscosities (hexadecane, decane, hexane and sunflower oil) as continuous phases; lecithin, PGPR (polyglycerol polyricinoleate) and span80 were used as emulsifiers.

The roughness affected the emulsification behaviour significantly. The smoother Cu surface exhibited droplet formation over the entire length of the droplet formation unit, while the rougher CuNi surface showed non-uniform filling of the plateau and much lower droplet formation frequency.

In spite of this different behaviour, monodispersed droplets ($CV < 10\%$) were produced by both systems (with span80 and PGPR), with a size 6 times the plateau height ($d_{\text{avg}} \approx 6.0\ \mu\text{m}$). The droplet size decreased with increasing viscosity ratio and remained constant above some critical value. The emulsification process was stable over a wider range of pressures as previously found for silicon based systems. The amount of PGPR influenced the pressure stability, but the system could be used effectively, while with lecithin and Span80 the stable pressure range was very small. The pressure and viscosity stability of these semi-metal systems with rough surfaces show that the EDGE system has potential for practical applications, especially since overall productivity is not affected.

1. Introduction

Emulsification is commonly applied in foods, cosmetics, pharmaceutical and chemical industries for the preparation of various high-tech products including (multiple) emulsions, microcapsules, e.g. for ultra sound imaging and encapsulation purposes¹⁻⁴, or microspheres e.g. used as spacers or in gel permeation chromatography (GPC)⁵. For a good overview of products made by emulsification the interested reader is referred through to the review paper by Vladislavljevic and Williams⁶.

The emulsion droplet size and size distribution strongly influence the stability and rheological behaviour^{5,7}. Traditional emulsification techniques (high pressure homogenizers, colloid mills, rotor stator systems) lead to droplet sizes that are rather polydisperse; basically, the occurrence of large droplets needs to be prevented leading to the use of more energy than strictly necessary for the production of monodispersed droplets. Besides, the heat and shear stresses can be detrimental to ingredients (starch, proteins etc.) or prevent their use in emulsion formulation⁸.

In recent years several energy efficient techniques (including membranes and microfluidic devices) have been introduced with the ability to produce monodispersed emulsions⁹. In these techniques droplet formation takes place through shear (membranes, T-, Y-, and cross junctions and flow focussing devices) or a spontaneous mechanism (grooved and straight-through microchannels). Most studied among these techniques are membrane emulsification which was introduced by Nakashima et al.,¹⁰ and microchannel emulsification proposed by the group of Nakajima¹¹. Reviews are available by Charcosset and co-workers⁸ for membrane emulsification, and specifically for pre-mix membrane emulsification by Nazir et al.,¹², and Maan and co-workers¹³ for spontaneous emulsification techniques. The most recent review is by Vladislavljević et al.,¹⁴ who evaluate all droplet formation techniques including T-, Y-, and cross junctions and flow focussing devices.

Membranes can produce droplets at much higher throughputs as compared to microfluidic devices¹⁴. In membrane emulsification, a to-be-dispersed phase is pressed through the pores of a membrane. Droplets are usually sheared-off at the surface and

carried away by a cross flowing continuous phase. The droplet size is controlled by the membrane pore size, the applied shear and the oil flux. Monodispersed emulsions with a coefficient of variation (CV) of around 10% may be produced. However, the technique can only be applied to the preparation of dilute emulsions (<10%) and an increase in dispersed phase fraction through recirculation results in increased polydispersity¹³. Pre-mix membrane emulsification can produce emulsions with high dispersed phase fraction (>50%), monodispersity of resulting emulsions is however much less as compared to direct membrane emulsification¹⁵. In microchannel emulsification, a to-be-dispersed phase is pushed from a side channel into the continuous phase channel through a shallow flat structure (the terrace). The to-be-dispersed phase forms a disc in the wider terrace area. As soon as part of the disc bulges into the larger channel of the continuous phase, the disc can reduce its surface area by splitting off spontaneously and forming a spherical droplet, as a result of Laplace pressure differences¹⁶. Thus droplets are sequentially produced at high monodispersity (CV≈5%) potentially leading to high dispersed phase fraction¹³. Mass parallelization of microchannels (>10⁴ channels on a single chip) worked efficiently for droplets sizes of around 10 μm producing uniform droplets at a dispersed phase flux of 1.5 ml/hr¹⁷. However, up-scaling for droplets <10 μm turned out to be a challenge¹⁸. Pressure gradients in the system and precision fabrication of narrow channels can lead to reduced efficiency (less active channels) and increased polydispersity.

We recently introduced a new emulsification system called EDGE (Edge based Droplet Generation) which is based on Laplace pressure differences similar as described for microchannel emulsification¹⁹. However, with this device multiple monodisperse droplets are generated simultaneously from a single droplet formation unit (DFU), unlike microchannel emulsification in which one droplet is formed at a time from one DFU. An EDGE-system consists of a large flat structure (the plateau) located between a dispersed and a continuous phase channel. Droplet formation through a typical EDGE device is shown in figure 3.1. When pressurized, the dispersed phase flows through the dispersed phase channel and spreads on the plateau. On reaching the edge of the plateau, the dispersed phase forms monodispersed droplets at various locations along the entire length of the edge of the plateau. EDGE emulsification was found to be robust against

fouling, simple in operation and can be successfully scaled-up on chip-level without affecting the monodispersity and efficiency of the system²⁰. It has been successfully applied to the preparation of single (O/W) emulsions, double (W/O/W) emulsions and foams²¹.

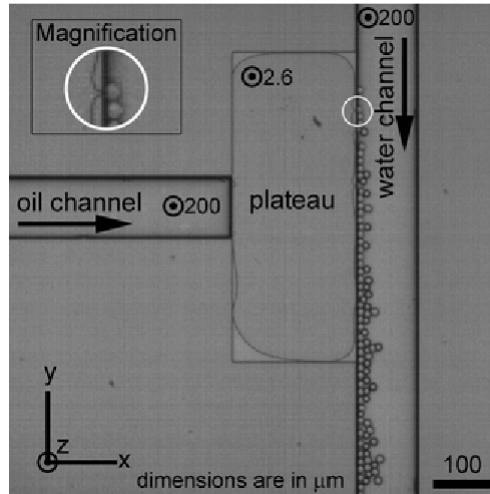


Figure 3.1: Droplet formation through a typical EDGE device (reprinted from van Dijke et al.,¹⁹.)

Until now, all EDGE systems have been in silicon or glass devices, which is not attractive to use in larger, industrial systems. We here explore the use of metal surfaces, as metal devices are preferable for industrial application, due to their resistance to cleaning, insusceptibility to fracture, and well-known surface properties. As a first step towards completely metal chips, we here use semi-metal EDGE chips. Despite the fast development of metal fabrication technology, manufacturing of precisely defined plateaus of micrometre sizes is currently not possible, and besides we need visual observation of droplet formation to compare with previous results obtained with silicon and glass chips. Therefore, we used EDGE systems with metal (Cu and CuNi) coated surfaces to investigate water-in-oil emulsification for droplet sizes $<10 \mu\text{m}$. Monodispersed water-in-oil emulsions are more complex to prepare compared to their oil-in-water counterparts because of surface wettability issues (possibly induced by the surfactants used) and the viscosities of dispersed and continuous phases⁵. We report here on the influence of metal surfaces on the operation of EDGE devices, the process stability and the product quality.

2. Materials and Methods

2.1. Chemicals

MilliQ ultra-pure water was used as dispersed phase. As continuous phases, n-hexadecane ($C_{16}H_{34}$, 99%) from Merck KGaA (Germany), decane ($C_{10}H_{22}$, $\geq 95\%$) from Fluka (Germany), n-hexane (C_6H_{14} , $\geq 97\%$) from Sigma Aldrich (Spain) and sunflower oil purchased from the local supermarket were used. PolyGlycerol PolyRicinoleate (PGPR) (Givaudan, Vernier, Switzerland), Sorbitan monooleate (Span80) (Sigma-Aldrich, Germany) and Alcolac-S Lecithin (American lecithin company, USA) were used as emulsifier. The viscosities of the continuous phases were measured in a rheometer (MCR 301, Anton Paar, Graz, Austria) with couette geometry (DG 26.7). Rate sweeps were performed with shear rates from 2 s^{-1} to 100 s^{-1} at a controlled temperature of $25\text{ }^\circ\text{C}$. Each of the 29 shear rates were applied for a constant time of 5 s. The equilibrium interfacial tensions at hexadecane/water interfaces with different surfactants were measured with a pendant drop method (PAT 1, profile analysis tensiometer, Germany). All the measurements for interfacial tension were performed at $25\text{ }^\circ\text{C}$.

2.2. Chip design

In EDGE systems, the plateau height is the only dimension that determines the droplet size and therefore needs to be precisely defined and maintained to ensure monodispersity. As a first step to fully metal systems, we designed a system in which the plateau consisted of metal, but that allowed observation of droplet formation through a glass cover plate. The microstructures were fabricated on glass plates ($1.5 \times 1.5\text{ cm}$) through wet etching technique (Micronit Microfluidics, Enschede, The Netherlands) with the bottom plate having channels (figure 3.2a) and the top plate engraved with the plateau (figure 3.2b). The channels were $500\text{ }\mu\text{m}$ and $400\text{ }\mu\text{m}$ wide (dispersed and continuous phase channels respectively) and $175\text{ }\mu\text{m}$ deep. Both channels and the plateau area in the bottom plate were coated with Cu or CuNi (300 nm) (indicated by the orange colour in figure 3.2) using standard sputtering technique; the systems are denominated accordingly as EDGE-Cu and EDGE-CuNi. Both plates were bonded together keeping the engraved part of the top (uncoated) glass plate in between the dispersed and continuous

phase channels, thus creating the plateau, with the bottom of the plateau being metallic, and the top being glass to facilitate visual inspection. The plateaus used were having dimensions of $200\ \mu\text{m} \times 1\ \mu\text{m}$ (length \times height) with widths of either $1000\ \mu\text{m}$ or $2000\ \mu\text{m}$.

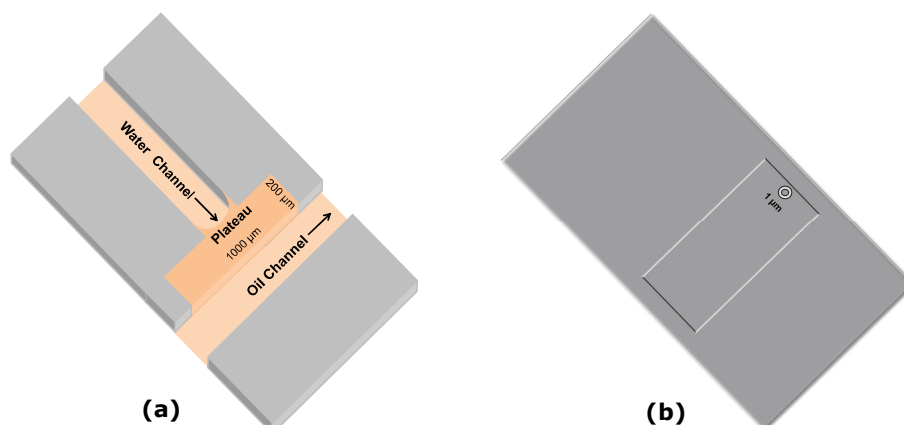


Figure 3.2: Schematic representation of metal EDGE system showing channels etched in the bottom plate (a) and the plateau etched in the top plate (b).

2.3. Experimental set-up

The continuous and dispersed phases were pushed into the respective channels through 0.030" PEEK tubing (Grace Davison Discovery Sciences, Deerfield, IL, USA). The continuous phase was pumped in through a 10mL Hamilton gastight Luer Lock syringe (Bonaduz, Switzerland) placed in a Harvard Apparatus (Holliston, MA, USA) PHD 2000 syringe pump. Typical flow rates for the continuous phase were maintained between 0.2 - 0.5 ml/hr. The dispersed phase was pumped through a pressurized vessel, and a digital pressure controller, controlled with Flowplot V3.25 and FlowView 2 V1.15 software (Bronkhorst, Ruurlo, The Netherlands) was used to set and regulate the applied pressure of the dispersed phase. The microchip was put in a custom made module (Micronit Microfluidics, Enschede, The Netherlands) and placed on the microscope table. The emulsification process was observed with a high-speed camera (motionPro HS-4, Redlake MASD Inc., San Diego, CA, USA) connected to a microscope (Axiovert 200 MAT, Carl Zeiss B. V., Sliedrecht, The Netherlands). The maximum magnification was 2500x and the maximum frame rate was $10,000\ \text{frames s}^{-1}$. The combination of magnification and frame

rate was limited by the amount of light reaching the high-speed camera. Image analysis software (Image Pro plus 4.5) was used to measure droplet size and distribution. Droplet images, used for droplet size and size distribution measurements, were taken near the plateau edge in continuous phase channel.

2.4. Surface characteristics

Roughness: The roughness of the metal coated surfaces was measured using an AFM (Nanoscope Multimode IIIa, Bruker) provided with a standard V-shaped silicon nitride tip (NP, Bruker). The roughness was measured in triplicate for each surface; the given values are the average of these three measurements which were within 1.6 and 3.0 nm (for Cu and CuNi respectively) of each other.

Contact angle: Two flat glass plates were coated separately with Cu and CuNi using a standard sputtering technique (Micronit Microfluidics, The Netherlands). The metal coated and uncoated glass plates (representing the bottom and top of the plateau) were further used for three phase contact angle measurements. The plates were immersed in the continuous oil phase and a drop of water phase of 150 μL was put on the surface. The contact angle was measured in triplicate after the shape of the drop becomes stable; the values mentioned in this paper are always the average of these three measurements that were typically within 2 degrees of each other.

3. Results and discussions

3.1. Surface characteristics

In EDGE systems, the plateau has the highest hydrodynamic flow resistance, and its wettability and topography is expected to greatly affect the behaviour of the dispersed phase on the plateau. For stable emulsification the continuous phase should preferentially wet the surface; hence the surface should be hydrophilic for o/w emulsification and hydrophobic for w/o emulsification (in our case contact angles should be $>90^\circ$). Three phase contact angles were measured for water droplets on surfaces dipped into hexadecane containing 2.5% (wt./vol.) PGPR. In a later section (3.5) we will discuss the influence of the surfactant type and concentration in detail.

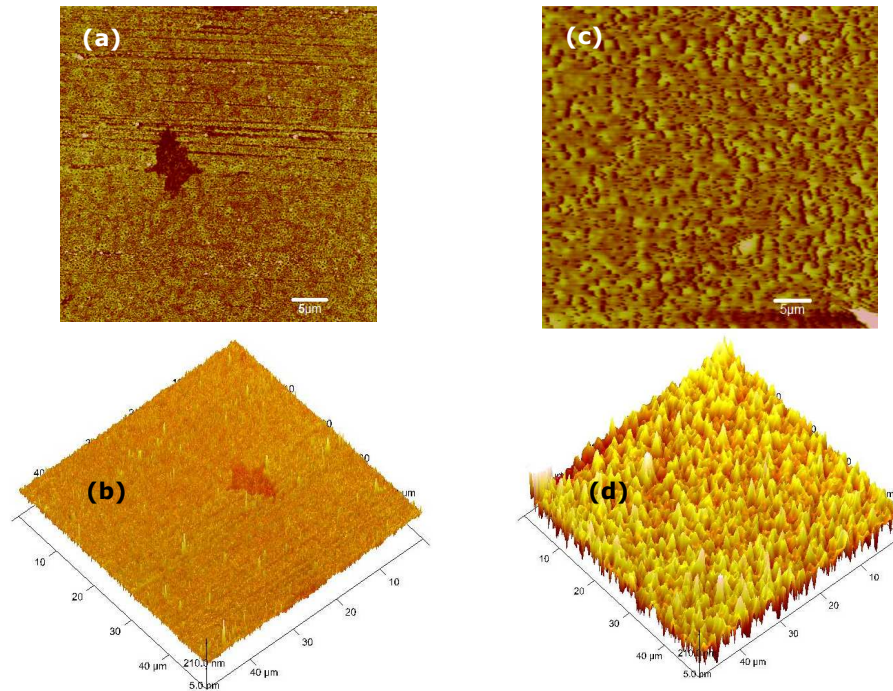


Figure 3.3: AFM images showing grain size and resulting surface roughness of the plateau in EDGE-Cu (a & b) and EDGE-CuNi (c & d)

Table 3.1 shows that all surfaces are equally hydrophobic ($>90^\circ$) and thus suitable for w/o emulsification. The root mean square roughness of both the surfaces as measured by AFM showed that the CuNi surface is clearly rougher than the Cu surface. The surface roughness of thin metal films is related to the grain size and increases with increasing grain size²², as is illustrated in the AFM images shown in figure 3.3; with Cu having the smaller grain size.

Table 3.1: Surface characteristics of Cu and CuNi surfaces.

Surface type	Contact angle ($^\circ$)	Root mean square surface roughness (nm)
Cu	151 ± 2	12 ± 1.5
CuNi	151 ± 2	61 ± 3.0
Glass	150 ± 2	6.0 ± 1.0

3.2. Description of plateau invasion and droplet formation

When using hexadecane containing PGPR (2.5 wt./vol. %) in the EDGE chips, this liquid was first pumped through the continuous phase channel, which leads to hexadecane being present on the plateau (1000 μm wide). Subsequently, the pressure on the to-be-dispersed phase was gradually increased and the respective channel was filled with water. The pressure during the entire (EDGE) process was monitored since it gives important information on the behaviour of the plateau. At the so-called invasion pressure, the dispersed phase entered the plateau replacing the hexadecane, and at further increasing pressure the dispersed phase moved towards the edge of the plateau and eventually started making droplets in the continuous phase channel at the breakthrough pressure. Upon further increase of the pressure, the droplet size remained constant over a wide pressure range but eventually increased rapidly at the so-called blow-up pressure, as is also illustrated in figure 3.5a.

Figure 3.4 shows the droplet formation through EDGE-Cu (a) and EDGE-CuNi (b) systems. Water is pushed through the water channel from right to left which flows on the plateau. Droplet formation can be seen along the edge of the plateau in the oil phase. For the EDGE-Cu system, initially the dispersed phase smoothly moved towards the edge generating 2-3 droplet formation points in the middle of the plateau just in front of the dispersed phase channel, at the breakthrough pressure. Upon further increase in pressure the dispersed phase spread towards the ends of the plateau, uniformly covering the whole surface and making droplets along the entire length of the edge. The total number of droplet formation points increased with increasing pressure and just before the blow-up pressure was reached (the pressure at which the system becomes unstable resulting in much larger droplets) 20 droplet formation points were observed. The droplet formation frequency at this pressure was 378 droplets per second (Hz). The droplet formation points were spaced irregularly with distances between points ranging from 10-100 μm . This behaviour was similar to the silicon systems where the points of droplet formation were also irregularly distributed with an interstitial distance of 10-125 μm . Also the frequencies and the total amount of oil that can be emulsified in a specific time through a specific

edge length are similar to those found for the silicon EDGE system (0.30 mL/h·m versus 0.33 mL/h·m for the EDGE-Cu).

In EDGE-CuNi, the dispersed phase after entering the plateau split into separate flow paths, often called ‘fingers’, most probably as a result of the roughness of the plateau as will be discussed at the end of this section. These fingers moved individually in a crisscross pattern and on reaching the edge, each finger generated a droplet formation point. At the breakthrough pressure there was only one droplet formation point along the edge, and by increasing the pressure gradually, the number of droplet formation points could be increased to 5, which were widely spaced (50-150 μm apart) in the middle of the plateau just before the blow-up pressure was reached. The droplet formation frequency at this pressure was 70 Hz which is much lower as compared to EDGE-Cu, as is also reflected in the amount of oil that can be processed with the EDGE-CuNi system (0.04 mL/h·m at most).

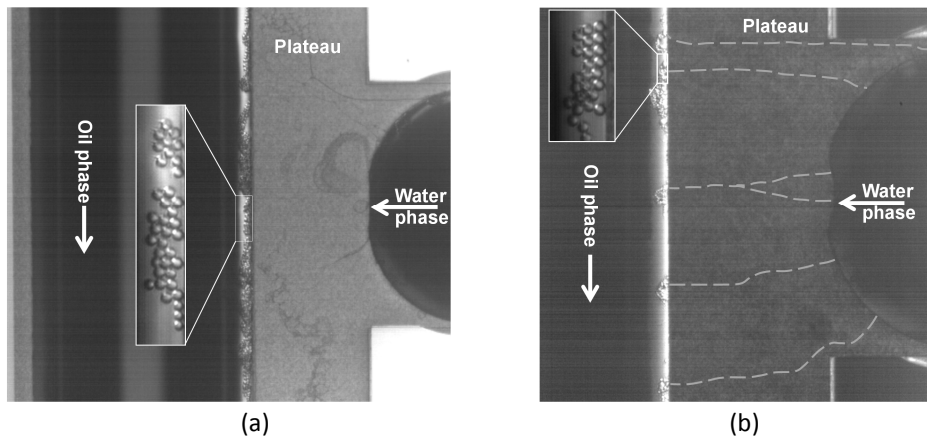


Figure 3.4: Top view of the (a) EDGE-Cu (image taken at 10X magnification) and (b) EDGE-CuNi (image taken at 16X magnification) system showing droplet formation; droplets can be seen in oil phase along the edge of the plateau together with the close-up image of the droplets. Dashed lines in EDGE-CuNi are showing the flow path of the fingers on the plateau. Because of the length of the plateaus, their upper and lower ends are not visible.

Luo and co-workers²³ numerically simulated the flow of two immiscible fluids between parallel plates having undulated surfaces, with the purpose to analyse the effect

of surface roughness on the motion of the fluid flow. They found that the roughness can cause pinning of the contact line as a result of which the contact line moves more slowly as compared to the tip of the (fluid-fluid) interface. This results in the deformation of the interface and fingering of the fluid front, as was seen for the CuNi surface, leading to a reduced droplet formation frequency. As roughness is a relevant factor in practical scaled-up systems, this is an important aspect to take into account for the design of micro systems.

3.3. Effect of the applied pressure on droplet size and size distribution

The minimum pressure required to invade the plateau with dispersed phase and to start the droplet formation can be calculated with Laplace's law given as²⁴:

$$\Delta P_{min} = \sigma \left[\frac{1}{R_1} + \frac{1}{R_2} \right] \cos \theta \quad 3.1$$

Where σ is the interfacial tension, ϑ is the contact angle and R_1 and R_2 are the radii of curvature of the water-oil interface corresponding to the plateau height (R_1) and width (R_2). Figure 3.5 shows the effect of the applied pressure on droplet size and size distributions, when using MilliQ ultra-pure water as dispersed phase and hexadecane with 2.5 % PGPR as continuous phase. In EDGE-Cu, the minimum pressure for droplet formation (breakthrough pressure) was reached at 65 mbar and droplets of 6.2 μm were obtained at this pressure. With increasing pressure, the average droplet size remained constant until the blow-up pressure (200 mbar) was reached. The coefficient of variation (CV) increased slightly with pressure, but remained acceptable (<10%) till blow-up occurred. The maximum droplet formation frequency at which the coefficient of variation was below 5% was 75 Hz. With EDGE-CuNi, the breakthrough pressure was 125 mbar which is a bit higher than with EDGE-Cu. Size of the droplets produced at this pressure was 4 μm , which is smaller as compared to the droplets produced by EDGE-Cu, but this size seems to be related to a very narrow pressure range since upon further increase of pressure the droplet size increased to 5.5 μm and remained constant throughout the pressure range until blow-up (250 mbar) occurred. With the EDGE-CuNi system the CV increased slightly with pressure but remained below 10% as long as the operating pressure remained below the blow-up pressure. Above the blow-up pressure, in both EDGE-Cu and EDGE-CuNi

systems, droplets of 25-30 μm were produced at some of the droplet formation points which led to a sudden increase of the average droplet size and the polydispersity ($\text{CV} > 40\%$).

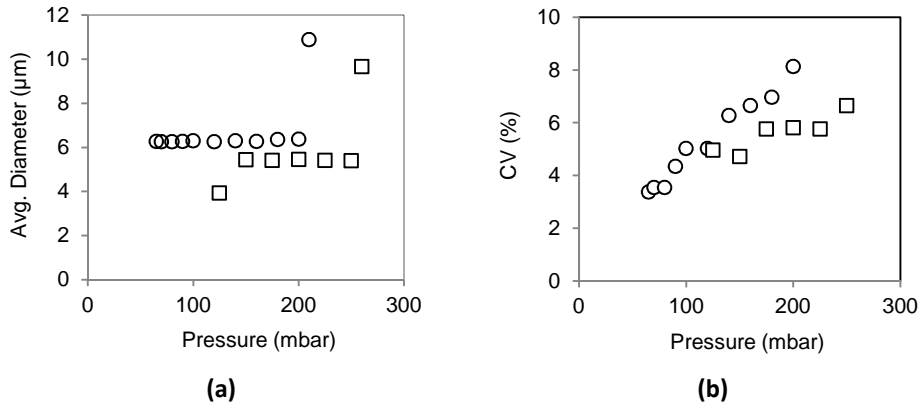


Figure 3.5: Effect of applied pressure on droplet size and size distributions for EDGE-Cu (o) and EDGE-CuNi (\square); the continuous phase was hexadecane with 2.5 % PGPR, the droplet phase was water.

The small difference in size (5.5 versus 6.2 μm) compared to the Cu system is most probably due to a small variation in plateau height, which could also partially explain the difference in the observed invasion pressure (see Laplace equation, variation of R_1), albeit not completely. We expect that the roughness of the systems influences the largest curvature in the Laplace equation (as is also reflected in the fingering behaviour), and that the value of R_2 is no longer the plateau width as could be assumed for the silicon systems that are virtually flat, but attains a lower value, therewith effectively increasing the invasion pressure. The finger formation is also related to the difference in blow-up pressure; with the finger length effectively adding to the total resistance in the system, which is known to increase the pressure range of microchannel emulsification systems²⁵. Finally, the roughness itself may add to the flow resistance on the plateau.

For our further investigations on viscosity effects and aspects related to surfactants, we used EDGE-Cu (2000 μm wide) based on its better performance regarding the plateau filling and overall productivity.

3.4. Effect of viscosity ratio

In silicon based EDGE systems, the droplet size is known to be a function of the viscosity ratio for oil-in-water emulsification, with a stable droplet size at high ratio of the viscosities of the dispersed and continuous phases. Water-in-oil emulsification therefore implies that we operate in the non-stable operation range of the EDGE systems, and thus the effect of viscosity ratio ($\xi = \eta_d/\eta_c$) needs to be investigated. We used water as dispersed phase with continuous phases (sunflower oil, hexane, decane, and hexadecane, each with 2.5% PGPR) having different viscosities (see table 3.2). Figure 3.6 shows the effect of the viscosity ratio on the average droplet sizes; as a comparison results by van Dijke and co-workers²⁴ are shown for oil-in-water emulsification (both CFD and measured values) with silicon based EDGE systems.

Table 3.2: Ratio of viscosity of dispersed water phase to different continuous oil phases

Dispersed phase	Viscosity (mPas)	Viscosity ratio ($\xi = \eta_d/\eta_c$)
Sunflower oil	49	0.02
Hexadecane	2.32	0.43
Decane	0.92	1.08
Hexane	0.29	3.40

Above a certain critical value (ξ_{crit}), the droplet size was not affected by the viscosity ratio and remained constant, as was also found for oil-in-water emulsification (van Dijke et al.,²⁴). Below ξ_{crit} , the droplet size increased with decreasing viscosity ratio. Kawakatsu et al.,²⁶ mentioned for a microchannel emulsification system, that a higher continuous phase viscosity delays the detachment of the droplet which results in more dispersed phase supplied during droplet formation and hence a larger droplet. Van Dijke et al.,²⁷ explained the effect of viscosity ratio on microchannel emulsification through CFD simulations and found that a higher viscosity of the continuous phase hinders the flow of that phase into the microchannel, which results in a lower pressure in the dispersed phase, which facilitates further growth of the droplets. Given the viscosity ratios used in

water-in-oil emulsification, we assume that similar phenomena occurs in EDGE-Cu systems.

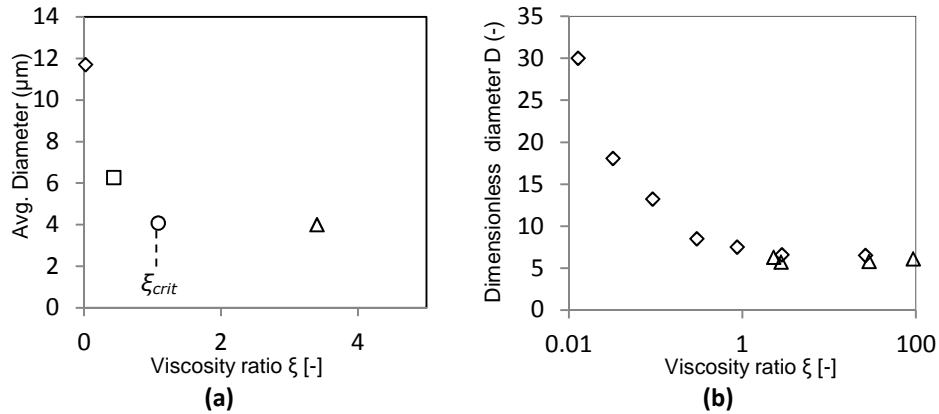


Figure 3.6: Effect of viscosity ratio on average droplet size in (a) EDGE-Cu using (◇) sunflower oil, (□) hexadecane, (○) decane and (Δ) hexane and (b) EDGE-silicon²⁴ with (◇) CFD and (Δ) measured values.

3.4. Effect of surfactants

The results presented until now have been obtained with surfactants that were used at concentrations that are appropriate for droplet formation; however their type and concentration strongly influence the droplet formation.

We first tried to analyse the emulsification behaviour without any surfactant in the continuous phase by pushing water into pure hexadecane. Water flowed continuously into hexadecane, albeit without forming any droplets. This shows that surfactant is required to keep the plateau wetted with the continuous phase.

Next, the effect of type of surfactants on emulsification was investigated with three different surfactants, PGPR, lecithin and span80 and their performance was compared. As a starting point, 2.5 (wt./vol.)% of each of these surfactants was dissolved in hexadecane; the obtained average droplet size and CV are shown in figure 3.7. With all three surfactants, the dispersed phase spread uniformly over the plateau and active droplet formation was observed at several locations along the plateau edge. The invasion

pressure is a function of the contact angle (which is virtually the same as shown in Table 3.3) and the interfacial tension (which is different for the three surfactants). Both PGPR and Span80 have low interfacial tensions, and have low invasion pressures, while with lecithin the invasion pressure is higher. It is expected that depending on the dynamic behaviour of the surfactants, the static interfacial tension mentioned in Table 3.3 can be the actual interfacial tension value at invasion pressure (very fast surfactant diffusion) or it may be higher as is expected for slow surfactant diffusion.

The differences in invasion pressure are expected to represent this dynamic behaviour, leading to larger differences in invasion pressures as expected from the static values only. Initially, the average droplet size was almost the same (at the respective breakthrough pressures) for all the surfactants and remained constant with increasing pressure. Emulsions produced by PGPR were uniform with CV increasing slightly and remaining below 10 % until blow-up pressure was reached. However, with especially lecithin and to a lesser extent with span80 the CV increased rapidly and polydispersity was observed soon after the breakthrough pressure was exceeded. This is related to surfactant interaction with the surface, which gives the plateau different wettability, resulting in irregular droplet formation. Clearly, the surfactant needs to be chosen with care, or alternatively, the surface should repel the surfactant that needs to be used. Since the PGPR emulsion systems showed good stability, they were analysed further. The PGPR concentration was varied (0.1-4 (wt./vol.) %). Figure 3.8 shows the effect of PGPR concentration on average droplet size, CV and pressure stability.

Complete wetting and continuous outflow was observed with 0.1 % PGPR, as was also the case with pure hexadecane. Droplet formation started at a concentration of 0.25%, giving a droplet size and CV of 7.2 μm and 20% respectively, indicating that droplet formation was not completely stable under these conditions. This was also reflected in very small pressure difference between the breakthrough pressure and the blow-up pressure.

Table 3.3: Water/hexadecane interfacial tensions and contact angles of water with Cu surface dipped in hexadecane with different surfactants.

Type of surfactants	Contact angle ($^{\circ}$)	Interfacial tensions (mN/m)
No surfactant	156 ± 2	52^a
PGPR	151 ± 2	3.3
Span80	152 ± 2	3.1
Lecithin	140 ± 3	4.3

a = ref. 28

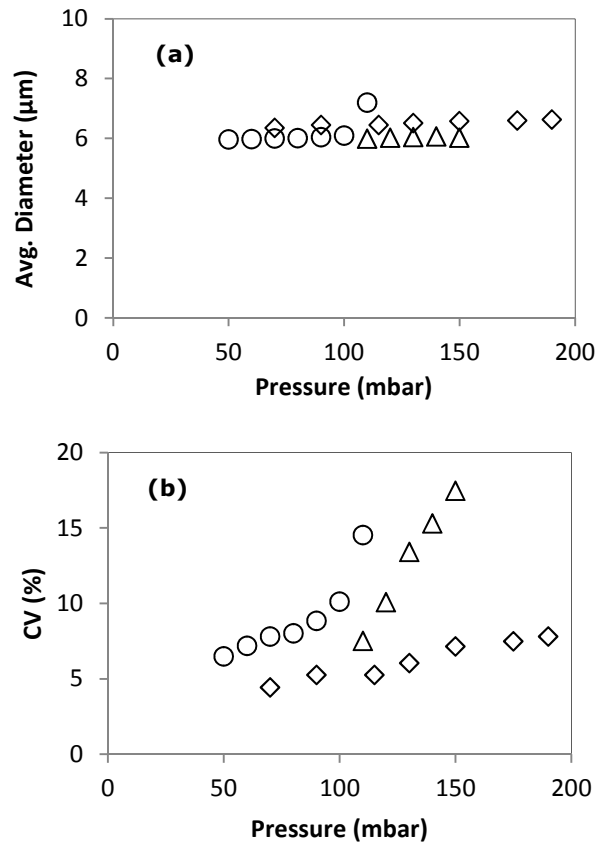


Figure 3.7: Effect of surfactant (span80 (o), PGPR (\diamond) and lecithin (Δ)) on average droplet size (a) and size distribution (b).

By increasing the surfactant concentrations, both the droplet size and the CV decreased. Above 2% PGPR concentration, the droplet size became constant at 6.1 μm and monodispersed emulsions with $\text{CV} < 10\%$ were produced. With increasing PGPR concentrations the breakthrough pressure decreased while the blow-up pressure first decreased

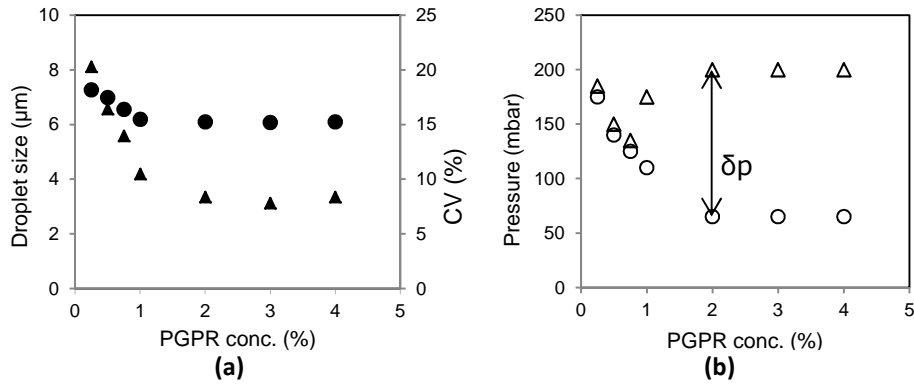


Figure 3.8: Effect of PGPR concentrations on average droplet size (\bullet), CV (\blacktriangle), breakthrough pressure (\circ) and blow-up pressure (Δ).

and then increased again, which could be due to surfactant surface interactions. At low concentration, the surface is not covered with surfactant, and the contact angle is higher than reported for the system with surfactant (see Table 3.1), leading to higher invasion pressures. The blow-up pressure is also influenced by the amount of surfactant (both on the solid surface and the liquid/liquid interface), since this determines how easily the liquid can flow over the surface, and may even allow liquid to move into 'rougher' areas. We expect this to be the case in the first part of the curve where the blow-up pressure becomes lower as function of the PGPR concentration. At higher concentrations, the solid surface is fully covered; however, the concentration in the liquid/liquid interface at the point of droplet formation will remain higher during expansion of the neck that keeps the droplet connected to the plateau, therewith facilitating droplet formation also at higher pressures.

Above 2% concentrations, both the breakthrough and blow-up pressures remained unchanged, most probably because of saturation of the solid and liquid/liquid interface. The stable pressure range ($\delta p = \text{blow-up pressure} - \text{breakthrough pressure}$) was

appreciable above 2% PGPR (140 mbar). Below 2% PGPR the stable pressure range decreased and below 1% it became very narrow, which limits the formulation that can be successfully emulsified.

4. Conclusion

Monodispersed water-in-oil emulsions were successfully prepared using semi-metal microfluidic EDGE systems. Cu and CuNi surfaces with similar hydrophobicity but different surface roughness were investigated, and emulsification behaviour was significantly affected by surface roughness. EDGE-Cu, with comparatively smooth surface, was uniformly filled with the dispersed phase and droplets were formed along the entire length of the plateau. The total productivity of EDGE-Cu was similar to that observed for silicon systems, which compared to the current systems are virtually flat. The EDGE-CuNi system with rougher surface did not exhibit uniform filling of the plateau resulting in lower droplet formation frequency. Both the systems produced monodispersed droplets and the emulsification was stable over a wide range of pressures. Only PGPR could produce uniform emulsions until the blow-up pressure was reached, while with lecithin and span80 polydispersity was observed slightly above the breakthrough pressure. The concentration of PGPR influenced the pressure stability of the system, however (above 2% concentration) the system could be used affectively. The EDGE process was affected by the viscosity ratio (η_d/η_c) even though the droplet size was stable over a wide range of viscosities. The viscosity and pressure stability of these semi-metal systems shows that translation of the systems into metal devices is promising and through the roughness may even improve their performance relative to the silicon based devices.

References

1. H. Sawalha, N. Purwanti, A. Rinzema, K. Schroën and R. Boom, *J. Membr. Sci.*, 2008, **310**, 484-493.
2. H. Sawalha, Y. Fan, K. Schroën and R. Boom, *J. Membr. Sci.*, 2008, **325**, 665-671.
3. L. M. C. Sagis, R. de Ruiter, F. J. R. Miranda, J. de Ruiter, K. Schroen, A. C. van Aelst, H. Kieft, R. Boom and E. van der Linden, *Langmuir*, 2008, **24**, 1608-1612.
4. F. J. Rossier-Miranda, K. Schroën and R. Boom, *Langmuir*, 2010, **26**, 19106-19113.
5. C.-J. Cheng, L.-Y. Chu and R. Xie, *J. Colloid Interface Sci.*, 2006, **300**, 375-382.
6. G. T. Vladislavljević and R. A. Williams, *Advances in Colloid and Interface Science*, 2005, **113**, 1-20.
7. S. Sugiura, M. Nakajima and M. Seki, *Langmuir*, 2002, **18**, 5708-5712.
8. C. Charcosset, I. Limayem and H. Fessi, *J Chem Technol Biot*, 2004, **79**, 209-218.
9. I. Lambrich and H. Schubert, *J. Membr. Sci.*, 2005, **257**, 76-84.
10. T. Nakashima, M. Shimizu and M. Kukizaki, *Key Eng. Mater.*, 1991, **61/62**, 513.
11. T. Kawakatsu, Y. Kikuchi and M. Nakajima, *J. Am. Oil Chem. Soc.*, 1997, **74**, 317-321.
12. A. Nazir, K. Schroën and R. Boom, *J. Membr. Sci.*, 2010, **362**, 1-11.
13. A. A. Maan, K. Schroën and R. Boom, *J Food Eng*, 2011, **107**, 334-346.
14. G. Vladislavljević, I. Kobayashi and M. Nakajima, *Microfluid Nanofluid*, 2012, DOI 10.1007/s10404-012-0948-0.
15. G. T. Vladislavljević, M. Shimizu and T. Nakashima, *J. Membr. Sci.*, 2004, **244**, 97-106.
16. S. Sugiura, M. Nakajima, S. Iwamoto and M. Seki, *Langmuir*, 2001, **17**, 5562-5566.
17. I. Kobayashi, Y. Wada, K. Uemura and M. Nakajima, *Microfluid Nanofluid*, 2010, **8**, 255-262.
18. I. Kobayashi, T. Takano, R. Maeda, Y. Wada, K. Uemura and M. Nakajima, *Microfluid Nanofluid*, 2008, **4**, 167-177.
19. K. C. van Dijke, G. Veldhuis, K. Schroën and R. M. Boom, *AIChE Journal*, 2010, **56**, 833-836.
20. K. C. van Dijke, G. Veldhuis, K. Schroen and R. M. Boom, *Lab Chip*, 2009, **9**, 2824-2830.
21. K. C. van Dijke, K. Schroën, A. van der Padt and R. M. Boom, *J Food Eng*, 2010, **97**, 348-354.
22. F. Meng and F. Lu, *Journal of Alloys and Compounds*, 2010, **501**, 154-158.
23. X. Luo, X.-P. Wang, T. Qian and P. Sheng, *Solid State Communications*, 2006, **139**, 623-629.
24. K. C. van Dijke, R. de Ruiter, K. Schroën and R. M. Boom, *Soft Matter*, 2010, **6**, 321-330.
25. K. C. van Dijke, K. C. G. P. H. Schroën and R. M. Boom, *Langmuir*, 2008, **24**, 10107-10115.
26. T. Kawakatsu, G. Trägårdh, C. Trägårdh, M. Nakajima, N. Oda and T. Yonemoto, *Colloid Surface A*, 2001, **179**, 29-37.
27. K. C. van Dijke, I. Kobayashi, K. Schroën, K. Uemura, M. Nakajima and R. M. Boom, *Microfluid Nanofluid*, 2010, **9**, 77-85.

28. H. B. d. Aguiar, A. G. F. d. Beer, M. L. Strader and S. Roke, *J. Am. Chem. Soc.*, 2010, **132**, 2122-2123.

Chapter 4

Preparation of Monodispersed Oil-in- Water Emulsions through Semi-Metal Microfluidic EDGE Systems

This chapter has been published as: Maan, A. A., Boom, R., Schroën, K. 2012. Preparation of monodispersed oil-in-water emulsions through semi-metal microfluidic EDGE systems. *Microfluid Nanofluid*, DOI DOI 10.1007/s10404-012-1097-1.

Abstract

EDGE (Edge based Droplet Generation) emulsification systems with the ability to produce multiple droplets simultaneously from a single nozzle, were used for the preparation of monodispersed oil-in-water emulsions. The devices (with plateau height of 1 μm) were coated with metals (Cu, CuNi and CuNi/Cu) and had different surface roughness and wettability properties. This influenced the emulsification behavior significantly. The large surface roughness of the CuNi/Cu coated system resulted in stronger non-uniform filling of the plateau compared to the smoother surfaces of Cu and less rough CuNi, and less droplet formation points in the CuNi/Cu coated system relative to the Cu and CuNi systems. The less hydrophilic CuNi surface however provided wider pressure stability than the more hydrophilic Cu and CuNi/Cu surface. A narrower pressure stability (Cu surface) and lower number of droplet formation points (CuNi/Cu surface) resulted in lower overall droplet formation frequency compared to CuNi system. All metal coated EDGE systems reliably produced monodispersed droplets (with sizes being 6 times the plateau height), similar to the silicon based EDGE systems having much smoother surfaces. The pressure stability for CuNi coated surfaces was wider while the droplet formation frequency was comparable to that with the silicon system. This indicated that the use of metal is not a limitation in these systems as initially expected, but may be used for more robust and productive emulsification systems, which lend themselves well for scale-out to practical productivity rates.

1. Introduction

Emulsions with uniformly dispersed droplets are important in the preparation of for example foods, cosmetics, pharmaceuticals and petrochemicals. Traditional techniques for emulsion preparation (colloid mills, high pressure homogenizers and rotor stator systems) are known for inefficient use of energy, and may negatively influence the product quality by heating and subsection of the product to shear stress, which limits the use of some ingredients (starch, proteins etc.) in emulsion formulation¹. Additionally, the produced emulsions are usually highly polydispersed; droplet sizes range from 1-5 μm for colloidal mills, 0.05-1 μm for high pressure homogenizers and 2-10 μm for blenders, with coefficients of variation (CV) approaching 40%^{2, 3}. This induces an increasing demand for systems which can provide a better control over droplet size and can produce emulsions using less energy.

Several microfluidic systems have been introduced in recent years which are able to produce uniformly sized droplets using much less energy as compared to the traditional emulsification systems⁴. Most common examples are T-, Y- junctions, flow focussing devices and microchannels, all using different droplet formation mechanisms. In T- and Y-junctions, a cross flowing continuous phase is used to shear off a droplet growing from a narrow pore through which the disperse phase is pushed⁵⁻⁷. In flow-focusing devices both the phases flow in the same direction with continuous phase flowing at much higher speed which causes longitudinal extension of the droplet resulting in droplet breakup^{8, 9}. Droplet formation in microchannels takes place through a spontaneous mechanism driven by Laplace pressure differences^{3, 10}.

All mentioned systems are single droplet formation techniques (droplets are produced sequentially from one droplet formation unit) and produce highly monodispersed emulsions (CV<10%)¹¹. Their single-nozzle productivity is not sufficient to be appropriate for large scale applications, while scale-up of these systems through mass parallelization (especially for narrow structures meant to produce droplets of sizes less than 10 μm) is a challenge because of the difficulties related to the flow control of phases, fabrication inaccuracies and pressure gradients resulting in low working efficiency^{12, 13}.

We have recently introduced a new droplet formation technique called EDGE (Edge-based Droplet Generation) which enables us to produce multiple monodispersed droplets concurrently from a single droplet formation unit (DFU)¹². An EDGE DFU is a wide and flat cavity called a plateau situated in between an oil channel and a continuous phase channel. Droplet formation from a typical silicon-based EDGE device is shown in figure 4.1. The dispersed phase is pressurized through the dispersed phase channel, spreads over the plateau and on reaching the edge of the plateau it spontaneously forms monodispersed droplets at several locations along the entire length of the plateau. The size of the droplets is determined by the height of the plateau: a scaling factor of 6-8 has been observed. Single emulsions (O/W), double emulsions (W/O/W) and foams have been successfully prepared through EDGE emulsification¹⁴. The technique is simple in operation, stable within a reasonable pressure range and can easily and robustly be scaled-up¹¹.

Several construction materials have been employed in the preparation of microfluidic devices; e.g. glass¹⁵⁻¹⁷, silicon^{12, 18} and polymer¹⁹⁻²¹ have been reported, but metals, being the preferred materials for industries, are still lacking in literature. Tong and his co-workers²² have claimed the preparation of o/w microspheres using stainless steel microchannels. Microchannels with uniform dimensions could not be fabricated because of multicrystal property of stainless steel. Droplets produced from individual channels were monodispersed, however, they did not report on the effects of metal surface characteristics on emulsification behaviour.

In the current study, we move the EDGE technology a step forward by using chips that have metallic surfaces (Cu and CuNi) and use them for the preparation of O/W emulsions with droplets of sizes <10 μm . The most important aspects which need to be considered are surface wettability and surface roughness, and to investigate these aspects before moving to a completely metal systems, we decided to use metal coated surfaces as a first step, and use that in combination with a glass cover plate to allow visual observation. We chose to use Cu and CuNi because these metals have been employed successfully in chips before, and we expect that changes in wettability and roughness will occur. We see this as first step toward stainless steel which is the preferred option for industry, but for which application in chips is still a challenge. We report here on the

pressure stability of the semi-metal chips, the number of droplet formation points, and the droplet formation frequency in relation to surface properties (topography and wettability), and compare their behaviour to 'standard' silicon EDGE chips.

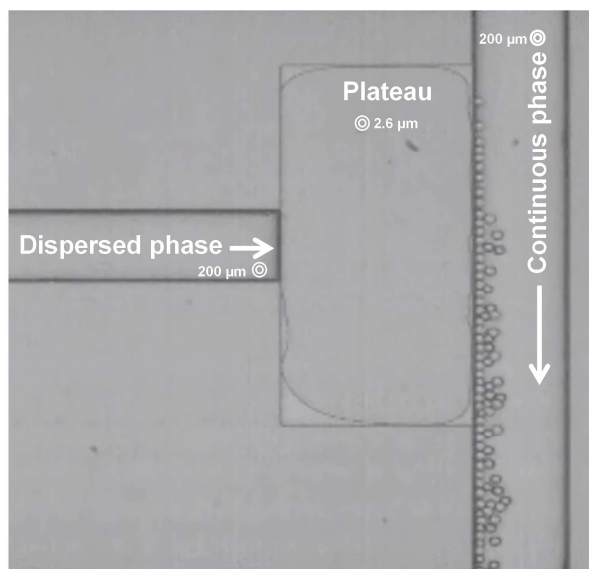


Figure 4.1: Droplet formation through a typical EDGE device (reprinted from van Dijke et al.¹²).

2. Materials and Methods

2.1. Chemicals

n-Hexadecane ($C_{16}H_{34}$, 99%) from Merck KGaA (Germany) was used as dispersed phase. MilliQ ultra-pure water with 0.5 % (wt./vol.) sodium dodecyl sulphate (SDS) from Sigma-Aldrich (Japan) was used as the continuous phase. The viscosities of the dispersed and continuous phases were 3.34 and 1.00 mPas respectively, and were measured using a rheometer (MCR 301, Anton Paar, Gran, Austria) with couette geometry. Rate sweeps were performed with shear rates from 2 to 100 s^{-1} at a controlled temperature of 20 °C. Each of the 29 shear rates were applied for a constant time of 5s.

2.2. Chip design

Construction of metal EDGE systems with precisely defined plateaus of micrometer size is currently not possible because of limitations in the precision of metal fabrication, even though the technology progresses fast. Therefore, to proceed with metal surfaces we designed a system in which the plateau and the channels consisted of metals and were covered by a glass plate to allow the visual observation of droplet formation. The microstructures were fabricated on glass plates (1.5×1.5 cm) through a wet etching technique (Micronit Microfluidics, Enschede, The Netherlands) with a bottom plate having the supply channels (figure 4.2a) and the top plate carved with the plateau (figure 4.2b). The supply channels (with depth of $175 \mu\text{m}$ and width of $500 \mu\text{m}$ and $400 \mu\text{m}$ for dispersed and continuous phase channels respectively) and the area specified for the plateau (in between the channels) were coated with Cu (300 nm), CuNi (300 nm) or CuNi/Cu (with 200 nm of Cu deposited on 100 nm seed layer of CuNi) using standard sputtering technique, as indicated by the orange color in figure 4.2.

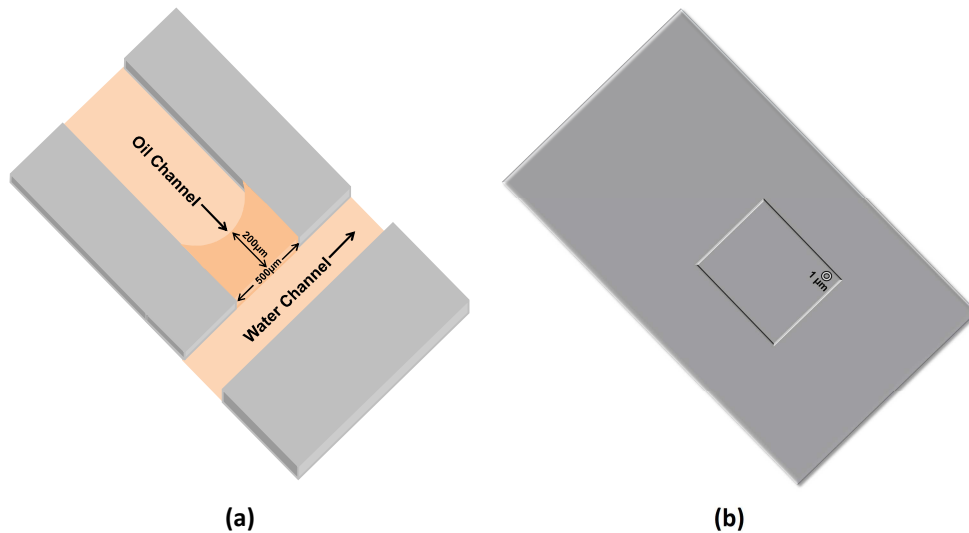


Figure 4.2: Schematic representation of semi-metal EDGE system with channels in the bottom plate (a) and the plateau in the top plate (b).

The systems were defined accordingly as EDGE-Cu, EDGE-CuNi and EDGE-CuNi/Cu. Both the plates were bonded together keeping the (engraved) plateau in

between the dispersed and continuous phase channels such that the bottom of the plateau was metal and the top being the glass enabling visual inspection of the emulsification process. The plateaus used in current experiments were 500 μm wide and 1 μm high. The length of the plateaus ranged from 200 μm (in the center) to 300 μm (at the ends). All the chips were oxidized either through annealing (EDGE-CuNi and EDGE-CuNi/Cu) at high temperature (575 $^{\circ}\text{C}$) or through plasma oxidation (EDGE-Cu) to render their surfaces hydrophilic.

2.3. Experimental procedure

The emulsification process was observed with a high-speed camera (motionPro HS-4, Redlake MASD Inc., San Diego, CA) connected to a microscope (Axiovert 200 MAT, Carl Zeis B. V., Sliedrecht, The Netherlands). MotionPro Studio software (Redlake MASD Inc.) was used to control the camera. The maximum magnification was 2500x and maximum frame rate was 10,000 frames s^{-1} . The combination of magnification and frame rate was limited by the amount of light reaching the high-speed camera sensor. The microchip was fixed in a custom made module (Micronit Microfluidics, Enschede, The Netherlands) and was placed on the microscope table. The continuous phase entered the system through 0.030" PEEK tubing (Grace Davison Discovery Sciences, Deerfield, IL) connected to a 10mL Hamilton gastight Luer Lock syringe (Bonaduz, Switzerland) placed in a Harvard Apparatus (Holliston, MA) PHD 2000 syringe pump. Typical flow rates were between 300-1000 $\mu\text{l}/\text{hour}$. The dispersed phase was pumped through PEEK tubing (0.030") connected to a pressurized vessel. A digital pressure controller controlled with Flowplot V3.25 and FlowView 2 V1.15 software (Bronkhorst, Ruurlo, The Netherlands) was used to set and regulate the applied pressure of the dispersed phase. Image analysis software (Image Pro plus 4.5) was used to measure the droplet size and size distribution.

2.4. Surface characteristics

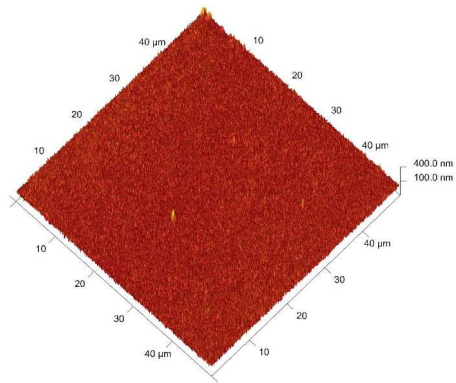
Roughness: The roughness of the metal coated surfaces was measured using an AFM (Nanoscope Multimode IIIa, Bruker) provided with a standard V-shaped silicon nitride tip (NP, Bruker). Triplicate measurements were made for each surface; we report the root mean square roughness values, which are the average of these three measurements.

Contact angle: Since our plateaus consisted of metal at the bottom and glass at the top, contact angles were measured separately for both the metal and glass surfaces. Flat glass plates were coated separately with Cu, CuNi and CuNi/Cu using the standard sputtering technique applied in chip manufacture (Micronit Microfluidics, The Netherlands). For both (metal) coated and uncoated glass plates, the three phase contact angle was measured using contact angle measuring system (G10, KRUSS GmbH, Germany). The plates (annealed or plasma oxidized) were immersed in the continuous water phase containing 0.5 % (wt./vol.) SDS, and a drop of hexadecane was put on the surface. The contact angle was measured in triplicate after the shape of the drop became stable; the mentioned values are always the average of these three measurements.

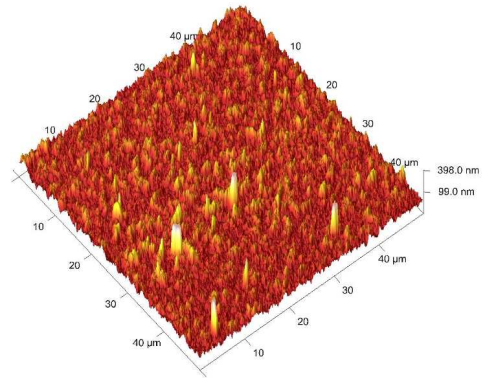
3. Results and discussions

3.1. Surface characteristics

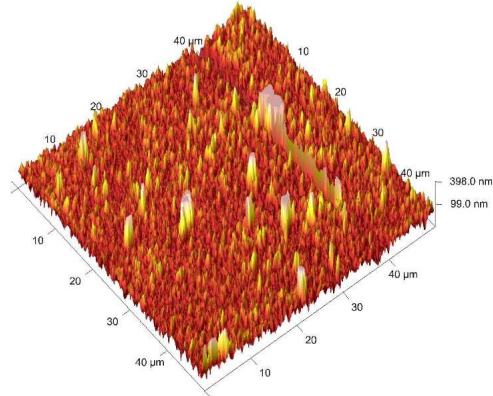
It is expected that topography and wettability of any microfluidic system and especially of the plateau in EDGE systems significantly influence the emulsification behavior. For successful emulsification through microfluidic devices, the continuous phase should preferentially wet the surface implying that the dispersed phase should have a three-phase contact angle of $>90^{\circ}$ ²³⁻²⁵. Kawakatsu et al.,²⁴ investigated the effect of contact angle on w/o emulsification through microchannels and found that stable emulsification was only possible at contact angle of above 120° . We measured three-phase contact angles of oil (hexadecane) droplets on the surfaces dipped into water containing 0.5 % (wt./vol.) SDS (table 4.1). All the surfaces were reasonably hydrophilic (contact angles $\gg 90^{\circ}$, while still showing an appreciable difference in contact angle) and were therefore suitable for O/W emulsification. Figure 4.3 shows the three dimensional surface topography of the metal coated surfaces. The CuNi/Cu is clearly rougher than CuNi which is rougher than Cu; as is also evident from root mean square roughness shown in table 4.1. All the surfaces were quite rough compared to glass (and silicon).



(a)



(b)



(c)

Figure 4.3: Three dimensional surface topography of Cu (a), CuNi (b) and CuNi/Cu (c) surfaces.

Table 4.1: Surface characteristics of silicon, glass and oxidised metal coated surfaces.

Surface type	Contact angle (°)	Surface roughness (nm)
Silicon	155 ^a	- ^b
Glass	160 ± 2	6.0 ± 1.0
Cu	160 ± 2	23 ± 1.0
CuNi	125 ± 2	42 ± 7.5
CuNi/Cu	145 ± 2	65 ± 3.5

a = ref. 26, b = silicon surfaces are virtually atomically flat

3.2. Invasion of the plateau and location of droplet formation points

Water containing 0.5 % (wt./vol.) SDS was first introduced through the respective channel in order to wet the plateau with continuous phase. Subsequently, the pressure on the to-be-dispersed phase was increased to fill the dispersed phase channel with hexadecane. The pressure on the to-be-dispersed phase was then gradually increased throughout the emulsification process and the spread of the dispersed phase onto the plateau was observed as a function of the applied pressure. The dispersed phase entered the plateau at the invasion (Laplace) pressure and with higher pressures started filling up the plateau. On reaching the edge, the dispersed phase started generating monodispersed droplets in the continuous phase at the breakthrough pressure. Figure 4.4 shows the droplet formation in typical EDGE-Cu and EDGE-CuNi/Cu systems. The droplets retained their uniformity with increasing pressure until blow-up pressure was reached. At this pressure, the droplet size increased rapidly at some droplet formation locations, resulting in polydispersed emulsions.

In silicon based EDGE systems (having smoother surfaces), the plateau was uniformly and regularly filled with the dispersed phase, and droplet formation was observed at seemingly regularly spaced droplet generation locations²⁶. Similarly, in EDGE-Cu system, the plateau was also filled almost uniformly with dispersed phase. However, the dispersed phase, upon reaching the edge of the plateau, split into so-called (small)

fingers (distributed throughout the length of the edge) with each finger giving rise to a droplet formation point. Droplet formation points were irregularly spaced with shortest and longest distances between them being 7 and 80 μm respectively.

In the EDGE-CuNi system the dispersed phase, after entering the plateau, moved towards its edge and almost in middle of the plateau it split into separate flow paths giving rise to fingers. Each finger, upon reaching the edge, started functioning as a droplet formation point. Initially, the fingers were unstable i.e. the fingers detached from the rest of the dispersed phase on the plateau, while generating droplets until the entire length of the finger disappeared. Then new fingers arose at approximately the same points. However, at somewhat increased pressures the fingers became stable and stayed connected with the dispersed phase. At the breakthrough pressure only the middle part of the plateau was filled with dispersed phase and droplet formation was observed only there. With increasing pressure the dispersed phase spreads towards the plateau ends; before blow-up pressure was reached the whole plateau was uniformly filled with dispersed phase and droplet formation points were present along the entire length of the edge. A total of 13 irregularly spaced droplet formation points were observed.

In figure 4.5a, the droplet formation points (DFP) are indicated in relation to the lower (-1) and upper (+1) end of the plateau; the lower and upper ends are defined relative to the stage of the microscope. The measurements were repeated with three different chips and total number of droplet formation points were found to be almost same with a variation of ± 1 . In EDGE-CuNi most of the DFPs maintained their locations throughout the applied pressure range, however in some cases, generation of new droplet formation points caused the surrounding DFPs to change their positions. This can be observed at 30 KPa where a DFP (\blacktriangle) was generated and surrounding DFPs adapted to it by slightly changing their positions. Some of the droplet formation points disappeared at some pressure and either completely vanished (\bullet) or re-appeared (\times) at higher pressure. The shortest and longest distances (at blow-up pressure) between droplet formation points (δ_{drop}) were 11 μm and 48 μm respectively.

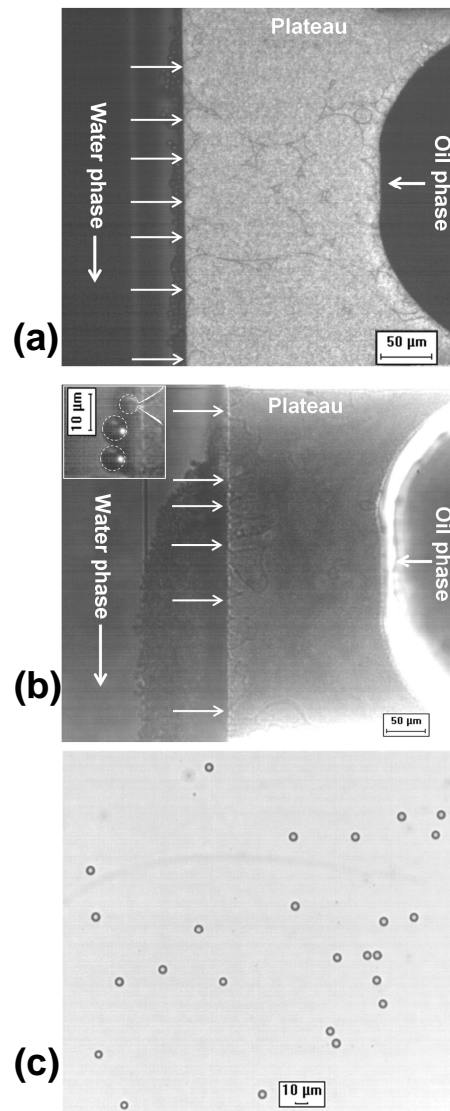


Figure 4.4: Droplet formation through EDGE-Cu (a) and EDGE-CuNi/Cu micro devices (b) with magnification of a droplet formation point in the top left corner. Dispersed phase (oil) is pushed from the dispersed phase channel (right) to the continuous phase (water) channel (left) through the plateau (middle). Disperse phase behavior (fingering) can be seen on the plateau while a clear image of droplets produced by EDGE-CuNi micro devices collected on a glass slide can be seen in figure c.

As mentioned, in the EDGE-CuNi/Cu system, the dispersed phase split into fingers soon after entering the plateau, which was initially not smoothly filled with dispersed phase, widely spaced fingers occurred and droplet formation (at breakthrough pressure) was observed only in middle part of the plateau. At higher pressure, more droplet formation points were formed (as also indicated in figure 4.5b).

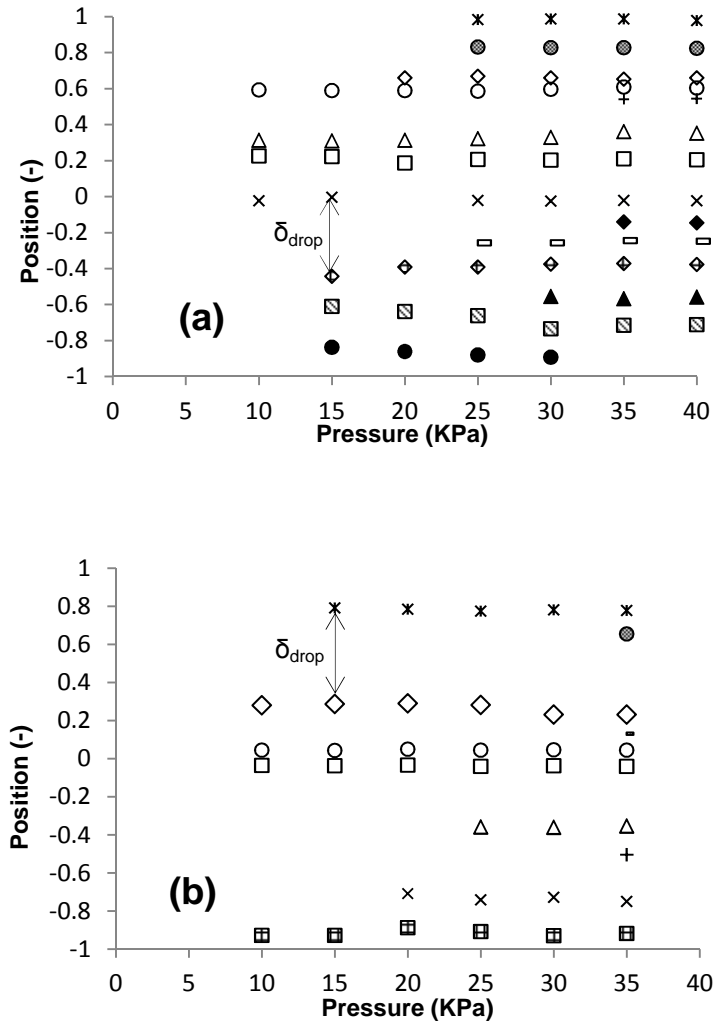


Figure 4.5: Droplet formation positions in EDGE-CuNi (a) and EDGE-CuNi/Cu (b) as a function of applied pressure with -1 and +1 indicating the lower and upper ends of the plateau respectively.

The area covered by the dispersed phase increased while the length of fingers decreased with increasing pressure. At blow-up pressure most of the plateau was uniformly filled with dispersed phase and in total 10 fingers arising from the dispersed phase were making droplets along the edge as can be seen in figure 4.4b.

In the EDGE-CuNi/Cu system the droplet formation points (DFPs), once they appeared, seemed to maintain their positions more than was observed in the EDGE-CuNi system throughout the applied pressure range. The positions did not change when a new DFP was generated in-between two already existing closely spaced DFPs, as can be seen at 35 KPa where a DFP (-) appears between two narrowly spaced DFPs (o) and (\diamond) (figure 4.5b). As mentioned, the total number of DFPs was 10 at maximum pressure with shortest and longest distances between them (δ_{drop}) being 21 μm and 70 μm respectively.

van Dijk et al.²⁶ investigated the droplet formation using silicon based EDGE systems and found that when a new DFP is generated by increasing pressure, all other points adopt to this resulting in a decrease in droplet formation distances and a shift in their positions. The distances between the droplet formation points were found to be scaling with 25x the plateau height. The DFPs were regularly spaced with distances between them being around 29 μm for a plateau height of 1.2 μm . This is different with the semi-metal EDGE chips investigated here: the droplet production seems here more irregular, but still has quite high pressure stability (except EDGE-Cu) and productivity (see section 3.3).

The effect of the surface roughness on the flow of two immiscible fluids flowing through parallel plates having undulated surfaces was analyzed by Luo and co-workers²⁷. It was found that roughness may cause fingering of the proceeding fluid interface because of local pinning of the contact line as a result of which the contact line locally moves more slowly as compared to the front tip of fluid-fluid interface. This results in strong deformation of the interface and fingering. This is also what we observed in semi-metal chips: the dispersed phase split into fingers when pushed onto the plateau. The higher surface roughness of the EDGE-CuNi/Cu system (table 4.1) resulted in fingers being formed soon after plateau invasion, as compared to the EDGE-CuNi system that formed

fingers in middle of the plateau, and EDGE-Cu system that formed fingers very close to the edge. Early fingering caused irregular filling of the plateau, which resulted ultimately in a lower number of droplet formation points (10 versus 13 for EDGE-CuNi). At low pressure (10 KPa) EDGE-Cu with minimum surface roughness had higher number of droplet formation points compared to EDGE-CuNi and EDGE-CuNi/Cu (8 versus 4 for both CuNi and CuNi/Cu systems); however, this value could not be greatly increased (maximum of 11) because of low pressure stability of the EDGE-Cu system (as will be discussed in next section). One should note that this fingering did not result in any coalescence or other instabilities during droplet formation. In that respect, the roughness (if not too high) may help to increase the productivity of the system: the droplet formation points may be located at closer distances resulting in a higher number of droplet formation points per unit length of the edge.

3.3. Pressure stability and productivity of the system

In EDGE emulsification, the pressure applied on the to-be-dispersed phase gives important information on emulsification behavior. The minimum pressure required to initiate the plateau invasion and droplet generation can be calculated by Laplace's law as²⁶

$$\Delta P = \sigma \left(\frac{1}{R_1} + \frac{1}{R_2} \right) \cos \theta \quad 4.1$$

Where σ is the interfacial tension, ϑ is the contact angle and R_1 and R_2 are the radii of curvature of the oil-water interface corresponding to plateau height (R_1) and its width (R_2) when completely filled. The effect of the applied pressure on the average droplet size and size distribution is shown in figure 4.6. For comparison, data points for a purely silicon based system (EDGE-silicon) are also given in the same figure.

With the EDGE-CuNi/Cu system, the breakthrough pressure was reached at 7 KPa; uniform droplets with an average size of 6.2 μm were produced at this pressure. At increasing pressures, the average droplet size remained constant albeit with a slight increase in CV, which stayed below 10%. Above 30 KPa, the droplet size increased rapidly leading to polydispersity (CV>10%). Ultimately, blow-up occurred at 38 KPa, with droplet sizes of 25-30 μm produced at some points resulting in highly polydispersed emulsions.

With the EDGE-CuNi system, droplet formation started at 5.5 KPa with droplets that were highly uniform with average size of 6.3 μm . the droplet size remained constant and monodispersed ($\text{CV} < 10\%$) for the entire pressure range until the blow-up pressure (42.5 KPa) was reached. At this pressure, the behavior was similar to that of the EDGE-CuNi/Cu system. The EDGE-CuNi system was exceptionally stable as function of the pressure.

Contrary to EDGE-CuNi and EDGE-CuNi/Cu, pressure stability of EDGE-Cu was very low with breakthrough and blow-up pressures being 9 KPa and 14 KPa respectively. Within this pressure range monodispersed droplets ($\text{CV} < 8\%$) with average size of 6.4 μm were produced. In fact, both EDGE-CuNi and EDGE-CuNi/Cu systems were much more stable as compared to the EDGE-Cu and EDGE-silicon as shown in Table 4.2. This stability is of great relevance for scale-up.

In addition to surface roughness which seems to facilitate the number of droplet formation points, the pressure stability of the systems may be linked to the contact angle or alternatively to the contact angle difference between top (glass) and bottom (silicon or metal coated) plate and it was found to increase with decreasing contact angle (or increasing contact angle difference). The EDGE-Cu system, having the largest contact angle ($\theta = 160^\circ$) and apparently no contact angle difference had the lowest pressure stability while the EDGE-CuNi system with its smallest contact angle and largest contact angle difference (table 4.1) had the highest stability. These findings are contrary to the simulations of van Dijk et al.,²⁸ according to which the pressure stability decreases by decreasing dispersed phase contact angle. Van Dijk and his co-workers²⁶ also investigated the effect of the surface contact angle on the droplet size during EDGE emulsification. It was found that the droplet size decreases with increasing contact angle if the system is operated with a high viscosity ratio (i.e. above critical value as reported by van Dijk et al.,²⁹ and in chapter 3 as is the case here) and within the monodispersed droplet formation regime. The results of the present study are contrary to these findings: here, the droplet size was the same for all the systems (including silicon) even though the systems exhibited different contact angles. It might be that dynamic interfacial tension effects that were not covered in the geometric analysis, could be responsible for creating a higher Laplace

pressure difference at higher expansion rates (frequency), therewith cancelling out the effect of the contact angle difference.

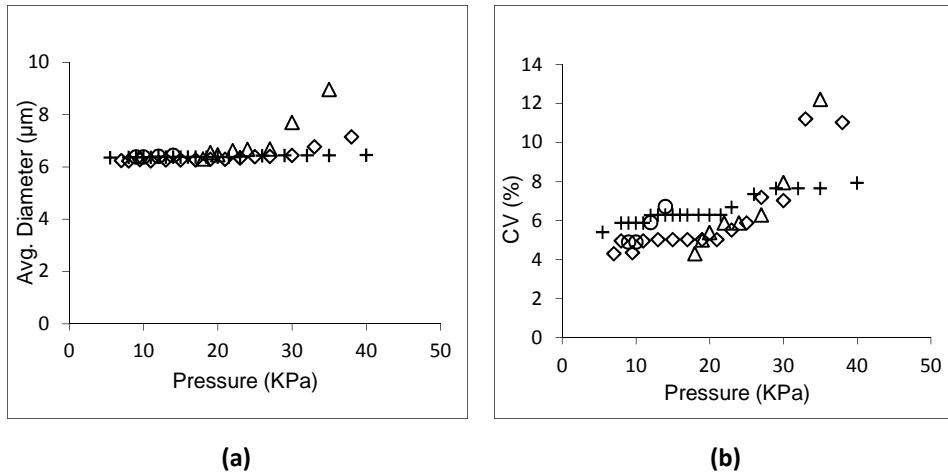


Figure 4.6: Average droplet diameter (a) and coefficient of variation CV (b) as a function of pressure using the EDGE-Cu system (o), EDGE-CuNi system (+), EDGE-CuNi/Cu system (◊) and EDGE-silicon system (Δ). The results were repeated three times using different chips and were found to be the same in each repetition.

Table 4.2 shows a comparison of the pressure stability and productivity of the silicon and metal based systems. The maximum droplet formation frequency for the EDGE-CuNi system was comparable to that reported for silicon based systems (when considering the frequency per droplet formation unit). As a result of the larger droplet size generated by the silicon EDGE system, which had a plateau height of 1.2 micron, the flux of the dispersed phase per hour per meter of the edge length is higher. At low pressure (10 KPa) EDGE-Cu having minimum roughness had highest frequency. However, maximum droplet formation frequency found for the EDGE-CuNi/Cu and especially for EDGE-Cu system was low compared to the EDGE-CuNi system. This can be attributed to the lower pressure stability (especially of EDGE-Cu system) and high roughness (of EDGE-CuNi/Cu). The surface roughness adds to the flow resistance on the plateau while the length of the fingers may effectively add to the total resistance in the system which is known to increase the pressure stability of microchannel emulsification systems²⁸. Low frequency of

EDGE-CuNi (at 10 KPa) compared to EDGE-CuNi/Cu can be attributed to unstable fingers in EDGE-CuNi at this pressure as already discussed in section 3.2. In this respect, metal systems show similar productivity to the silicon systems, as long as their roughness is not too large. In addition they exhibit wider pressure stability as compared to completely flat (silicon) systems, and this is an important step towards practical application of these systems.

Table 4.2: Comparison of EDGE systems consisting of different surfaces

Chip type	Stable press. range (KPa)	No. of droplet formation points/500 μm		Avg. drop size (μm)	Frequency (Hz)		Max. Dispersed phase flux ($\text{m}^3/\text{hr.m}$)
		@10 KPa	Max.		@ 10KPa	Max.	
EDGE-silicon	18 - 30	-	15 ^a	7.1 ^b	-	2750 ^b	3.70×10^{-6}
EDGE-Cu	9 - 14	8	11	6.4	123	336	3.37×10^{-7}
EDGE-CuNi	5.5 – 42.5	4	13	6.3	64	2596	2.43×10^{-6}
EDGE-CuNi/Cu	7 - 35	4	10	6.2	74	1584	1.41×10^{-6}

A = ref. 26

b = ref. 14

4. Conclusion

Metal-coated microfluidic EDGE systems having different surface roughness and wettability were investigated for monodispersed oil-in-water emulsification. The plateau in the EDGE-CuNi/Cu system, having large surface roughness, was not filled uniformly, which resulted in a smaller number of droplet formation points per unit length. This ultimately leads to a lower droplet formation frequency. Droplet formation with the less hydrophilic EDGE-CuNi system was stable over a wider range of pressures than with the more hydrophilic EDGE-Cu and EDGE-CuNi/Cu surface. The productivity of the EDGE-CuNi system was found similar to the silicon based systems.

The results indicate that a moderate surface roughness may help to decrease the distances between the locations at which droplet formation takes place and hence may increase the total number of droplet formation points per unit length of the edge. This, together with their high pressure stability, may increase the productivity of the system (compared to flat silicon based systems), which is significant for scale-out and the development of practical applications.

References

1. C. Charcosset, I. Limayem and H. Fessi, *J Chem Technol Biot*, 2004, **79**, 209-218.
2. M. Saito, L. J. Yin, I. Kobayashi and M. Nakajima, *Food Hydrocolloid*, 2006, **20**, 1020-1028.
3. S. Sugiura, M. Nakajima and M. Seki, *Langmuir*, 2002, **18**, 5708-5712.
4. I. Lambrich and H. Schubert, *J. Membr. Sci.*, 2005, **257**, 76-84.
5. S. van der Graaf, M. L. J. Steegmans, R. G. M. van der Sman, C. G. P. H. Schroën and R. M. Boom, *Colloid Surface A*, 2005, **266**, 106-116.
6. M. L. J. Steegmans, K. C. G. P. H. Schroën and R. M. Boom, *Langmuir*, 2009, **25**, 3396-3401.
7. M. L. J. Steegmans, C. G. P. H. Schroën and R. M. Boom, *Chemical Engineering Science*, 2009, **64**, 3042-3050.
8. A. S. Utada, L. Y. Chu, A. Fernandez-Nieves, D. R. Link and D. A. Weitz, *MRS Bull*, 2007, **32**, 702-708.
9. A. S. Utada, E. Lorenceau, D. R. Link, P. D. Kaplan, H. A. Stone and D. A. Weitz, *Science*, 2005, **308**, 537-541.
10. I. Kobayashi, M. Nakajima, K. Chun, Y. Kikuchi and H. Fujita, *AIChE J*, 2002, **48**, 1639-1644.
11. K. C. van Dijke, G. Veldhuis, K. Schroën and R. M. Boom, *Lab Chip*, 2009, **9**, 2824-2830.
12. K. C. van Dijke, G. Veldhuis, K. Schroën and R. M. Boom, *AIChE Journal*, 2010, **56**, 833-836.
13. I. Kobayashi, T. Takano, R. Maeda, Y. Wada, K. Uemura and M. Nakajima, *Microfluid Nanofluid*, 2008, **4**, 167-177.
14. K. C. van Dijke, K. Schroën, A. van der Padt and R. M. Boom, *J Food Eng*, 2010, **97**, 348-354.
15. M. L. J. Steegmans, A. Warmerdam, K. G. P. H. Schroën and R. M. Boom, *Langmuir*, 2009, **25**, 9751-9758.
16. S. van der Graaf, T. Nisisako, C. G. P. H. Schroën, R. G. M. van der Sman and R. M. Boom, *Langmuir*, 2006, **22**, 4144-4152.
17. R. K. Shah, H. C. Shum, A. C. Rowat, D. Lee, J. J. Agresti, A. S. Utada, L.-Y. Chu, J.-W. Kim, A. Fernandez-Nieves, C. J. Martinez and D. A. Weitz, *Materials Today*, 2008, **11**, 18-27.
18. I. Kobayashi, K. Uemura and M. Nakajima, *Food Biophys*, 2008, **3**, 132-139.
19. H. Liu, M. Nakajima and T. Kimura, *J. Am. Oil Chem. Soc.*, 2004, **81**, 705-711.
20. H. Liu, M. Nakajima, T. Nishi and T. Kimura, *Eur. J. Lipid Sci. Technol.*, 2005, **107**, 481-487.
21. V. Barbier, M. Tatoulian, H. Li, F. Arefi-Khonsari, A. Ajdari and P. Tabeling, *Langmuir*, 2006, **22**, 5230-5232.
22. J. Tong, M. Nakajima, H. Nabetani, Y. Kikuchi and Y. Maruta, *J. Colloid Interface Sci.*, 2001, **237**, 239-248.
23. J. Tong, M. Nakajima, H. Nabetani and Y. Kikuchi, *J. Surfactants Deterg.*, 2000, **3**, 285-293.
24. T. Kawakatsu, G. Trägårdh, C. Trägårdh, M. Nakajima, N. Oda and T. Yonemoto, *Colloid Surface A*, 2001, **179**, 29-37.
25. I. Kobayashi, M. Nakajima and S. Mukataka, *Colloid Surface A*, 2003, **229**, 33-41.

26. K. C. van Dijke, R. de Ruiter, K. Schroën and R. M. Boom, *Soft Matter*, 2010, **6**, 321-330.
27. X. Luo, X.-P. Wang, T. Qian and P. Sheng, *Solid State Communications*, 2006, **139**, 623-629.
28. K. C. van Dijke, K. C. G. P. H. Schroën and R. M. Boom, *Langmuir*, 2008, **24**, 10107-10115.
29. K. C. van Dijke, I. Kobayashi, K. Schroën, K. Uemura, M. Nakajima and R. M. Boom, *Microfluid Nanofluid*, 2010, **9**, 77-85.
30. A. Maan, K. Schroën and R. Boom, *Microfluid Nanofluid*, DOI 10.1007/s10404-012-1037-0.

Chapter 5

Effect of Surface Wettability on Microfluidic Emulsification

This chapter has been submitted as: Maan, A. A., Sahin, S., Mujawar, L., Boom, R., Schroën, K..Effect of surface wettability on microfluidic emulsification.

Abstract

In most microfluidic emulsification devices, the channel sizes are such that the wettability of the surface does not play a major role. However when using much smaller channel dimensions in emulsification devices as is the case in EDGE (Edge based Droplet Generation) systems in which the to-be-dispersed phase needs to flow across a large shallow area, this is expected to play an important role. Therefore we took these microfluidic chips as models to evaluate the effect of wettability on emulsification and found remarkable effects while varying the contact angle between 90 and 160°. The highest contact angle ($\vartheta = 160^\circ$) produced monodispersed emulsions with average droplet size of 5.0 μm and coefficient of variation (CV) below 10%, as expected from previous work; however, the pressure stability of these systems was very low. The pressure stability was greatly enhanced at contact angles below 150°; the plateaus were filled over their entire length, and the observed droplet generation frequencies increased (up to a factor of 2.0 and 3.5 for Tween20 and Tween60 respectively) at comparable pressures. The emulsion became highly polydispersed when the contact angle was below 100°; this is due to the wetting of the surface with dispersed phase.

These effects are also expected to play an important role in other devices, in which small dimensions are used, especially for emulsion production. As the pressure stability is crucial for practical application, we expect that adequate optimisation of the wetting behaviour may greatly enhance the applicability of spontaneous emulsification systems in general.

1. Introduction

The last few years have shown a rapid growth in the application of microfluidic systems in various fields including chemistry, biology, medicine, physical sciences, energy generation and display technology¹. An emerging application is in the preparation of emulsions. Microfluidic devices give accurate control over droplet size, shape and internal structure². The resulting highly monodispersed droplets find their applications amongst others in microencapsulation, micro-reaction systems and fabrication of colloidal particles³⁻⁵.

Emulsions can be made through different formation mechanisms, for example through shear of a (cross flowing or co-flowing) continuous phase in T-, Y-junctions, by using flow focussing devices and by using co-flow systems⁶⁻⁸. In microchannels, droplets may be formed by a spontaneous mechanism driven by Laplace pressure differences^{9, 10}. This is also the case in the recently introduced EDGE system, in which simultaneous multiple droplet formation takes place from a single, wide nozzle¹¹.

Contrary to most droplet generation systems, EDGE has two distinct channel depths. The shallowest part (the plateau) is the key element for steady operation. It was already shown that the EDGE chips can be scaled up rather simply by making plateaus wider and/or by applying more plateaus in series^{11, 12}. The process is influenced by several factors including plateau dimensions, dispersed phase flow rate and viscosity ratio of (dispersed and continuous) phases; these factors have been well documented in literature¹¹⁻¹³.

One of the parameters that have not yet been systematically investigated is the wettability of the surface. Especially in channels with very small dimensions, such as the plateau of an EDGE chip, this is expected to be important for successful emulsification: the dispersed phase needs to be able to invade the plateau, but it should remain wetted by the continuous phase to induce droplet snap off. The effect of surface wettability on preparation of w/o emulsions was touched upon by Kawakatsu et al.,¹⁴ for microchannels, and they reported that monodispersed droplets could only be produced if the contact angle of water (measured on the surface submerged in oil phase) is above 120°. However,

systematic information regarding the effect of surface wettability on the stability and productivity of the systems is still lacking. In the current study, we investigated the effect of surface wettability on (o/w) emulsification through EDGE systems, and report on the efficiency, pressure stability and productivity of these systems.

2. Experimental

The EDGE chips used in our investigations consisted of multiple plateaus (48 in total) which are triangular, as can be seen in figure 5.1. The channels and plateaus were fabricated in silicon wafers and were covered with a glass plate. Both glass and silicon surfaces were hydrophilized to make them suitable for o/w emulsification. The tapered plateaus (900 nm deep) consisted of an oil inlet of 200 μm (wide) and a wide outlet (where droplet formation takes place) of 1200 μm . The plateaus were fed by an oil channel (500 μm wide and 200 μm deep) at the side of the narrow inlet (200 μm) and the plateaus ejected the droplets into a water channel (200 μm wide and 200 μm deep) at the broader (1200 μm) outlet.

Chips with different surface wettability were prepared by coating the surfaces with silanes: triethoxysilylbutyraldehyde from Gelest Inc. (Morrisville, USA), chloro(methyl)phenylsilane from Aldrich (Old Brickyard, United Kingdom) and 3-cyanopropyltriethoxysilane from Aldrich (Seelze, Germany). For contact angle measurements, separate, smooth silicon and glass plates were coated by immersing the cleaned (rinsed with water and ethanol followed by plasma cleaning) surfaces into the silane solutions prepared in ethanol (3-cyanopropyltriethoxysilane, 2.5 % vol/vol) or toluene (triethoxysilylbutyraldehyde and chloro(methyl)phenylsilane, 1 % vol./vol.), for one hour. The plates were then rinsed with the respective solvents (toluene or ethanol) to remove any unreacted materials, and were dried with nitrogen. The surfaces were then immersed in the continuous water phase (containing 2.5 % (wt./vol.) Tween20 or Tween60) and a drop of dispersed phase (hexadecane) was put on the surface. An image of the droplet was captured after its shape became stable and was used for contact angle measurement by using image analysis software (Image Pro plus 4.5). The contact angle measurements were made in triplicate and the values mentioned in this paper are always

the average of these three measurements. For the modification of the channels and plateaus in the chip, solutions (for modification) and liquids (for cleaning) were introduced with a syringe pump; the chips were used for emulsification immediately after modification.

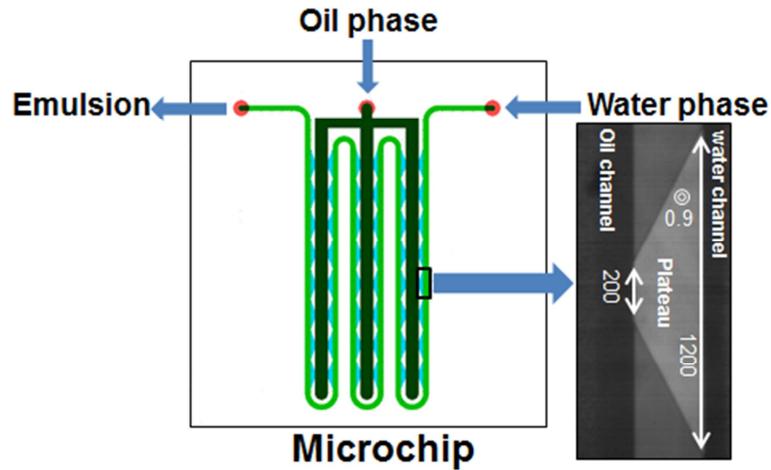


Figure 5.1: Drawing of the EDGE chip with magnification of a droplet formation unit.

3. Results and discussions

It is generally known that surface properties are of essence for emulsification in microfluidic devices. Some authors varied contact angles between 130-150° through changes in temperature, which however also influences the viscosity¹⁵. Kawakatsu and co-workers used silanes to modify the surfaces for water-in-oil emulsification, but mainly focussed on droplet sizes. This is the first time that the contact angle is directly linked to process stability.

Table 5.1 lists the silanes used for surface modification, the type of surfactant and the resulting contact angles on silicon and glass. For untreated surfaces the contact angle was independent of the surfactant used. The contact angle on the modified surfaces depends not only on the silane but also on the type of surfactant used; the surfaces modified with the same silane (triethoxysilylbutyraldehyde or 3-cyanopropyltriethoxysilane) gave different contact angles with different surfactants. This

observation is in agreement with those of e.g. Kawakatsu and co-workers¹⁴, who observed different contact angles for water droplets made on silicon and glass surfaces, hydrophobically modified through silanization (n-octyltriethoxysilane), while using different surfactants (Sodium bis(2-ethylhexyl) sulfosuccinate and sorbitan fatty acid esters).

Table 5.1: Equilibrium contact angles resulting from different silane treatments using different surfactants.

Microchip	Type of silane	Surfactant	Contact angle (θ)	
			Silicon	Glass
EDGE-A20	Untreated (silicon dioxide)	Tween20	160 \pm 2	160 \pm 2
EDGE-B20	Triethoxysilylbutyraldehyde	-	144 \pm 1	142 \pm 2
EDGE-C20	3-Cyanopropyltriethoxysilane	-	151 \pm 2	150 \pm 2
EDGE-D20	Chloromethylphenylsilane	-	91 \pm 2	93 \pm 3
EDGE-A60	Untreated (silicon dioxide)	Tween60	160 \pm 2	160 \pm 2
EDGE-B60	Triethoxysilylbutyraldehyde	-	153 \pm 1	152 \pm 1
EDGE-C60	3-Cyanopropyltriethoxysilane	-	143 \pm 4	145 \pm 1
EDGE-D60	Chloromethylphenylsilane	-	93 \pm 4	92 \pm 4

Emulsification was started by wetting the plateaus with the aqueous phase by injecting it through continuous phase channel using a syringe pump. Hexadecane was then injected into the dispersed phase channel with a digital pressure controller (Bronkhorst, The Netherlands) at low pressure (100 mbar) until all dispersed phase channels were filled with hexadecane. Pressure was then gradually increased and emulsification behaviour was analysed as a function of applied pressure with a high speed camera attached to a microscope, and the captured images were analysed through image analysis software (Image pro plus 4.5).

At higher pressures, the dispersed phase entered the plateau, smoothly covering the plateau and moving towards its edge, where the interface became instable and generated droplets into the continuous phase at the so-called "break-through" pressure. The filling behaviour of the plateau was affected by the surface (O/W) contact angle. At contact angles above 150°, the far corners of the plateau were not filled with dispersed

phase; about 80 μm was left unfilled at both corners as can be seen in figure 5.2a. This observation is in good agreement with the findings of van Dijk et al.,¹² who reported this effect to be larger for triangular shaped plateaus than for rectangular ones. However, for contact angles below 150°, the dispersed phase filled the plateaus completely by moving towards the far corners (see figure 5.2b), which increased the productivity of the plateau. The spreading of a liquid on a solid surface increases by decreasing its contact angle with the surface as was reported by Mao and co-workers¹⁶, who investigated the spreading of a water drop on glass, stainless steel and paraffin wax surfaces and found that the spread of the droplet was highest on glass due to its lower contact angle, followed by stainless steel and paraffin wax.

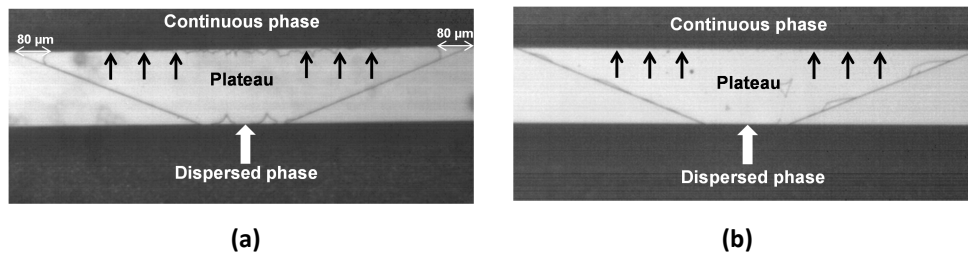


Figure 5.2: Filling behaviour of the plateau with **a.** unfilled ($\vartheta = 160$) and **b.** filled ($\vartheta < 150$) corners. Continuous phase was Tween60 and dispersed phase pressure was 190 mbar.

According to the geometric model of van Dijk et al.,¹³ the droplet size should decrease with increasing the dispersed phase contact angle in EDGE emulsification. In our case, however, the droplet size remained unaffected by the contact angle as can be seen in figure 5.3. Droplet size, for all contact angles, remained constant (around 5.0 μm) and uniform (CV<10%) with increasing pressure until some critical pressure was reached above which very large droplets (>25 μm) were observed at some (2-3) droplet formation points. This increased the average droplet size slightly whereas the polydispersity (CV) increased rapidly resulting in unstable emulsification.

Van Dijk et al.¹⁷ simulated the effect of surface contact angle on microchannel emulsification by computational fluid dynamics and found that the pressure stability of the system decreases by decreasing the dispersed phase contact angle. However, our results are contrary to these simulations as can be seen in figures 5.3 and 5.4.

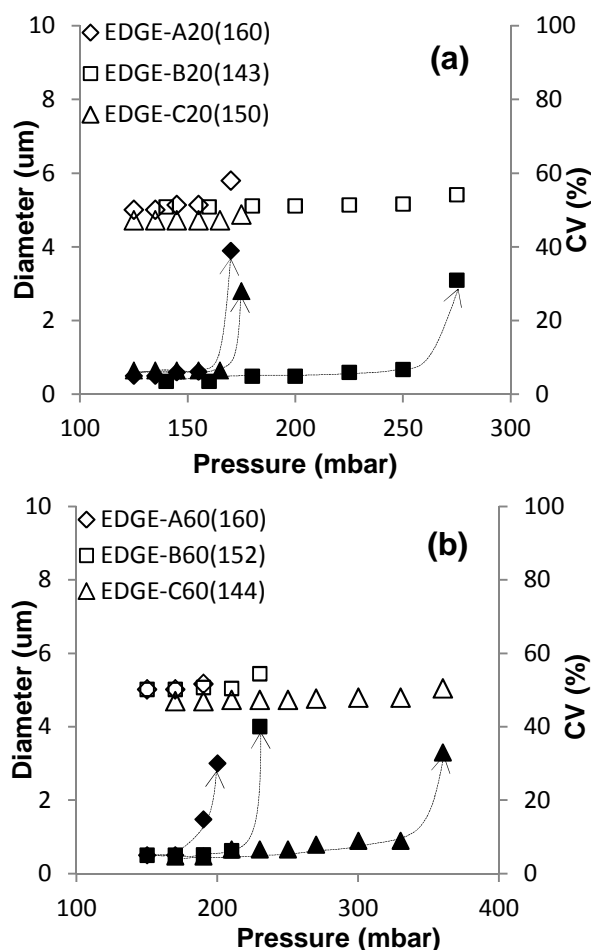


Figure 5.3: Effect of surface contact angle on average droplet size (unfilled markers) and CV (filled markers) with increasing pressure using **a.** Tween20 and **b.** Tween60 with contact angles of respective EDGE chips shown in brackets. The results were repeated thrice by using different chips and pressure stability was found to be the same in every repetition.

Unmodified chips had the largest contact angles ($\vartheta = 160^\circ$) and produced monodispersed emulsions, however, the pressure range in which these emulsions remained monodispersed was quite narrow. With slightly lower contact angles, ($160^\circ > \vartheta > 150^\circ$) the pressure range for monodispersed emulsification was increased slightly, however at contact angle $< 150^\circ$ monodispersed emulsions could be produced over a wide pressure range.

In general the pressure stability of the systems increased with decreasing contact angle (figure 5.4) and the systems had a large pressure range in which they were stable when the contact angle became $<150^\circ$. The lowest contact angles were found for chloromethylphenylsilane modified chips, which lead to polydispersed emulsions with droplets ranging from 5 to 100 μm , probably because of the wetting of the plateau surface with dispersed phase.

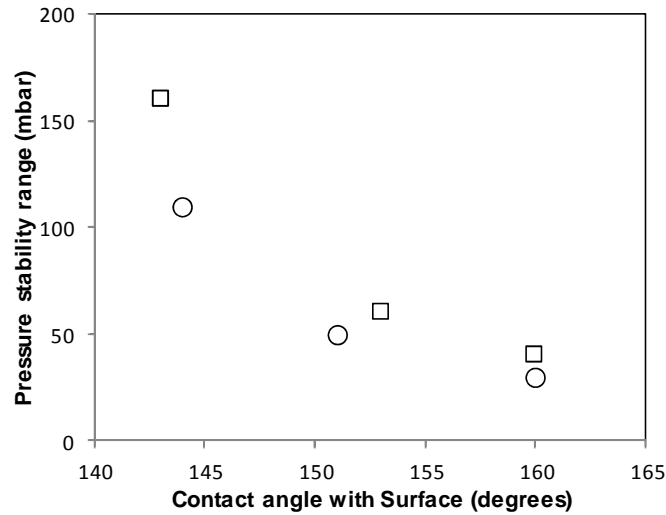


Figure 5.4: Effect of surface contact angle on pressure stability of the system using Tween20 (o) and Tween60 (□) as surfactants.

Table 5.2 gives an overview of the pressure stability and productivity of the systems. When the applied pressure was kept constant, the total number of droplet formation points per unit length of the edge was not affected, but the droplet formation frequency (per unit length of the edge) was highest in the chips with the lowest contact angles that were able to produce emulsions (i.e., excluding chloromethylphenylsilane modification, which resulted in wetting of the plateaus by the dispersed phase).

The droplets are initially connected to the plateau through a neck that spontaneously breaks when the droplet has reached a certain size. We hypothesize that at larger contact angles, the oil water interface has more convex shape and the local (Laplace) pressure in the tip of such an interface is expected to be higher. This hinders the

deformation of the interface into a neck and delays the collapse of the neck to make a droplet, resulting in lower droplet formation frequencies, while blow-up occurs at only a slight increase in dispersed phase flow. As the convexity of the interface is smaller at lower contact angles, the neck formation and droplet detachment become comparatively easier. This results in increased droplet formation frequency and systems that can be operated at higher pressures. For both surfactants the highest frequencies were found at the lowest contact angles (58 Hz and 123 Hz respectively), obtained for two different modification agents.

One should keep in mind that the droplet formation points (in all cases) were irregularly distributed along the edge and that the total number of droplet formation points and droplet formation frequency were different at different locations in the chip. The locations seem to be random: with different experiments, the droplet formation points were also at different places; but when active at constant applied pressure, they remain on the same spot.

Table 5.2: Effect of surface contact angle on pressure stability and productivity of the system.

Microchip	Surfactant	Pressure stability (mbar)	Droplet formation points/400 μm		
			@ 150 mbar	@ 150 mbar	Max.
EDGE-A20	Tween20	125 - 155	3	10	-
EDGE-B20	-	140 - 250	5	22	58
EDGE-C20	-	125 - 175	5	18	-
			@ 190 mbar	@ 190 mbar	
EDGE-A60	Tween60	150 - 190	4	11	-
EDGE-B60	-	150 - 210	4	13	-
EDGE-C60	-	170 - 330	6	40	123

It is clear that for a good design of EDGE emulsification systems the contact angle is crucial: it should be relatively low to allow good pressure stability and high productivity,

while at the same time it should be sufficiently large to still induce spontaneous droplet formation.

4. Conclusion

The surface contact angle is crucial in microfluidic emulsification, not only for the spontaneous droplet formation itself, but also for the pressure stability of the system, which is very important for scale-out of the systems. In addition, the efficiency and productivity of the system were improved not only due to increased pressure stability but also because of better plateau filling behaviour (allowing the dispersed phase to reach the far corners of the plateau) and increased droplet formation frequency. Similar effects are expected to play a role in other microfluidic emulsification systems; especially those having narrow channel dimensions.

Acknowledgement

We would like to thank Higher Education Commission (HEC) of Pakistan for partially funding this research; and NanoNextNI for support of this project.

References

1. T. M. Squires and S. R. Quake, *Rev. Mod. Phys.*, 2005, **77**, 977-1026.
2. M. Seo, C. Paquet, Z. Nie, S. Xu and E. Kumacheva, *Soft Matter*, 2007, **3**, 986-992.
3. A. S. Utada, E. Lorenceau, D. R. Link, P. D. Kaplan, H. A. Stone and D. A. Weitz, *Science*, 2005, **308**, 537-541.
4. Z. T. Cygan, J. T. Cabral, K. L. Beers and E. J. Amis, *Langmuir*, 2005, **21**, 3629-3634.
5. A. A. Maan, K. Schroën and R. Boom, *J Food Eng*, 2011, **107**, 334-346.
6. S. van der Graaf, M. L. J. Steegmans, R. G. M. van der Sman, C. G. P. H. Schroën and R. M. Boom, *Colloid Surface A*, 2005, **266**, 106-116.
7. M. L. J. Steegmans, K. C. G. P. H. Schroën and R. M. Boom, *Langmuir*, 2009, **25**, 3396-3401.
8. P. B. Umbanhowar, V. Prasad and D. A. Weitz, *Langmuir*, 2000, **16**, 347-351.
9. S. Sugiura, M. Nakajima, S. Iwamoto and M. Seki, *Langmuir*, 2001, **17**, 5562-5566.
10. I. Kobayashi, M. nakajima, K. Chun, Y. kikuchi and H. Fujita, *AIChE J*, 2002, **48**, 1639-1644.
11. K. C. van Dijke, G. Veldhuis, K. Schroën and R. M. Boom, *AIChE Journal*, 2010, **56**, 833-836.
12. K. C. van Dijke, G. Veldhuis, K. Schroen and R. M. Boom, *Lab Chip*, 2009, **9**, 2824-2830.
13. K. C. van Dijke, R. de Rooter, K. Schroën and R. M. Boom, *Soft Matter*, 2010, **6**, 321-330.
14. T. Kawakatsu, G. Trägårdh, C. Trägårdh, M. Nakajima, N. Oda and T. Yonemoto, *Colloid Surface A*, 2001, **179**, 29-37.
15. K. B. Fujii, I. Kobayashi, K. Uemura and M. Nakajima, *Microfluid Nanofluid*, 2010, DOI 10.1007/s10404-010-0708-y.
16. T. Mao, D. C. S. Kuhn and H. Tran, *AIChE Journal*, 1997, **43**, 2169-2179.
17. K. C. van Dijke, K. C. G. P. H. Schroën and R. M. Boom, *Langmuir*, 2008, **24**, 10107-10115.

Chapter 6

Microfluidic Preparation and Self Diffusion PFG–NMR Analysis of monodisperse Water-in- Oil-in-Water double Emulsions

This chapter has been published as: Hughes, E., Maan, A. A., Acquistapace, S., Burbudge, A., Johns, M. L., Gunes, D. Z., Clausen, P., Syrbe, A., Hugo, J., Schroën, K., Miralles, V., Atkins, T., Gray, R., Homewood, P., Zick, K., 2012. Microfluidic preparation and self diffusion PFG-NMR analysis of monodisperse w/o/w double emulsions. Journal of colloid and interface science, Doi.org/10.1016/j.jcis.2012.07.073.

Abstract

Monodisperse water-in-oil-in-water (W/O/W) double emulsions have been prepared using microfluidic glass devices designed and built primarily from off the shelf components. The systems were easy to assemble and use. They were capable of producing double emulsions with an outer droplet size from 100 to 40 μm . Depending on how the devices were operated; double emulsions containing either single or multiple water droplets could be produced. Pulsed-field gradient self-diffusion NMR experiments have been performed on the monodisperse water-in-oil-in-water double emulsions to obtain information on the inner water droplet diameter and the distribution of the water in the different phases of the double emulsion. This has been achieved by applying regularization methods to the self-diffusion data. Using these methods the stability of the double emulsions to osmotic pressure imbalance has been followed by observing the change in the size of the inner water droplets over time.

1. Introduction

Double emulsions, in particular, water-in-oil-in-water (w/o/w) double emulsions, are of interest in a number of application and research areas. In the food industry, research has been aimed at using double emulsion technology as a means of reducing the fat content of foods without impacting the taste¹. In pharmaceutical and cosmetic research the emphasis has been placed on double emulsions as delivery or encapsulation solutions for various actives^{2, 3}. With the introduction of microfluidic production of monodisperse double emulsions^{4, 5}, the increased control of droplet fabrication has led to novel areas of research of particle and material production^{6, 7}. For applications of encapsulation and delivery there are still issues regarding the long-term stability of the double emulsions which can only be resolved by understanding the physical mechanisms that lead to the destabilization of the double emulsions⁸. Key to providing this understanding is a noninvasive quantitative measurement of both the distribution of water and the inner water droplet size distribution of w/o/w emulsions, without any assumptions regarding the distribution shape.

Pulsed field gradient nuclear magnetic resonance (PFG-NMR) is a common non-invasive technique to study the size distribution and dynamics of single emulsion systems^{9, 10} with advantages that it can be used on concentrated opaque emulsions and is a non-destructive technique. The main drawback of the analysis of NMR data of emulsions is that it normally involves assuming a certain characteristic shape for the droplet size distribution, such as a log-normal distribution⁹. PFG-NMR has also been applied to double emulsions¹¹⁻¹³ and while the models used are quite sophisticated, in terms of their ability to account for the possible presence of water transport within the double emulsion, they still assume a certain shape for the size distribution of the inner water droplets.

Recently, in simple polydisperse emulsions, Hollingsworth and Johns¹⁴ have applied regularization methods to diffusion NMR data to obtain the size distribution of the droplets directly. Using this approach no assumptions are made about the shape of the size distribution. In this paper, we present a novel extension to their methodology such that it can be readily applied to multiple emulsions, in particular, water-in-oil-in-water

(w/o/w) double emulsions. This is accomplished by the unique inclusion of both restricted water diffusion within the inner droplet spheres as well as hindered water diffusion around the larger oil droplets into the required analysis. However, exchange of water between droplets on the timescale of the diffusion observation time in the PFGNMR experiment is ignored.

To develop and test the new extended NMR approach we have resorted to using monodisperse double emulsions as model systems produced using microfluidic techniques^{5, 15, 16}. This has involved developing microfluidic devices based on flow-focussing geometries¹⁷ to generate the monodisperse double emulsions. A second objective of the work presented here was thus the adaption and development of microfluidic devices that were capable of producing sufficient quantities of stable monodisperse double emulsions for use in standard high field NMR spectrometers. Typical microfluidic devices for making multiple emulsions require two junctions with opposite surface wetting properties. In the first instance, we have taken a pragmatic approach to overcome the difficulties of requiring both hydrophobic and hydrophilic surfaces on the microfluidic device. Our solution was to utilize two commercially available microfluidic chips with a single droplet generator on each and where each chip had different surface properties^{4, 18}. The chips are aligned in such a manner that the perturbation of the flow fields within the microfluidic channels is minimized as much as possible across the interface of the chips.

Under certain flow conditions and surface tension properties of the fluids, stable jets can be established within the microfluidic channels¹⁹⁻²¹, we have taken advantage of these conditions to make w/o/w double emulsions, where a single water droplet in oil droplet is always formed¹⁶. We have found that this mode of generation of the double emulsions is very stable, allowing the junctions on the microfluidic chip to be well separated, on the order of several millimetres. This has led to the design of a single monolithic double emulsion microfluidic device with two flow-focussing junctions which allows for simple chemical surface modification of the device due to their large separation distance^{22, 23}.

Finally, the importance of the development work in NMR and microfluidics to understanding double emulsion stability is demonstrated. In a series of NMR diffusion experiments on monodisperse double emulsions as a function of time, the long term stability of the double emulsion towards osmotic pressure imbalance is followed. For the first time, in a concentrated emulsion, in a non-destructive manner, the change in the size of the inner water droplets is tracked. Since the double emulsion has a low polydispersity, diffraction like phenomena are observed in the experimental NMR diffusion data²⁴⁻²⁶. The positions of the maxima and minima in the data are given by the size of the inner water droplets. With time, these positions shift, due to the loss of water from the inner droplets of the double emulsion to the outer water phase. It is demonstrated that the full analysis of the NMR data using the inversion regularization approach corresponds well with the simple analysis of measuring the changing position of the diffraction minima.

2. NMR theory

The equation relating the free diffusion coefficient D , to the echo response S , for a pulse gradient NMR experiment is given by the following equation²⁷,

$$\frac{S}{S_0}(g, \Delta) = \exp\left(-(\gamma\delta g)^2 D \left(\Delta - \frac{\delta}{3}\right)\right) \quad 6.1$$

Where, S_0 is the echo signal in the absence of gradients, δ is the gradient pulse duration, g is the gradient strength, γ is the gyromagnetic ratio, D is the diffusion observation time.

For the problem of the echo response for diffusion within a sphere, there are two main solutions found in the literature. The first assumes that dephasing of the magnetization at long diffusion observation times follows a Gaussian distribution. Murday and Cotts published the following equation²⁸.

$$\ln \frac{S(2\Delta, \delta, g)}{S_0} = \frac{2\Delta}{T^2} - 2\gamma^2 g^2 \sum_{m=1}^{\infty} [\alpha_m^2 (\alpha_m^2 a^2 - 2)]^{-1} \times \left(\frac{2\delta}{\alpha_m^2 D} - \frac{(2 + \exp[-\alpha_m^2 D(\Delta - \delta)] - 2\exp(-\alpha_m^2 D\delta) - 2\exp(-\alpha_m^2 D\Delta) + \exp[-\alpha_m^2 D(\Delta + \delta)])}{(\alpha_m^2 D)^2} \right) \quad 6.2$$

Where, α is the radius of the droplets, α_m are the m th roots of the Bessel equation $\left(\frac{1}{\alpha r}\right) J_{\frac{3}{2}}(\alpha r) = J_{\frac{5}{2}}(\alpha r)$.

The second general solution is an exact solution to the problem of diffusion within a sphere, but assumes that the gradient pulses are short compared to the diffusion observation time and to the ratio of $a^2/2D$ where a is the radius of the sphere and is known in the literature as the short gradient pulse solution. The complete equation is given by^{29, 30}.

$$\frac{S(g, \Delta)}{S_0} = \frac{9[\gamma g \delta \alpha \cos(\gamma g \delta \alpha) - \sin(\gamma g \delta \alpha)]^2}{(\gamma g \delta \alpha)^2} + 6 \sum_{n=0}^{\infty} \sum_k \frac{(2n+1)\alpha_{nk}^2}{\alpha_{nk}^2 - n^2 - n} \exp\left(-\frac{\alpha_{nk}^2 D \Delta}{\alpha^2}\right) \left[\frac{\gamma g \delta \alpha j'_n(\gamma g \delta \alpha)}{\alpha_{nk}^2 - (\gamma g \delta \alpha)^2}\right]^2 \quad 6.3$$

where the spherical Bessel functions are defined as $J'_n(\lambda r') = \sqrt{\frac{\pi}{2r'}} J_{n+\frac{1}{2}}(\lambda r')$ and α_{nk} are the roots of $J'_n(\alpha_{nk}) = 0$ as outlined by Veeman²⁹. When $\Delta \gtrsim a^2/6D$ and $\delta \ll \Delta$ then one may use only the first term of the above equation

$$\frac{S(g)}{S_0} = \frac{9[\gamma \delta g \alpha \cos(\gamma \delta g \alpha) - \sin(\gamma \delta g \alpha)]^2}{(\gamma \delta g \alpha)^6} \quad 6.4$$

A good approximation to the above equation has been shown to be³¹,

$$\frac{S(g)}{S_0} = \exp\left(-\frac{1}{5} \gamma^2 \delta^2 g^2 \alpha^2\right) \quad 6.5$$

Equations (6.4) and (6.5) are identical down to $S(g)/S(0) > 0.15$.

Figure 6.1 shows the results from Equations (6.2), (6.4), and (6.5) for diffusion in a sphere of radius, α of 25 μm , diffusion observation time, Δ , of 3 s, gradient pulse width, δ of 2 ms and the free diffusion coefficient, D_{H_2O} of $2.3 \times 10^{-9} \text{ m}^2/\text{s}$. Both the curves from Equations (6.2) and (6.5) overlap which means that under these simulation parameters the system is well within the long diffusion time limit. All three equations completely overlap down to an $S(g)/S(0)$ ratio of 0.3. After, Equation (6.4) deviates markedly and shows characteristic "diffraction" maxima of diffusion within a single sphere²⁴.

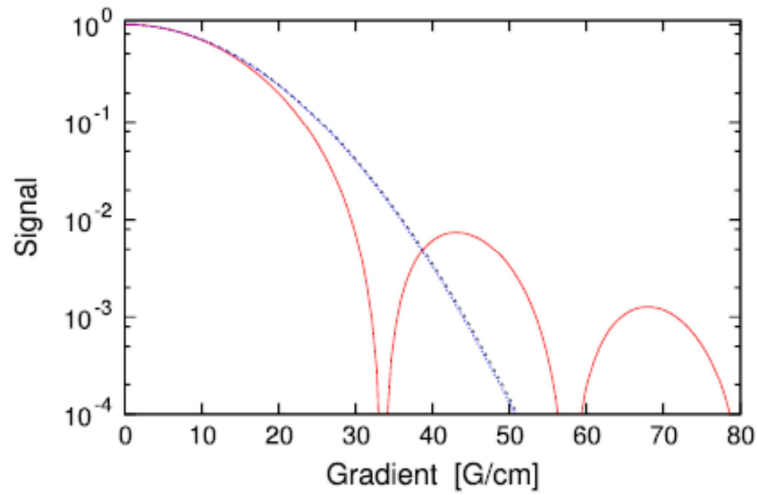


Figure 6.1: Plots of diffusion within a sphere using Equation (6.2) (blue dashed), (6.4) (red line), and (6.5) (dashed black). (For interpretation of the references to colour in this figure legend, the reader is referred to the web version of this article.)

2.1. Regularized numerical inversion analysis of self-diffusion NMR data of double emulsions

In a water-in-oil-in-water double emulsion, the diffusion signal of the water resonance can be modeled using a linear combination of equations for free diffusion for the water of the external phase and for diffusion within a sphere for the internal water phase. If we assume that there is no exchange of water between droplet or between the inner and outer phase on the time scale of the diffusion observation time then the only difficulty in analyzing the diffusion data is to account for the polydispersity or probability distribution $P(a)$, of the water droplets in the double emulsion. In the literature¹⁰, for simple emulsions, the majority of papers have analyzed the dispersed phase of the emulsion by applying a non-linear least squares approach based on the Murday and Cotts equation, Equation (6.2) in the form

$$b(a) = \frac{\int_0^\infty a^3 P(a) S(g,a) da}{\int_0^\infty a^3 P(a) da} \quad 6.6$$

the most convenient approach to handle this equation is to assume a known distribution of droplet sizes. This is typically taken to be a log-normal distribution and the diffusion

data is fit to a median radius and the width of the distribution. However, for real systems this assumption can lead to errors. Hollingsworth and Johns¹⁴ have treated Equation (6.6) as a first-order Fredholm equation and used inverse regularization methods to obtain for a simple emulsion, $P(a)$ from the experimentally discrete values of $b(g)$. They show that Equation (6.6) can be rewritten as,

$$b_i = \sum_{j=1}^m R(g_i, a_j) P(a_j) \delta_j \quad 6.7$$

where the denominator in Equation (6.6) is neglected as it is a constant for a given emulsion. Each b_i is the i th attenuation signal for the corresponding gradient value g_i . $P(a_j)$ represents the probability density of the solution at the j th quadrature interval. The matrix R is a transfer matrix and represents the value of the attenuation for discrete values of g and a . δ_j represents the weighting of the quadrature intervals. Equation (6.7) can be written in matrix form as,

$$\mathbf{b} = \mathbf{R}\mathbf{P} \quad 6.8$$

We are now interested in finding \mathbf{P} given \mathbf{b} and \mathbf{R} . This must be done using regularization methods through the introduction of a smoothing matrix that stops \mathbf{P} becoming oscillatory as a solution is reached. The equation that is then minimized is,

$$H = \min\{\|\mathbf{R}\mathbf{P} - \mathbf{b}\|^2 + \lambda^2 \|\mathbf{L}\mathbf{P}\|^2\} \quad 6.9$$

\mathbf{L} is a matrix that contains coefficients that can be simply the unit matrix or the coefficients of the integral of the second derivative. We have followed Hollingsworth and Johns¹⁴ and chosen the latter using the matrix coefficients found in the paper by Wilson³²

$$\mathbf{L} = \begin{pmatrix} 6 & -4 & 1 & 0 & \dots & 0 & 0 & 0 \\ -4 & 6 & -4 & 1 & \dots & 0 & 0 & 0 \\ 1 & -4 & 6 & 1 & \dots & 0 & 0 & 0 \\ 0 & 1 & -4 & 6 & \dots & 0 & 0 & 0 \\ \vdots & \vdots & \vdots & \vdots & \ddots & \vdots & \vdots & \vdots \\ 0 & 0 & 0 & 0 & \dots & 6 & -4 & 1 \\ 0 & 0 & 0 & 0 & \dots & -4 & 6 & -4 \\ 0 & 0 & 0 & 0 & \dots & 0 & -4 & 6 \end{pmatrix} \quad 6.10$$

For a given value of λ a unique solution for \mathbf{P} can be found. The difficulty is to find the best value for λ that gives a physically meaningful result. Large values of λ produce too smooth

a solution, while small values will give non-physical oscillations in the solution for \mathbf{P} . The choice of λ should be based on a combination of prior knowledge of the physical state of the system and an unbiased assessment of the goodness of fit and the noise present in the experimental data.

The transfer matrix for a simple emulsion is derived solely from Equations (6.2) or (6.3) depending on the model chosen. For a double emulsion the transfer matrix is derived from both Equations (6.1) and either (6.2) or (6.3). Therefore Equation (6.7) becomes,

$$b_i = \sum_{j=1}^m R(g_i a_j) P(a_j) \delta_j + \sum_{j=1}^m Q(g_i, D_j) P(D_j) \delta_j \quad 6.11$$

In matrix form this equation can be expressed in the following manner

$$b = \left[\begin{pmatrix} R & 0 \\ 0 & 0 \end{pmatrix} + \begin{pmatrix} 0 & 0 \\ 0 & Q \end{pmatrix} + \begin{pmatrix} P(a) \\ P(D) \end{pmatrix} \right] \quad 6.12$$

where \mathbf{Q} is the transfer matrix and contains values for Equation (6.1) as a function of D and g and \mathbf{R} is the transfer matrix and contains values for Equation (6.2) as a function of a and G . The probability distribution \mathbf{P} , is then split in two equal parts to contain the probability distribution for the droplet size, $P(a)$ and the diffusion distribution, $P(D)$ for the hindered diffusion of the outer water of the double emulsion around the oil droplets. In this form, Equation (6.9) will have two smoothing parameters, λ_a for the radius distribution and λ_D for the diffusion distribution and the matrix \mathbf{L} has a block diagonal form consisting of two \mathbf{L} matrices for λ_a and λ_D .

The final equation, which can be found in Numerical Recipes³³, that is solved using a non-negative least squares algorithm based on the algorithm of Lawson and Hanson^{34, 35} is,

$$(\mathfrak{R}^T \mathfrak{R} + \lambda L) P = \mathfrak{R}^T b \quad 6.13$$

where \mathfrak{R} now is the combination of R and Q matrices in Equation (6.12).

3. Experimental

3.1. Materials

The three phases of water-in-oil-in-water double emulsions were prepared with either only MilliQ water, 1% sodium dodecyl sulfate (SDS) solution or 1% Tween20

(Polyoxyethylene (20) sorbitan monolaurate) solution for the inner water droplets, sunflower oil with 2% polyglycerol polyricinoleate (PGPR) for the oil droplets and water with 1 or 2% b-lactoglobulin for the continuous outer aqueous phase in imidazole (20 mM) buffer at pH 7.

3.2. Microfluidic apparatus

For the first experiments, two standard flow focussing droplet generating microfluidic glass chips were used. These were purchased from Dolomite Ltd. (Part nos. 3000158 (hydrophilic) and 3000301 (hydrophobic)). A schematic of the chips and the assembly are shown in figure 6.2. The width of the channel at the flow-focussing geometry is 105 μm and the depth is 100 μm . Before and after the junction the channels widen to a width of 300 μm but the depth remains constant at 100 μm . The overall chip dimensions are 22.5 by 15.0 mm with a thickness of 4 mm. The flow focussing junction is positioned half way along the chip. The two chips were mounted in a custom built holder. A Viton gasket of thickness 0.3 mm and through holes with a diameter of 300 μm was placed between the chips to make a water-proof seal. The position of the two chips in the holder was adjusted with the aid of a microscope so that the channels were aligned with the minimum mismatch. The position was fixed by closing the clamps at the center of the holding device.

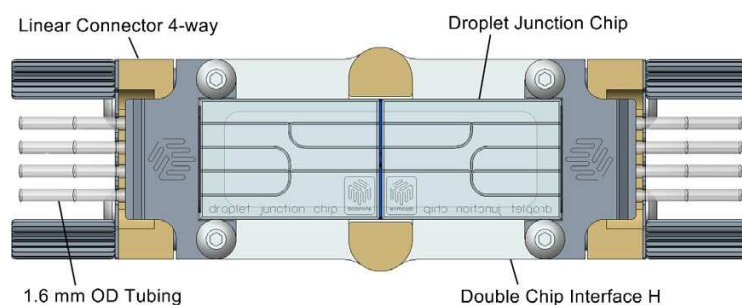


Figure 6.2: The setup of the two chips within the holder. Only the two flow focussing junctions are utilized.

For the later experiments, custom designed microfluidic chips were built with smaller junction and channel dimensions. Two chip systems were designed with junction

diameters of 75 and 50 μm . The junctions were placed 2.5 mm from the chip edge and the overall dimensions of the microfluidic chips were 15 \times 11 mm and a new holder was constructed based on figure 6.2. The same gasket used for the commercial microfluidic chips was used with the new designs.

Finally, a single double emulsion chip was designed based on the geometry of the commercially available 100 μm junction design. The two junctions were separated by a distance of 1 cm. The microfluidic chip was first surface treated to make it hydrophobic at both junctions and then the hydrophobic coating at one junction was removed using an alkali treatment. The position of the change of the surface conditions from hydrophobic to hydrophilic between the two junctions was not controlled precisely.

Liquids were applied to the chips by three pressure controlled pumps (Mitos Part no. 3200016). Tubing of inner diameter 300 μm and 1/16th inch outer diameter was used to connect the chip to the pumps. The oil flow and outer liquid flow was split off the chip using Upchurch Y-junctions (Part no. P-512). Care was taken to make the length of the tubing in both arms between the chip and the Y-junction the same. For the inner water, a flow resistor was placed in-line between the pressure pump and the chip. This consisted of a 20 cm length of tubing of inner diameter 250 μm . Two 400 mL external pressure reservoirs were used for the oil and external phase which were capable of holding inside a 250 mL flask. For the internal water phase, the reservoir of the pressure pump was used. Droplet formation was observed using an Olympus SZX16 microscope equipped with an Olympus XM10 camera. Samples of the emulsions were collected on a microscope slide and the size of the droplets measured using an Axioplan microscope from Zeiss, Germany. The images were used to estimate the size and uniformity of the droplets. A correction to the size of the inner water droplet diameters obtained by microscopy was applied³⁶.

The fluids on the chip were pressure driven without flow meters inline, therefore, when the droplet generation conditions were stable, samples were collected over 1 min periods, weighed, left overnight to dry and then weighed again to obtain an estimate of the flow rates of the different water and oil phases.

For NMR, the output tube from the chip was submersed in a beaker filled with the outer aqueous phase. The double emulsions were then collected, under water in an inverted cut-off NMR tube of length 3.5 cm and outer diameter 4 mm. When full, the tubes were placed in 5 mm NMR tubes for the NMR analysis.

3.3. NMR

All NMR experiments were performed on a Bruker Avance DSX400 wide bore NMR spectrometer. The Larmor frequency for protons was 400.13 MHz. All experiments have been performed with either a Bruker micro-imaging probe with a single tuned proton 15 mm RF insert or a dedicated self-diffusion NMR probe (Bruker diff25) with a 5 mm proton RF insert. The proton 90° pulse was 24.5 μ s when using the imaging probe and 12.5 μ s when using the diffusion probe. Bruker BAFPA40 and a GREAT60 gradient amplifiers were used for the pulse field gradient measurements. The temperature was set to 25.0 $^\circ$ C and was calibrated using a standard ethylene glycol sample (Bruker Biospin). The temperature was maintained using the gradient cooling water system flowing through the gradient system of the probe. The gradient amplifiers were calibrated using a doped 1% water in D_2O sample (Bruker Biospin) to give a self-diffusion coefficient for the water of 1.90×10^{-9} m²/s. The pulsed-gradient stimulated echo pulse sequence²⁷ was used for the diffusion experiments employing trapezoidal shaped gradient pulses with a rise time of 0.3 ms. Diffusion experiments used to obtain the water droplet size and the amount of outer water were acquired with 128 points. The gradient pulse magnitude was varied linearly and the range depended on the sample. Further details will be given in the results section for individual experiments. A proton T_1 measurement on the double emulsion was acquired for each sample to obtain the correct recycle delay to use. Typically, the water T_1 in the double emulsion was 2.9 s. The gradient pulse, δ , for the pulse field gradient experiments was 1 and 2 ms. The diffusion observation time, Δ , was set depending on the properties of the emulsion, typically for protons, experiments were performed with different Δ s, varying from 3 s to 8 s. Figure 6.3 shows the pulse sequence used for the diffusion experiments.

Data analysis of the NMR diffusion experiments were performed using in-house software programmed in the Python programming language using the Numpy and Scipy scientific libraries³⁷. The programs are available by request from the corresponding author.

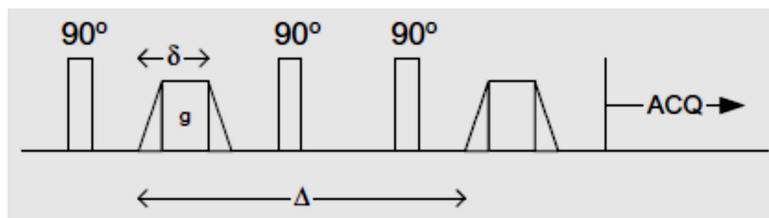


Figure 6.3: The pulsed-field stimulated echo pulse sequence using trapezoidal gradients.

4. Results

4.1. Droplet production in two step regime

When no emulsifier was present in the inner water phase, water droplets were easily formed at the first flow focussing junction on the hydrophobic chip. The droplets then passed unperturbed across the interface between the two chips and arrived at the second junction on the hydrophilic chip. Figure 6.4 shows a typical set of images of how the two chip system performed.

Figure 6.4a shows the generation of water droplets on the hydrophobic chip. figure 6.4b shows the section between the two chips and the droplets passing unperturbed, from one chip to the other. Finally, in figure 6.4c the oil surrounding the water droplets is then pinched off at the second flow focussing hydrophilic junction to form water-in-oil-in-water double emulsions. Under these specific conditions, the water droplets, as they pass through the second junction, are squeezed and split into two. Figure 6.5 shows a representative sample of a double emulsion prepared in the two step mode. Both inner and outer droplet size are regular and the number of water droplets in each oil droplet is controlled. The average inner water droplet diameter measured from the image is 74 μm (uncorrected) and the outer oil droplet size is 165 μm . The number of water droplets within the oil droplets can be varied by altering the flow conditions. However, the size range is limited, if small inner water droplets on the order of 30-45 μm are prepared

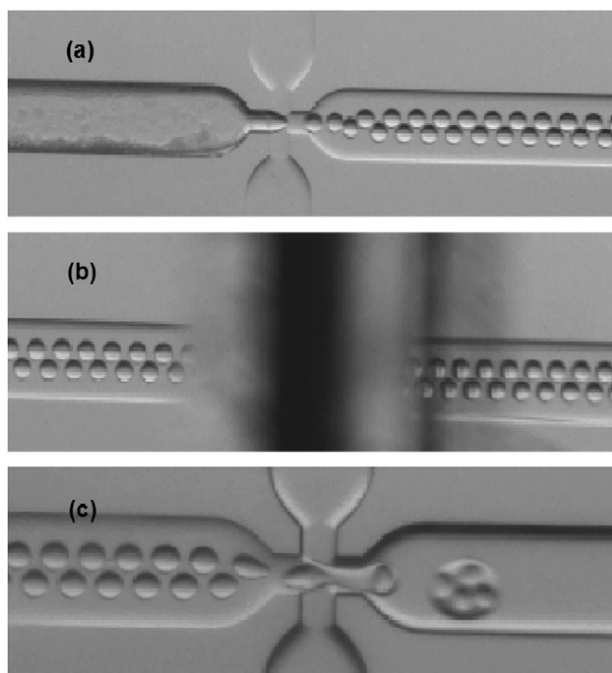


Figure 6.4: Generation of water-in-oil-in-water double emulsion in a two step fashion. (a) Water in oil droplets are formed at the first junction. (b) Water in oil droplets pass across the junction from one chip to the other unperturbed. (c) Double emulsion formed in second flow focussing junction. In this case, as the droplets pass through the junction, they are squeezed and split into two. The large channel width is $300\ \mu\text{m}$ and the junction widths are $100\ \mu\text{m}$.

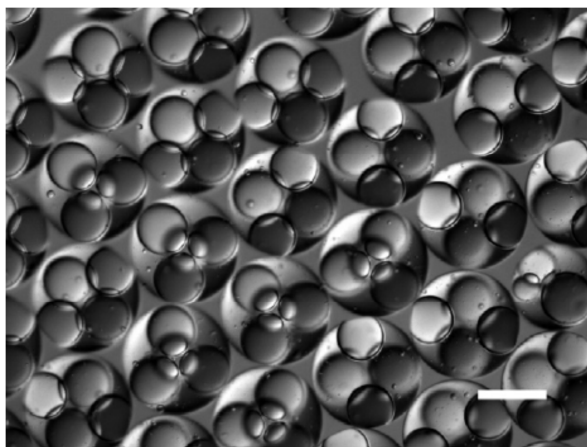


Figure 6.5: Representative sample of double emulsion produced when operating the chip in the two step mode. Scale bar = $100\ \mu\text{m}$.

then the oil droplets become much larger, as increased oil flow is necessary to produce the small inner water droplet size.

4.2. Droplet production in jetting regime

When 1% SDS was added to the inner phase, water droplets were no longer formed at the first flow focussing junction on the hydrophobic chip under similar flow conditions as in figure 6.4. Instead a stable jet was formed that travelled the length of both chips.

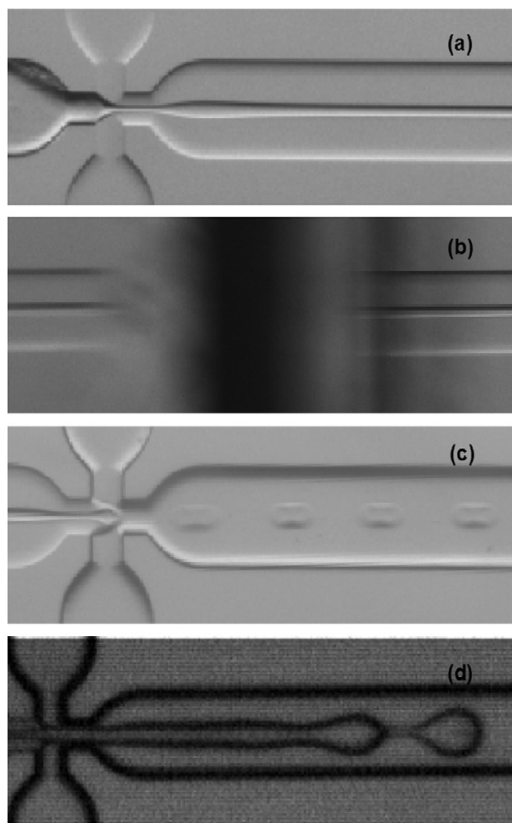


Figure 6.6: Generation of double emulsion in a single step. (a) The water jet is formed in first junction. (b) The water jet crosses the junction unperturbed. (c) The jet arrives at the second junction and is broken up into droplets in a dripping mode. (a-c) Corresponds to 1% SDS in the inner water phase. (d) Corresponds to 1% Tween20 in the inner water phase. The large channel width is 300 μm and junction widths are 100 μm .

The jet passed across the interface between the two chips and through the second flow-focussing junction on the hydrophilic chip. By adjusting the flow conditions of the three phases, the jet could be maintained, but droplets could also be formed at the second junction as shown in figure 6.6.

Table 6.1: Summary of physical parameters of the liquid used and estimation of flow and droplet sizes for 1% SDS and 1% Tween20 in the inner water phase.

	SDS	Tween20
Inner water pressure (mbar)	270	1440
Oil pressure (mbar)	300	1100
Outer water pressure (mbar)	170	300
Flow inner water ($\mu\text{L/h}$)	108 ± 13	2037 ± 191
Flow oil ($\mu\text{L/h}$)	935 ± 26	3765 ± 35
Flow outer water (mL/h)	21.0 ± 0.5	43.8 ± 0.9
Oil diameter (μm)	86.8 ± 0.8	165.0 ± 1.7
Inner water diameter (μm)	47.1 ± 1.2	133.6 ± 2.4
Inner water diameter ^a (μm)	39.9 ± 1.3	116 ± 2.2
Inner water viscosity (mPa s)	1	1
Oil viscosity (mPa s)	49.0	49.0
Oil viscosity (2% PGPR) (mPa s)	65 ± 2	65 ± 2
Outer water viscosity (2% bLG) (mPa s)	1.1	1.1
Inner water/oil surface tension (mN/m)	2	5

a = Corresponds to corrected inner water droplet diameter. Flows estimations calculated using corrected inner water droplet diameter.

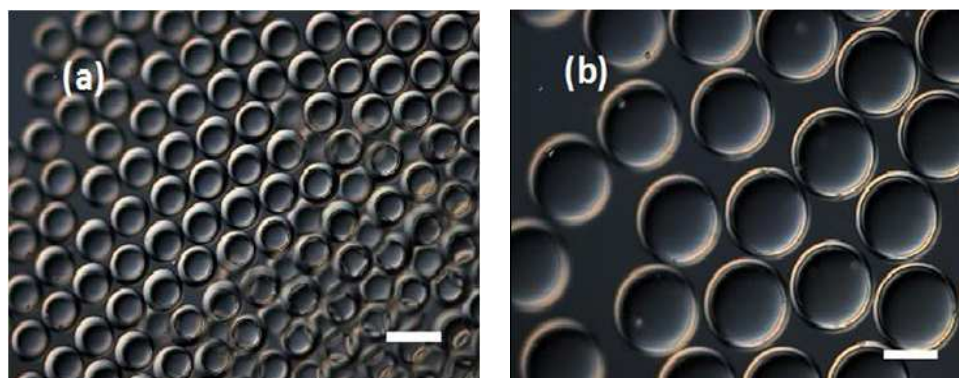


Figure 6.7: Representative sample of double emulsion produced when operating the chip in the jetting mode. (a) With 1% SDS in the inner aqueous phase, (b), with 1% Tween20. Scale bar 200 μm .

In this mode single water droplets were formed in the oil droplets and the diameter of the oil droplets could be varied between 65 and 95 μm . The inner water droplet diameter could be varied independently of the outer oil droplet diameter over the range of 35–55 μm . Fig. 6.7a gives a representative sample of the double emulsion formed when using 1% SDS in the inner water phase. The conditions to produce the droplets are given in table 6.1.

The droplet production rate (water and oil) was found to be 1.0 mL/h and the volume ratio of water droplet to oil droplet was 1:8.7. The surfactant in the inner water phase was then changed to Tween 20, a food grade emulsifier. Again, a stable jet could be formed, but the flow conditions needed were much higher. Under these conditions, the double emulsion did not form at the second junction exactly, but a jet was formed which broke up into droplets in the large channel (Fig. 6.6d). The droplet production rate of the water and oil was found to be 5.7 mL/h by weighing. The final droplet diameters were larger, 116 μm and 165.0 μm for the water and oil respectively (see fig. 6.7b) and the ratio of inner water to oil in the droplets was approximately 1:2.

4.3. Reduced junction diameter and single microfluidic chip designs

The simple solution of bringing two microfluidic chips together to produce double emulsions was further explored by designing microfluidic chips with smaller junction and channel geometries. Microfluidic flow focussing chips were designed with junction geometries with widths and depths of 75 and 50 μm . In both cases, double emulsion droplets were obtained with an overall reduction in size. A summary of typical operating conditions can be found in table 6.2 and representative microscopy images in figure 6.8. Again, a 1% SDS aqueous solution was used for the inner phase, sunflower oil with 2% PGPR for the oil phase and an aqueous buffered solution of 1% b-LG was used for the outer phase.

Finally, an attempt was made to design a single microfluidic double emulsion chip. The design was based on the 100 μm junction designs. Two junctions were placed on a 22.5-15 mm chip separated by a distance of 1 cm. The chip was made hydrophobic and then one junction was treated with sodium hydroxide to make it again hydrophilic. Figure

6.8c shows the double emulsion droplets formed from this device and the conditions are given in table 6.2. In the jetting regime in which the chips were operated, the size of the oil droplets produced by the three different junction sizes can be estimated by calculating

Table 6.2: Operating conditions for flow focussing microfluidic chips as a function of junction cross Section 50 and 75 μm were made up of two separate chips connected by a gasket. 100 μm junction chip was a single chip with the hydrophobic and hydrophilic junction with the cross over point mid-way between the two junctions.

Junction diameter (μm)	50	75	100
Inner water pressure (mbar)	498	147	191
Oil pressure (mbar)	480	129	181
Outer water pressure (mbar)	450	90	186
Oil diameter (μm)	42.7 ± 0.7	61.1 ± 1.2	69.8 ± 1.8
Inner water diameter (μm)	24.7 ± 1.2	31.1 ± 1.5	43.1 ± 1.4
Inner water diameter ^a (μm)	21.1 ± 1.1	26.4 ± 1.3	37.0 ± 1.3
Flow inner water ($\mu\text{L/h}$)	32 ± 8	24 ± 4	130 ± 21
Flow oil ($\mu\text{L/h}$)	248 ± 32	274 ± 29	745 ± 36
Flow outer water ($\mu\text{L/h}$)	10.0 ± 0.3	7.9 ± 0.7	32.8 ± 0.7

a = corrected inner water droplet diameter. Flow estimations calculated using corrected inner water droplet diameter.

the volume of a cone that has same height and diameter of the junction cross section. The expected estimated diameter of droplets produced by the three sizes are then 79, 59, and 39 μm which are comparable to that found experimentally and reported in table 6.2.

The production of double emulsions in the jetting regime using either the double chip approach or the single chip solution was sufficiently stable over time that samples could easily be collected for further analysis. It was found that as the double emulsion droplet size was reduced they became more stable for the given surfactant system used. Below an oil droplet diameter of 100 μm the production rate and stability of the emulsions was sufficient to perform NMR experiments that took just under an hour to perform.

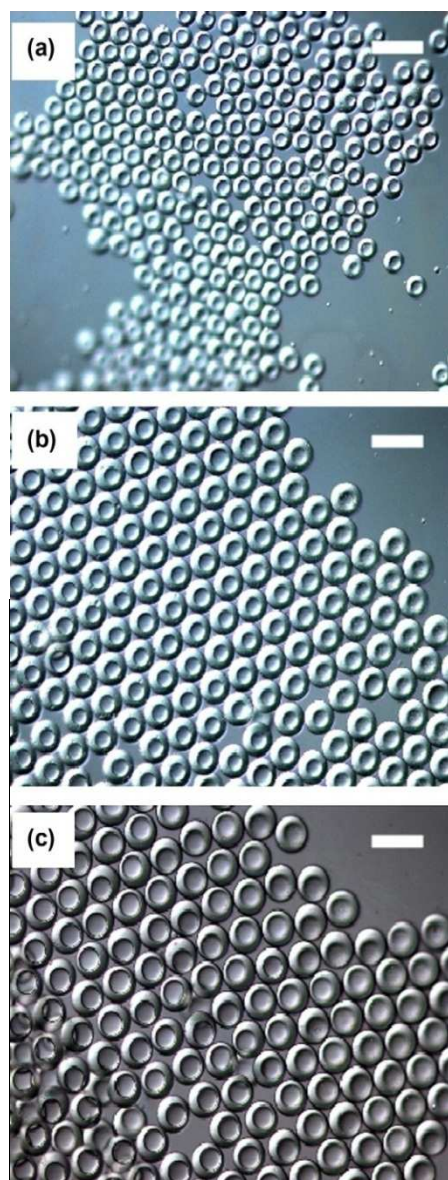


Figure 6.8: Representative examples of droplets produced from microfluidic chips with junction sizes of (a) 50 μm , (b) 75 μm and (c) 100 μm . 100 μm junction chip was a single chip device with junctions separated by a distance of 1cm. 50 μm and 75 μm chip devices consisted of two separate glass chips. Scale bar 100 μm .

4.4. NMR analysis

A sample of the double emulsion containing 1% SDS in the inner water phase was collected for NMR analysis. From microscope images, the diameter of the inner water droplets and outer oil droplets were $39.3 \pm 1.3 \mu\text{m}$ and $86.8 \pm 0.8 \mu\text{m}$ respectively. The uniformity of the two types of droplets were 1.8% (water) and 0.8% (oil). The PGSTE echo response for the water in the double emulsion is shown in figure 6.9a. The data is shown in a semi-log plot so that the maxima at large gradient strength is clearly observed. The maxima arises from the low polydispersity of the emulsions. The data in figure 6.9a is fit using Equations (6.1) and (6.4) and the numerical inversion regularization method. The results for the inner and outer water content of the double emulsion are shown in figure 6.9b, the percentage of inner water was 82% and the outer water was 18%. For the water contained inside the inner water droplets 98% by volume is found with a diameter of $43.2 \pm 1.0 \mu\text{m}$ with a minor secondary peak at $19.3 \mu\text{m}$. The apparent diffusion coefficient of the outer water from the analysis gives a value of $1.22 \times 10^{-9} \pm 0.05 \times 10^{-9} \text{ m}^2/\text{s}$. The diameter obtained by the NMR method agrees well with the microscopy data only after the correction due to lens effect of the double emulsions is taken into account.

In a second NMR experiment, two double emulsions of different inner water droplet size were collected sequentially in an NMR tube so that the height of each sample filled approximately half of the NMR detector coil. From microscopy images, the inner water droplet diameter of the two emulsions was $40.0 \pm 1.4 \mu\text{m}$ and $50.6 \pm 1.8 \mu\text{m}$. The NMR diffusion results are summarized in figure 6.10. The percentage of outer water and inner water was 46% and 54% respectively. In the distribution of droplet diameters two distinct diameters are resolved with values of $37.1 \pm 1.0 \mu\text{m}$ and $52.1 \pm 0.6 \mu\text{m}$. The percentage of each component was 22% and 32% respectively. The apparent diffusion coefficient of the outer water component was found to be $1.26 \times 10^{-9} \text{ m}^2/\text{s}$.

It was noted, for this system, when the data was analyzed using the Murday Cotts equation, the two different inner water droplet diameters were not resolved and a single value was obtained which came somewhere close to the average of the two sizes. Only with the short pulse approximation approach were the two droplet sizes resolved.

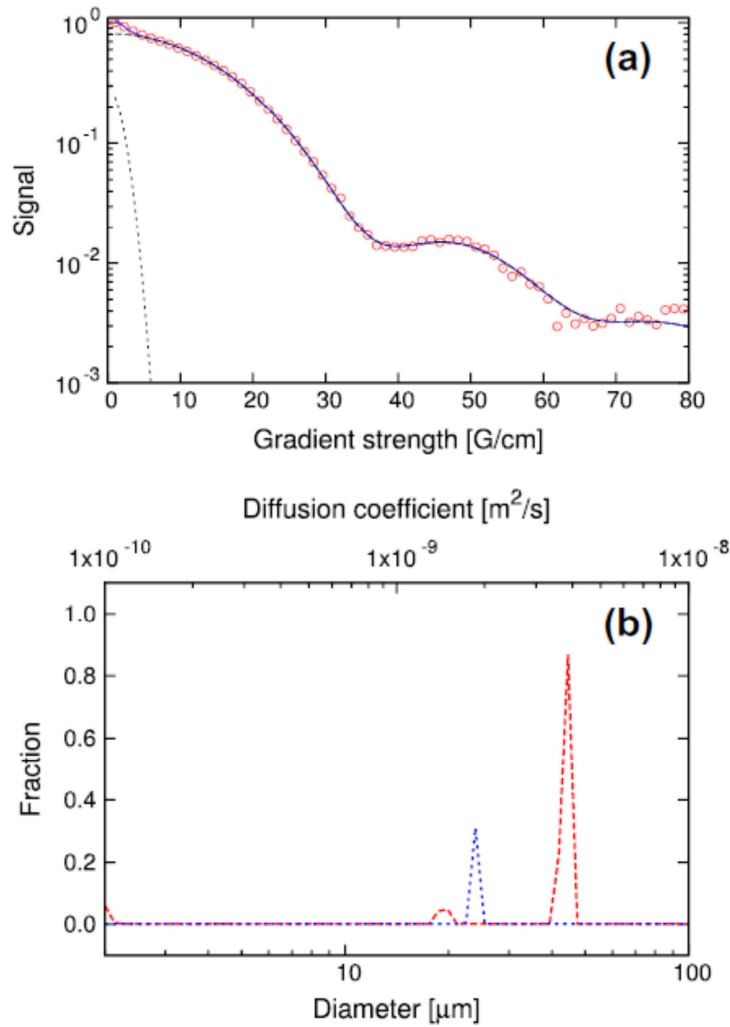


Figure 6.9: Numerical regularized inversion analysis of water ^1H self-diffusion NMR data using the SGP equation obtained from double emulsion prepared using 1% SDS in the inner water droplet phase. (a) Fit of PGSTE data showing the curves arising from the water inside the double emulsion and outside the phase. (b) Distribution of inner water droplet size (---) and apparent diffusion coefficient of external water (...). Experimental conditions $\delta = 2$ ms, $\Delta = 3$ s. From fit, outer water $D_{\text{app}} = 1.9 \times 10^9$ m^2/s and inner water droplet diameter = 43 μm . The percentage of each component was 23% (outer water) and 77% (internal water droplets). For clarity, only 64 of the 128 experimental data points are displayed.

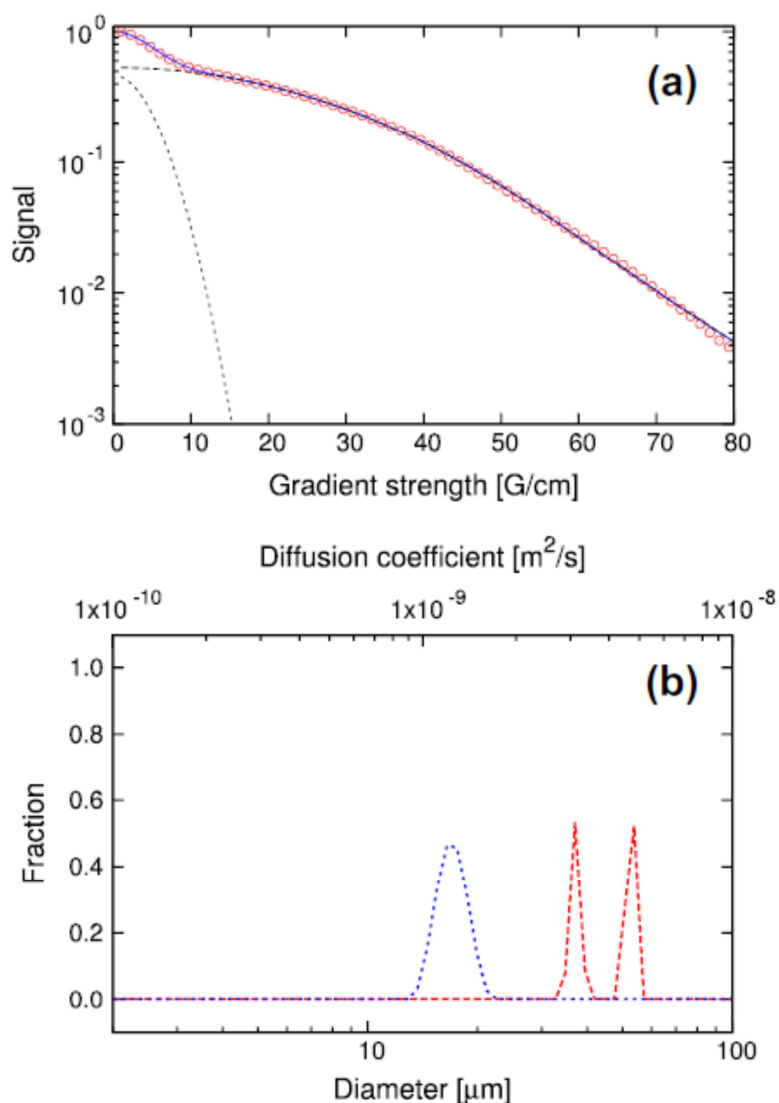


Figure 6.10: Numerical inversion analysis of water ^1H self-diffusion NMR data using SGP equation for diffusion within a sphere obtained from double emulsion prepared using 1% SDS in the inner water droplet phase. Two different sized droplets are present in the NMR tube. (a) Fit of PGSTE data showing the curves arising from the water inside the double emulsion and outside the phase. (b) Distribution of inner water droplet size (---) and apparent diffusion coefficient of external water (...). Experimental conditions $\delta = 1$ ms, $\Delta = 3$ s. From the fit, the outer water $D_{app} = 1.25 \times 10^9$ m 2 /s, droplet 1 diameter = 37 μm and droplet 2 diameter = 54 μm . The percentage of each component of water was 46% (outer water), 21% for droplets 1 and 33% for droplets 2.

To check whether this was just a problem with the numerical inversion, the data was fit using a non-linear least squares approach. The fitting function was allowed to have two droplet diameter components present, but again, the Murday Cotts equation gave a solution where only one main inner droplet diameter was needed. The solution using the short pulse approximation equation, again gave a solution where the two different droplet sizes were present in a ratio of approximately 50:50. The results are summarized in table 6.3.

Table 6.3: Summary of regularized numerical inversion fitting of diffusion data for two double emulsions layered on top of each other.

	Murday Cotts eqs. (6.1) and (6.2)	SGP eqs. (6.1) and (6.4)	Microscopy
Outer water (%)	46.8	46	
Inner water (%)	53.2	54	
$D_{app} (\times 10^9) (m^2/s)$	1.3	1.22 ± 0.07	
Diameter (μm)	48	37.1 ± 1.0 52.1 ± 0.6	$40.0 \pm 1.4 \mu m$ $50.6 \pm 1.8 \mu m$

4.5. Stability of monodisperse emulsions over time

The long term stability of the monodisperse double emulsions with respect to osmotic pressure imbalance over time was followed by NMR. Two monodisperse double emulsions made from the single double emulsion microfluidic chip with 100 μm flow-focussing junctions were collected in 4 mm NMR tubes and allowed to cream. By microscopy, the outer diameters of the two emulsions were 91 and 89 μm and the initial inner water droplet diameters were 66(57) and 56(48) μm respectively, with the corrected value in brackets. The stability of the double emulsions was followed by PGSTE NMR of the water signal to give the inner water diameter of the emulsions as a function of time. Figure 6.11a shows the NMR data collected over a period of 4 days for the monodisperse double emulsion with an outer diameter of 91 μm . From the graph one can see that the position of the first minima moves to larger q values or smaller diameter values as a function of time. This is an indication that the inner water droplet diameter is

decreasing. The fact that diffusion data as a function of time, all show a minima, indicates that the overall polydispersity of the inner water droplets of the double emulsion remains low as a function of time.

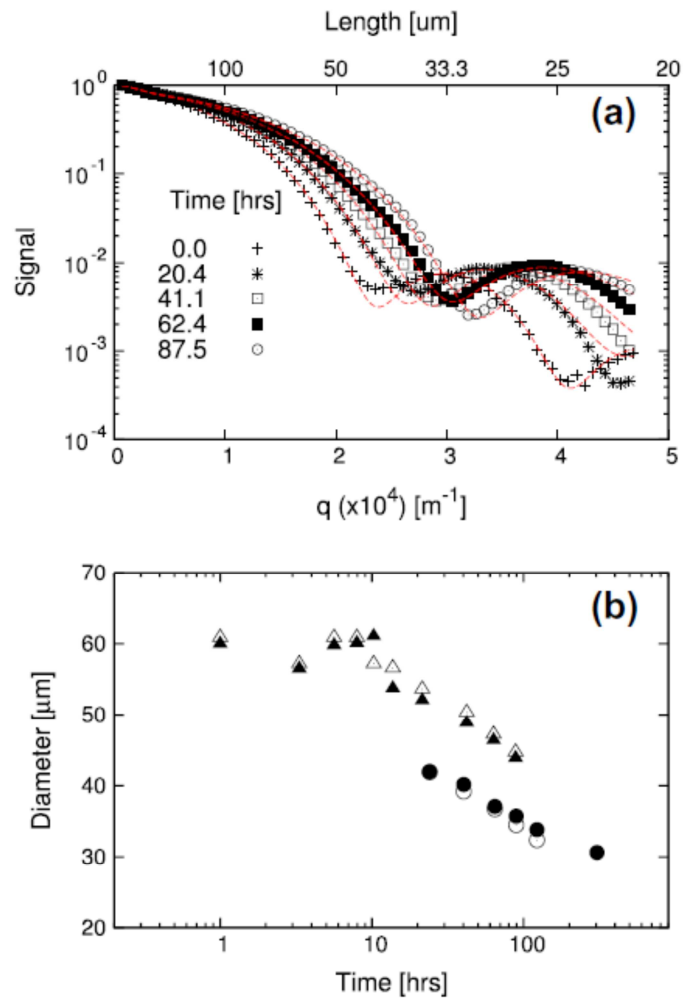


Figure 6.11: (a) Regularized numerical inversion analysis of PGSTE data of the water signal in a monodisperse emulsion as a function of time prepared using 1% SDS in the inner aqueous phase, 1% b-LG in buffer for the outer phase and sunflower oil containing 2% PGPR. (b) Plot of the inner water droplet size for two double emulsions with different initial sizes of 48 (circles) and 57 μm (triangles). The filled symbols arise from calculating the diameter from the position of the first minimum and the open symbols represent the analysis using the regularized numerical inversion approach.

The reduction in inner water diameter as a function of time is due to a difference in osmotic pressure between the inner and outer water phases of the double emulsions. Analysis of the NMR data to give the inner water diameter can be made in two ways, the first is to measure the position of the first minima and take the reciprocal multiplied $\sqrt{1/2}$ to give the diameter or to fit the data as before by applying the Equations. (6.1) and (6.4) using the regularized numerical inversion approach. The results for both emulsions are plotted in figure 6.11b on a logarithmic time scale. The two analysis methods overlap reasonably well. The more complete data set (triangles) would appear to show that there is an initial induction period where the inner droplet size remains nearly constant and then decreases due in part to the establishment of a diffusion gradient across the oil interface of the migrating species. Given the uncertainty in the data, the rate of decrease in the inner water droplet diameter of the two emulsions are essentially the same.

The rate of change in volume of the inner droplets due to the osmotic imbalance is dependent on a number of factors^{38, 39} such as the diffusion coefficient of the water in the oil layer, the relative surface areas of the droplets, the thickness of the oil film and changes in the relative concentration of the dissolved species in the two water environments as water transport takes place. A full analysis of the data in figure 6.11 is beyond the scope of this paper, even though the monodisperse emulsion should represent an ideal system, the fact that emulsion is concentrated and the difference in densities of the water and oil will make the emulsion geometry non-concentric makes a simple treatment of the data difficult. The general linearity of the data in figure 6.11 would suggest that further experimental work using self-diffusion NMR on concentrated monodisperse emulsions will provide useful insight into the stability of double emulsions.

5. Discussion

The microfluidic solutions to make monodisperse double emulsions described in this paper are based on the use of two chips of differing hydrophilicity or finally, on a single microfluidic chip where the junctions are far enough apart to make chemical surface modification a simple procedure. It would appear that the single microfluidic approach is the more elegant solution, but this may not necessarily be the case. The two microfluidic

chip approach has some advantages when the surfactants used over time modify the surface properties of the microfluidic chip making the hydrophilic surfaces less and less hydrophilic. This problem can be reversed by dismantling the system and washing the hydrophilic microfluidic chip with a suitable solution without affecting the hydrophobic microfluidic chip. One disadvantage of the two microfluidic chip approach is the disturbance of the gasket to the flow of the liquids when the system is operated in a jetting mode. It was observed that with the two microfluidic chip approach, the flow rates of the inner water and oil phase had to be higher to make the jet pass through the gasket and continue to the second junction without phase inverting.

Further improvement on the design in terms of alignment can be envisaged by implementing etched channels on the chips to improve the co-alignment. The production of double emulsions has been shown to work by producing a jet and was achieved by introducing a surfactant into the inner phase to reduce the surface tension between the inner water phase and oil phase. Stable jet formation within microfluidic channels has been discussed extensively^{19, 20, 40} and can be understood simply in terms of minimizing the Raleigh instability of the jet by increasing the flow rates of the two liquids to an extent that body of fluid moves faster along the channel than the instability can propagate back along itself. This can be followed by calculating the Weber number between the inner water phase and oil phase. The reduction in Weber number can be achieved by reducing the interfacial tension between the two phases as has been demonstrated, or by reducing the viscosity ratio of the two liquids. For real food grade systems, the second approach might be a better avenue to explore as there is a trend to reduce the number and amount of surfactants used in processed foods.

The double emulsions produced were stable enough to perform NMR experiments to determine the size of the inner water droplets and the distribution of water. The analysis of the data was based upon a regularized numerical inversion approach. This approach requires the introduction of a coefficient k to stop the solution becoming oscillatory due to the noise in the experimental data. The value of which must be chosen using a variety of approaches such as L-curve⁴¹ and generalized cross-validation methods⁴². Since the experiments have been performed upon monodisperse emulsions, k

can be chosen quite arbitrarily as it was found that the range of values could be used without affecting the overall results significantly. This will not be case for using the method on more polydisperse systems.

6. Conclusion

To understand the physical chemical properties that give rise to stable double emulsions quantitative characterization of the double emulsion is required in terms of the water distribution within the inner and outer phases and size distribution of the inner water droplets. Experimental NMR self-diffusion methods offer a means to bring this quantification about, at the same time the techniques offer other desirable attributes in that they are non-destructive, can work with opaque materials and work on statistically significant sample sizes.

Developments outlined in this paper have enabled systematic studies on double emulsions, firstly, technical developments of microfluidic devices have enabled the production of double emulsions in sufficient quantities for analysis. Secondly, NMR-PFG diffusion analysis has been adapted such that it can be readily applied to multiple emulsions and inform on water distribution and inner water droplet size distribution without the assumption of a specific distribution shape. Thirdly, we have demonstrated the use of this technique to quantify the evolution in the droplet size distribution with time for two different emulsions due to the osmotic pressure difference between the inner and outer water populations.

The work outlined in this paper should lead to better understanding of the physicochemical properties underpinning the stability of double emulsions. The work is also applicable to polydisperse double emulsions and should lead to applications in characterizing food emulsions at low field^{43, 44}. In this paper we have concentrated on following and characterizing the water in double emulsions, but the work is also applicable to follow the release and encapsulation of dissolved species within the water such as sodium salts or pharmaceutical actives⁴⁵⁻⁴⁷ where the double emulsion is being used as a delivery system.

References

1. F. Leal-Calderon, F. Thivilliers and V. Schmitt, *Curr. Opin. Colloid Interface Sci.*, 2007, **12**, 206–212.
2. Y. zalp, N. zdemir, S. Kocagz and V. Hasirci, *J. Microencapsulation*, 2001, **18**, 89–110.
3. H.C. Shum, D. Lee, I. Yoon, T. Kodger and D.A. Weitz, *Langmuir*, 2008, **24**, 7651–7653.
4. S. Okushima, T. Nisisako, T. Torii and T. Higuchi, *Langmuir*, 2004, **20**, 9905–9908.
5. A.S. Utada, E. Lorenceau, D.R. Link, P.D. Kaplan, H.A. Stone and D.A. Weitz, *Science*, 2005, **308**, 537–541.
6. A.O. Saeed, J.P. Magnusson, E. Moradi, M. Soliman, W. Wang, S. Stolnik, K.J. Thurecht, S.M. Howdle and C. Alexander, *Bioconjugate Chem.*, 2011, **22**, 156–168.
7. J. Thiele and S. Seiffert, *Lab Chip – Miniaturisat. Chem. Biol.*, 2011, **11**, 3188–3192.
8. K. Pays, J. Giermanska-Khan, B. Pouligny, J. Bibette and F. Leal-Calderon, *J. Controlled Release*, 2002, **79**, 193–205.
9. K.J. Packer and C. Rees, *J. Colloid Interface Sci.*, 1972, **40**, 206–218.
10. M.L. Johns and K.G. Hollingsworth, *Prog. NMR Spectrosc.*, 2007, **50**, 51–70.
11. J.P. Hindmarsh, J. Su, J. Flanagan and H. Sing, *Langmuir*, 2005, **21**, 9076–9084.
12. X. Guan, K. Hailu, G. Guthausen, F. Wolf, R. Bernewitz and H.P. Schuchmann, *Eur. J. Lipid Sci. Technol.*, 2010, **112**, 828–837.
13. R. Bernewitz, G. Guthausen and H.P. Schuchmann, *Magn. Reson. Chem.*, 2011, **49**, S93–S104.
14. K.G. Hollingsworth and M.L. Johns, *J. Colloid Interface Sci.*, 2003, **258**, 383–389.
15. L.-Y. Chu, A.S. Utada, R.K. Shah, J.-W. Kim and D.A. Weitz, *Angew. Chem. Int.*, 2007, **Ed. 46**, 8970.
16. A.R. Abate, J. Thiele and D.A. Weitz, *Lab Chip*, 2011, **11**, 253–258.
17. S.L. Anna, N. Bontoux and H.A. Stone, *Appl. Phys. Lett.*, 2003, **82**, 364–366.
18. T. Nisisako, S. Okushima and T. Torii, *Soft Matter*, 2005, **1**, 23–27.
19. A.S. Utada, A. Fernandez-Nieves, H.A. Stone and D.A. Weitz, *Phys. Rev. Lett.*, 2007, **99**, 0945021–0945024.
20. A.S. Utada, A. Fernandez-Nieves, J.M. Gordillo and D.A. Weitz, *Phys. Rev. Lett.*, 2008, **100**, 0145021–0145024.
21. M.A. Herrada, A.M. Ganan-Calvo and P. Guillot, *Phys. Rev.*, 2008, **E 78**, 0463121–0463127.
22. A.R. Abate, J. Thiele, M. Weinhart and D.A. Weitz, *Lab Chip*, 2010, **10**, 1774–1776.
23. W.-A.C. Bauer, M. Fischlechner, C. Abell and W.T.S. Huck, *Lab Chip*, 2010, **10**, 1814–1819.
24. P.T. Callaghan, A. Coy, D. MacGowan, K.J. Packer and F.O. Zelaya, *Nature*, 1991, **351**, 467–469.
25. P.T. Callaghan, S.L. Codd and J.D. Seymour, *Concepts Magn. Reson.*, 1999, **11**, 181–202.

26. P.T. Callaghan, D. MacGowan, K.J. Packer and F.O. Zelaya, *J. Magn. Reson.*, 1990, **90**, 177–182.
27. J.E. Tanner, *J. Chem. Phys.*, 1970, **52**, 2523–2526.
28. J.S. Murday and R.M. Cotts, *J. Chem. Phys.*, 1968, **48**, 4938–4945.
29. W.S. Veeman, *Ann. Rep. NMR Spectrosc.*, 2003, **50**, 202–216.
30. B. Balinov, B. Jönsson, P. Linse and O. Söderman, *J. Magn. Reson. Ser. A*, 1993, **104**, 17–25.
31. P.T. Callaghan, K.W. Jolley and R.S. Humphrey, *J. Colloid Interface Sci.*, 1983, **93**, 521–529.
32. J.D. Wilson, *J. Mater. Sci.*, 1992, **27**, 3911–3924.
33. W.H. Press, S.A. Teukolsky, W.T. Vetterling and B.P. Flannery, *Numerical Recipes in C: The Art of Scientific Computing*, second ed., Cambridge University Press, New York, NY, USA, 1992.
34. C.L. Lawson and R.J. Hanson, *Solving Least Squares Problems*, Prentice Hall, Englewood Cliffs, NJ, 1974.
35. C.L. Lawson, R.J. Hanson, *Solving Least Squares Problems*, Classics in Applied Mathematics, SIAM, Philadelphia, 1995.
36. R.M. Erb, D. Obrist, P.W. Chen, J. Studer and A.R. Studart, *Soft Matter*, 2011, **7**, 8757.
37. E. Jones, T. Oliphant and P. Peterson, et al., *SciPy: Open source scientific tools for Python*, 2001.
38. R. Mezzenga, B.M. Folmer and E. Hughes, *Langmuir*, 2004, **20**, 3574–3582.
39. F. Leal-Calderon, S. Homer, A. Goh and L. Lundin, *Food Hydrocolloids*, 2012, **27**, 30–41.
40. M.L. Cordero, F. Gallaire and C.N. Baroud, *Phys. Fluids*, 2011, **23**, 094111.
41. E. Castro-Hernández, V. Gundabala, A. Fernández-Nieves and J.M. Gordillo, *New J. Phys.*, 2009, **11**, 075021.
42. G. Wahba, *Statist. Decis. Theory Relat. Top.*, 1982, **III (2)**, 383–418.
43. M.A. Voda and J. van Duynhoven, *Trends Food Sci. Technol.*, 2009, **20**, 533–543.
44. J.P.M. van Duynhoven, G.J.W. Goudappel, G. van Dalen, P.C. van Bruggen, J.C.G. Blonk and A.P.A.M. Eijkelenboom, *Magn. Reson. Chem.*, 2002, **40**, S51–S59.
45. W. Fieber, V. Hafner and V. Normand, *J. Colloid Interface Sci.* 2011, **356** 422–428.
46. K.I. Momot and P.W. Kuchel, *Concepts Magn. Reson.*, 2003, Part A **19A**, 51–64.
47. H. Metz, K. MSder, *Int. J. Pharm.*, 2008, **364**, 170–175.

Chapter 7

General Discussion

Part of this chapter will be published as: Maan, A. A., , Boom, R., Schroën, K. Future aspects of microfluidic emulsification for food preparation.

The high energy efficiency and excellent emulsion quality that can be obtained with microfluidic droplet generators (chapters 1 and 2) inspired a further study into whether these systems can be used at larger scale. EDGE emulsification systems are distinct among all microfluidic droplet generators for their ability to produce multiple droplets at the same time from a single channel or plateau ¹, and therefore the EDGE systems were taken as a starting point.

This chapter, summarizes the main results of the work done on metal coated EDGE systems for preparation of w/o and o/w emulsions, and will elaborate on the effects of surface wettability and surface roughness. In the second part of the chapter, various emulsification systems will be compared and an outlook on scale-up of the emulsification systems for food applications will be given. The chapter will conclude with some general remarks.

1. Thesis highlights

Emulsions were prepared successfully with semi-metal microfluidic devices, which is the first essential step towards fully metallic systems, thought necessary for food production, and directly linked to general acceptance of the technology. The emulsification behaviour was found to be significantly affected by the surface properties (roughness and wettability) of the metal (Cu, CuNi and CuNi/Cu) coated surfaces. A plateau with smooth surfaces (roughness <20 nm) was completely and uniformly filled with dispersed phase. At increased roughness (20-40 nm) the dispersed phase, on reaching the edge of the plateau, split into so-called fingers while at even larger roughness (>40 nm) strong fingering and only partial filling of the plateau occurred. The increase in roughness decreased the total number of droplet formation points. In spite of the different patterns of plateau filling, monodispersed droplets with sizes almost 6 times the plateau height were produced with all the surfaces, although marked differences in pressure stability occurred (chapters 3 and 4); these effects could even be so great that they more than compensated for the reduced number of droplet formation points, effectively leading to a productivity per meter plateau edge, that was as large as with smooth surfaces.

Metal surfaces are different from glass or silicon surfaces both by their increased roughness, and by their different surface energy, leading to different wettability and contact angles. To differentiate the effects of the wettability of the plateau surfaces from the effects of their roughness, silicon based EDGE chips were modified by silanization and the oil-water-surface contact angle was varied between 90° and 160°. Silanization modifies the surface with a single molecular layer and does not influence the overall roughness of the surface. The droplet size was not influenced by the contact angle, but the efficiency and performance of the system was significantly better with oil-water contact angles below 150°. The plateaus filled completely with dispersed phase, and the pressure stability and the maximum droplet formation frequencies were significantly higher. At even lower contact angles (<100 °), emulsification became unstable (chapter 5).

These findings on the surface roughness and contact angle are both essential for industrial application of microfluidic devices, as they are relevant for the choice of the materials and formation processes that can be successfully applied. In addition, they give insight in the droplet formation mechanism: roughness affects the invasion and blow up pressures by splitting the dispersed phase into fingers thus changing the value of R_2 (see eqs. 3.1 and 4.1) and increasing the total resistance in the system whereas the wettability affects the convexity of the interface on the plateau which determines that how easily and rapidly the interfacial instability and droplet formation will take place. While in general it is thought that the plateau should be wetted by the dispersed phase, and that a higher contact angle is better, we here see that there is an optimum.

2. Comparison of microfluidic systems

There is a range of microfluidic emulsification systems available. One can roughly distinguish systems that rely on shear/flow for droplet break-up (T or Y shaped junctions, coflow or flow focusing nozzles and cross-flow membrane emulsification systems), and systems that rely on spontaneous droplet break-up (the microchannel systems, including flow-through, and EDGE systems). These two classes will now be compared. A fast overview can be obtained from table 7.1.

In shear-driven systems the droplet size is influenced by the flow rate of both the dispersed and continuous phases^{2,3}. Microfluidic Y-junctions are exceptions to this as the droplet size in Y-junctions is affected only by the continuous phase flow rate⁴ implying that control of the emulsification with these systems is comparatively easy. Contrary to this, the droplet size in spontaneous emulsification systems is not dependent on the flow rate of the dispersed phase as long as it is below a critical value. Above this value, polydisperse, larger droplets are obtained. The continuous phase flow does not influence the droplet formation at all (chapters 2, 3 and 4).

Table 7.1: Comparison of shear driven and spontaneous emulsification systems for various process parameters affecting the process of emulsification.

Process parameters	Shear/Flow driven systems	Spontaneous systems
Viscosity ratio	+	-
Interfacial tension	+	-/0
Continuous phase flow	+	0
Dispersed phase flow	+	-
Re-circulation of emulsion	+	0
Surface wettability	-	‡
Surface roughness	0	‡

(+) effect is large and the system is sensitive to this effect, (-) effect is small, (0) no effect, (‡) the effect can be used to tune the system’s stability and productivity.

It has been reported that the emulsification in microfluidic Y-junctions is not affected by the viscosity ratio of disperse and continuous phase⁵. In other shear driven systems (T-junctions and flow focussing devices) a higher viscosity of the dispersed phase results in larger droplets⁶⁻⁸. In spontaneous emulsification, the droplet size is constant as long as the ratio of the viscosity of the dispersed phase to that of the continuous phase is above a critical value; below this value the droplets become larger (as also described in chapters 2 and 3). As the viscosities of most food grade oils are high, and small changes in

viscosity that may occur during processing will not influence the droplet size; this gives spontaneous emulsification systems an advantage over shear-driven systems.

The interfacial tension is an important parameter in microfluidic emulsification, and co-determines the droplet size (in shear driven systems); although it should be mentioned that the actual, time-dependent interfacial tension during emulsification is hard to determine in any microfluidic system, maybe with the exception of Y-junctions that have been used to estimate the interfacial tension at extreme extension rates⁹. In shear-driven systems, the droplet size decreases continuously with decreasing interfacial tension^{4, 10-12}. The expansion rates during the formation of droplets are often high, which means that the actual value of the interfacial tension is unknown and may vary over the time of formation of a droplet. In spontaneous emulsification systems, a large interfacial tension is beneficial for stable emulsification (chapter 2), as it implies a larger driving force for droplet snap-off. It does not have an influence on the droplet size as such. The droplet formation in spontaneous emulsification is relatively slow, and therefore dynamic interfacial tension effects are much less pronounced. Therefore, a lower emulsifier concentration can be used compared to the shear-driven systems¹³; this is helpful for food applications.

Besides direct effects on the liquid/liquid interfacial tension, the contact angle may also be influenced indirectly by emulsifiers (¹⁴, chapter 2 and 3). In all microfluidic systems, the surface should be preferentially wetted by the continuous phase for stable droplet formation. This is also true for e.g. jetting, in which contact with the wall is minimal. Depending on the channel size, the effects of changes in wettability will have more or less effect on the stability of the emulsification process. This also implies that for the shallow plateau that is used with EDGE systems, these effects are prominent, as illustrated in chapter 5.

The surface roughness in EDGE devices can significantly influence the emulsification behaviour as is reported in chapters 3 and 4; roughness (around 20 nm) can help to increase the system productivity by increasing the total number of droplet formation points (chapter 4). For other microfluidic devices, the roughness is not expected

to influence the emulsification as long as the geometries are precisely and accurately fabricated throughout the system. Typically larger channel dimensions will be used compared to the height of the plateaus used in EDGE, and that will cancel out most effects of the nano-sized roughnesses, unless related to the wettability changes mentioned earlier.

The above discussed comparison is summarised in table 7.1. The process of spontaneous emulsification is simpler in operation, is less affected by the process parameters and may be used in recirculation mode to increase the volume fraction of the dispersed phase if needed. This is in contrast to shear-driven systems in which recirculation and flow directly influences the droplet size distribution. As was shown in this thesis, the use of metals can be an extra advantage in spontaneous emulsification systems: the metal surface characteristics (roughness and wettability) can be used to tune the productivity and stability of the system.

3. Outlook on scale-up for food applications

For most food applications, the average emulsion droplet size needs to be below $10\ \mu\text{m}$ ¹⁵. This droplet size can be produced by almost all microfluidic systems as long as a single droplet generator is considered. Table 7.2 gives a qualitative comparison of spontaneous emulsification systems (i.e. microchannels and EDGE) together with shear driven systems, for systems with a single droplet formation unit.

Table 7.2: Qualitative comparison of microfluidic emulsification techniques for single droplet formation unit.

	Process control (++) simple (--) complex	Droplet Size (++) Large (--) Small	Productivity (++) High (--) Low	Monodispersity (++) High (--) Low
Microchannels	++	--	+	++
EDGE	++	--	+	++
Shear driven systems	++	-	++	++

With a single droplet generating unit, shear driven systems can produce emulsions at much higher frequencies compared to spontaneous emulsification systems, while both systems produce highly monodisperse emulsions. However, when parallelized (for droplets of around 100 μm)¹⁶⁻¹⁸ the shear driven systems show complex dynamic behaviour and weak coupling between the various droplet formation units^{18, 19}. This effect is expected to be even more pronounced when channel dimensions are narrowed to produce droplets smaller than 10 μm , as the Laplace pressure then becomes higher. Control of the flow of the phases at each separate droplet formation unit will need to be very accurate to control droplet size, and this is a major challenge. Table 7.3 gives a qualitative comparison of the shear driven systems to the spontaneous emulsification devices (i.e. microchannels and EDGE), considering a mass-parallelized system for production of droplets of around 5 μm .

Table 7.3: Qualitative comparison of microfluidic emulsification techniques for parallelized systems when considering <5 μm droplets.

	Process control (++) simple (--) complex	System efficiency (++) High (--) Low	Productivity (++) High (--) Low	Monodispersity (++) High (--) Low
Microchannels	++	-	-	++
EDGE	++	++	++	++
Shear driven systems	-	+	+	+

Microchannels, when parallelized, can efficiently produce droplets of around 10 μm ²⁰, however, for smaller droplets the system efficiency reduces significantly due to pressure gradients in the system¹⁵. During droplet generation, the local pressure in the active microchannel drops, due to the lower Laplace pressure of a droplet relative to the Laplace pressure of an interface on the terrace. This causes a somewhat lower pressure in adjacent microchannels, which then become inactive. This effect, described earlier by Abrahamse et al.²¹, implies that in mass parallelised systems the total number of active microchannels may be as low as a few per cent (depending on the total design of the system). EDGE systems (as shown in table 7.3) generate many droplets at the same time,

while all pressure fluctuations are damped by the wide and narrow plateau. Therefore, these hydrodynamic coupling effects are not observed with the EDGE systems. Therefore, these systems are more convenient to scale up for smaller droplets and hence may be most appropriate for larger scale food applications. For scale up to commercial production levels, a straight-through EDGE sieve may be chosen, in contrast to the flat layout presented throughout the thesis, which was chosen as these are more suitable to investigate the process.

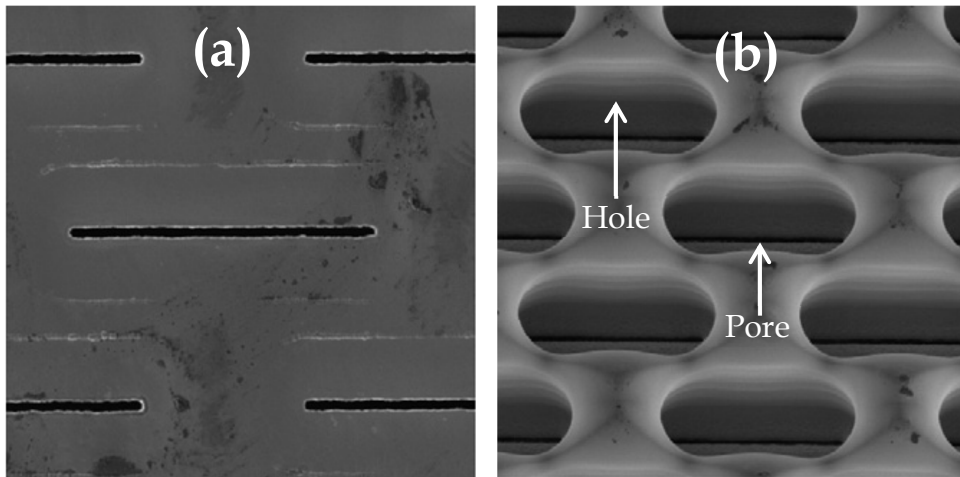


Figure 7.1: Straight-through nickel sieves (a) front view (b) back view²².

For straight-through EDGE systems, metal sieves similar to those presented by Nazir et al.,²² (figure 7.1) for pre-mix emulsification can be of interest. These sieves consist of a slit-like top geometry that extends into the sieve to a certain depth, leading to a more open structure with hole,s as can be seen in the back view of the sieve. The plateau may be fed with the dispersed phase from the back side, and will then spread through the narrow slits and form droplets on the front surface. As long as the depth of the slits is appropriate, we expect stable emulsification with the size of the droplets related to the width of the slit. Although the width of the currently available nickel sieves is still too large for the production of droplets below 10 μm , while the roughness and wettability need to be addressed, the fast developments in fabrication techniques are

expected to make our requirements realistic in the near future. Foods may contain different surface active components which may interact with the surface to change its wettability thus influencing the process of emulsification. Therefore, in the production of foods, interaction of various food components with the surface of the metal used needs to be addressed.

Besides single emulsions, double emulsions and encapsulation systems (i.e., solids or other components inside a phase that needs to be dispersed into an emulsion) are of great relevance for food applications, and also for these systems microfluidic devices may have specific advantages. It was already shown that double emulsions can be produced by EDGE systems²³; in which the inner emulsions were prepared with classic techniques to make the droplets small enough to pass through the shallow plateau; hence the number and size of the inner droplets was difficult to control. We expect that double emulsions with monodispersed inner droplets can be produced by designing a system with shallow and deep plateaus having different local surface properties. This is a subject for future research.

Since the stability of double emulsions is an issue that will decide whether it is worthwhile to design the complex EDGE devices described earlier, we used flow-focussing devices (chapter 6) for the production of relatively large (around 40 μm), easily observable double emulsions. Monodispersed emulsions with a controlled number and size of inner droplets were successfully prepared at quantities large enough for NMR analysis. With this technique the inner droplet size and the stability of the emulsions in time could be determined. The results are encouraging and justify the development of EDGE technology for the production of double emulsions. While flow-focussing devices are difficult to control on larger scales, the EDGE systems will enable scaling out into robust systems that can produce the double emulsions in larger quantities.

4. Concluding remarks

Microfluidic devices show great potential for emulsification. This thesis shows that the fabrication of these systems in metal, necessary for large scale production of food emulsions, may have advantages. The droplet formation process is more stable (allows

larger pressure to be used), benefits from just an intermediate contact angle, and the complex hydrodynamic coupling present in other systems is not observed, therefore the EDGE systems may be scaled out more easily.

The influence of the surface roughness and the contact angle also points to the fact that the EDGE droplet formation process is more complex than is previously thought. The role of the fingering behaviour of the dispersed phase, and its relation with the enhanced pressure stability are scientific challenges that are open to future investigation.

References

1. K. C. van Dijke, G. Veldhuis, K. Schroën and R. M. Boom, *AIChE Journal*, 2010, **56**, 833-836.
2. T. Nisisako, T. Torii and T. Higuchi, *Chemical Engineering Journal*, 2004, **101**, 23-29.
3. S. L. Anna, N. Bontoux and H. A. Stone, *Appl. Phys. Lett.*, 2003, **82**, 364-366.
4. M. L. J. Steegmans, K. C. G. P. H. Schroën and R. M. Boom, *Langmuir*, 2009, **25**, 3396-3401.
5. M. L. J. Steegmans, J. De Ruiter, K. G. P. H. Schroën and R. M. Boom, *AIChE Journal*, 2010, **56**, 2641-2649.
6. Z. Nie, M. Seo, S. Xu, P. Lewis, M. Mok, E. Kumacheva, G. Whitesides, P. Garstecki and H. Stone, *Microfluid Nanofluid*, 2008, **5**, 585-594.
7. J. Husny and J. J. Cooper-White, *Journal of Non-Newtonian Fluid Mechanics*, 2006, **137**, 121-136.
8. J. H. Xu, S. W. Li, J. Tan, Y. J. Wang and G. S. Luo, *AIChE Journal*, 2006, **52**, 3005-3010.
9. M. L. J. Steegmans, A. Warmerdam, K. G. P. H. Schroën and R. M. Boom, *Langmuir*, 2009, **25**, 9751-9758.
10. C. Cramer, P. Fischer and E. J. Windhab, *Chemical Engineering Science*, 2004, **59**, 3045-3058.
11. M. L. J. Steegmans, C. G. P. H. Schroën and R. M. Boom, *Chemical Engineering Science*, 2009, **64**, 3042-3050.
12. J. H. Xu, G. S. Luo, S. W. Li and G. G. Chen, *Lab Chip*, 2006, **6**, 131-136.
13. N. Yamazaki, K. Naganuma, M. Nagai, G. H. Ma and S. Omi, *Journal of Dispersion Science and Technology*, 2003, **24**, 249-257.
14. S. Sugiura, M. Nakajima, T. Oda, M. Satake and M. Seki, *J. Colloid Interface Sci.*, 2004, **269**, 178-185.
15. I. Kobayashi, T. Takano, R. Maeda, Y. Wada, K. Uemura and M. Nakajima, *Microfluid Nanofluid*, 2008, **4**, 167-177.
16. V. Barbier, M. Tatoulian, H. Li, F. Arefi-Khonsari, A. Ajdari and P. Tabeling, *Langmuir*, 2006, **22**, 5230-5232.
17. A. Kawai, S. I. Matsumoto, H. Kiriya, T. Oikawa, K. Hara, T. Okawa, T. Futami, K. Katayama and K. Nishizawa, *Tosoh Research & Technology Review*, 2003, **47**, 3-9.
18. M. Hashimoto, S. S. Shevkoplyas, B. Zasońska, T. Szymborski, P. Garstecki and G. M. Whitesides, *Small*, 2008, **4**, 1795-1805.
19. L. Wei, W. K. Y. Edmond, S. Minseok, N. Zhihong, G. Piotr, A. S. Craig and K. Eugenia, *Soft Matter*, 2008, **4**, 258-262.
20. I. Kobayashi, Y. Wada, K. Uemura and M. Nakajima, *Microfluid Nanofluid*, 2010, **8**, 255-262.
21. A. J. Abrahamse, R. van Lierop, R. G. M. van der Sman, A. van der Padt and R. M. Boom, *J. Membr. Sci.*, 2002, **204**, 125-137.
22. A. Nazir, K. Schroën and R. Boom, *J. Membr. Sci.*, 2011, **383**, 116-123.
23. K. C. van Dijke, K. Schroën, A. van der Padt and R. M. Boom, *J Food Eng*, 2010, **97**, 348-354.

Summary

An emulsion results when two immiscible liquids (e.g. oil and water) are mixed together by dispersing one of them into the other in the form of droplets in the presence of an appropriate emulsifier and/or stabilizer. Many emulsion based products are used in everyday life in the form of foods (milk, butter, mayonnaise etc.), cosmetics (facial creams, body lotions, hair products etc.), pharmaceuticals (drug delivery systems, vitamin drops etc.) and chemicals (paints, sprays, lubricants etc.). Amongst others, appearance, rheology, stability etc. depend on size of the dispersed droplets and their size distributions. Classic methods for emulsion preparation rely on intense flow, resulting in polydisperse emulsions, while most of the energy applied is lost as heat which may be detrimental to some ingredients, and to so-called double emulsions that can be used to encapsulate components.

Microfluidic devices have potential for preparing emulsions (including double and multiple emulsions), as they can produce emulsions with well controlled droplet sizes and at high energy efficiency, which improves product properties and shelf life, but also reduces the total energy expenditure. Not only single emulsions but also double and multiple emulsions can be successfully produced, although the scale at which this can be done is still limited. Given the potential for emulsification, this thesis focusses mostly on spontaneous emulsification systems particularly the EDGE systems that use Laplace pressure differences for droplet formation. The primary goal was to gain insight into the process and into the parameters important to the scale-up of EDGE emulsification using metal based systems, as a first step towards industrial systems for droplets of around ≤ 5 μm . In addition, we touched upon the preparation of w/o/w double emulsions, albeit with flow-focusing devices.

An overview on spontaneous emulsification systems having potential for food applications is given in chapter 2. Several design and process parameters, which influence the process of emulsification, are discussed in detail, together with various products that have been made with this technology. The energy efficiency of spontaneous emulsification

systems is compared with other systems showing that spontaneous emulsification is much more energy efficient as compared to classic emulsification techniques. For scale up of emulsification, EDGE systems are considered more applicable due to their stable operation and easy parallelization compared to other microfluidic systems, especially for droplets of sizes $\leq 5 \mu\text{m}$. As one of the pivotal points for implementation in the industry, the step toward other construction materials such as metals is identified and the work dedicated to this is covered in chapters 3-5.

The emulsification with metal (Cu and CuNi) coated EDGE systems having different surface roughnesses and wettabilities was investigated in chapters 3 to 5. An increase in surface roughness prevented the uniform filling of the droplet generation area, the so-called plateau, and the total number of droplet formation points decreased; however at the same time the droplet formation frequencies on the remaining droplet formation points increased. The overall maximum productivity was therefore not affected. Contrary to what is conventionally assumed, a higher contact angle is not always better: the pressure stability of the system was largest with an (oil-water-plateau surface) contact angle in between 100° and 150° , leading to a higher overall maximum productivity than with a higher contact angle. Apart from the effects of the plateau surface roughness and wettability, the emulsification was also influenced by the ratio of the viscosities of the dispersed and continuous phases. The scaling of this effect is similar as for other spontaneous emulsification techniques. The emulsification depended on the surfactant used, and its concentration is important to prevent undesired wettability changes of the surface during the process.

As EDGE systems are not yet stable enough for the preparation of water-in-oil-in-water (w/o/w) double emulsions, flow-focusing devices were used for their preparation, as described in chapter 6. Monodispersed droplets with outer droplet sizes of 40–100 μm were produced using different flow focusing geometries. The number and size of the inner droplets could be controlled by changing the method of operation (i.e. two step or jetting mode) or by changing the flow rates of the phases. Self-diffusion NMR analysis was used for determining the inner droplet sizes and the water distribution in different phases of

the double emulsion which was used to investigate the stability of these complex emulsion in time.

Finally, EDGE emulsification is compared to other microfluidic emulsification systems in the general discussion and an outlook is given for application of microfluidic emulsification at commercial scale in food products. EDGE systems are unique among microfluidic emulsification systems due to their ability to produce multiple monodisperse droplets simultaneously from one unit and their remarkable robustness and efficiency when scaled up (on chip level) for droplets of sizes $\leq 5 \mu\text{m}$. Stable operation during long term processing and appreciable performance with metal based systems are important aspects for realizing larger-scale emulsification systems to be applied in the food industry in the near future.

Acknowledgements

The time when I started my Masters at University of Agriculture, Faisalabad, I knew very little about practical science; thanks to Dr. Masood Sadiq Butt for giving me very tough time. My ever increasing interest in scientific research was the result of his kind supervision which ultimately urged me to do PhD. Special thanks to Higher Education Commission (HEC) for providing me the financial assistance for PhD. I still remember the day when I received the scholarship award letter from HEC and cannot explain in words how excited I was. In the course of producing current thesis, I received various forms of assistance from various people who deserve acknowledgement and appreciation. I am glad to use this opportunity to express my gratitude to all of them but apologise in advance if someone is missed.

First of all I would like to thank Food Process Engineering group of Wageningen University for providing me the scientific support. My special gratitude goes to my daily supervisor, Karin Schroen, whose kindness starts right from my first day in Netherlands. She helped me in various matters including arrangement of residence, bank account and many others apart from the scientific guidance. Karin I simply have no words to thank you for all of your support. I am really grateful to my promoter, Remko Boom, who always appreciated my work and encouraged me to do more. It will be most unfair if I miss the technicians, Strubel Maurice and Sewalt Jos, at this occasion. Maurice and Jos, thank you for all the technical assistance which ensured smooth running of my experiments.

I worked with Eric Hughes at Nestle research centre, Switzerland, for four weeks. Working with Eric was a good experience, I learnt new techniques which broadened my vision about my research. Eric, thank you for your hospitality and for the technical and scientific guidance.

To be far away of my family in a country with totally different culture was a bit challenging in the beginning. It was the company of my Pakistani friends which helped me to adjust to this new environment and was further helped by international friends. Kashif Khan, Akmal Nazir, Masood Iqbal, Imtiaz Rashid, Ghulam Mustafa, Ghulam Abbas, Abbas Gul, Zeeshan Hassan, Hamid Shah, Mazhar Ali, Mazhar Iqbal, Mazhar Khan, Sajid bhai,

Hafiz Sultan, Liyakat Mujawar, Sheikh Mustafa, Sheikh Wisaam, Hassan Sawalha, Shahrul Ismail and Sami Sahin, thank you very much for your love and co-operation you showed to me during my stay in Wageningen.

Last but not least, I would like to thank my family and friends back home in Pakistan for their support through prayers and best wishes. My humble gratitude to my parents for their love, affection and care they showed to me throughout my life. My brothers (Qasim, Shahid, Asim, Zahid and Asad), sister (Shazia), bhabi (Sumera) and uncles (Ehsan Ali and Manzoor Ali) always encouraged me to go further in my studies. I cannot forget the support of my wife (Javairia) and daughter (Fatima) during last year of my PhD. Thank you Javairia for your co-operation and moral support, you looked after the home almost alone when I was extremely busy in experiments and thesis writing. My lovely Fatima, I will never forget your smile which made me relax whenever I was tired of my work. At the end, I would like to say thanks to all those who have been supportive to me at any stage of life but were missed to be mentioned here.

About the author

Abid Aslam Maan was born in Lahore, Pakistan, on May 5, 1983. His education started at Lahore from where he completed his higher secondary school certificate in 2001. In bachelor, he started studying agricultural sciences at University of Agriculture, Faisalabad, with major subject of food technology. After getting B.Sc.(Hons.) degree in 2005 he started his masters at the same university. During his research he focussed on the functional properties of protein isolates from legumes for their application in baking industry. After finishing M.Sc.(Hons.) in 2007, he started working as Quality Assurance Executive in a local dairy company "Millac Foods (pvt.) Ltd."



In March 2008, Abid got admission to the PhD programme at Food Process Engineering group of Wageningen University (The Netherlands) through a fellowship from Higher Education Commission (HEC) of Pakistan under their overseas scholarship scheme. The PhD project, under the supervision of Prof. Remko Boom and Prof. Karin Schroën, was aimed to understand the influence of the metal surface characteristics on microfluidic emulsification especially the EDGE emulsification in order to contribute to the realisation of the metal-based EDGE-systems on industrial scale. The results of this research are presented in this thesis most of which have been published in peer-reviewed journals.

Email: abid.maan@gmail.com

List of publications

Maan, A. A., Schroën, K., Boom, R., 2011. Spontaneous droplet formation techniques for monodispersed emulsions preparation-perspectives for food applications. *Journal of food engineering* 107, 334-346.

Maan, A. A., Schroën, K., Boom, R., 2012. Monodispersed water-in-oil emulsions prepared with semi-metal microfluidic EDGE systems. *Microfluid Nanofluid*, DOI 10.1007/s10404-012-1037-0.

Maan, A. A., Boom, R., Schroën, K. 2012. Preparation of monodispersed oil-in-water emulsions through semi-metal microfluidic EDGE systems. *Microfluid Nanofluid*, DOI 10.1007/s10404-012-1097-1

Hughes, E., **Maan, A. A.,** Acquistapace, S., Burbudge, A., Johns, M. L., Gunes, D. Z., Clausen, P., Syrbe, A., Hugo, J., Schroën, K., Miralles, V., Atkins, T., Gray, R., Homewood, P., Zick, K., 2012. Microfluidic preparation and self diffusion PFG-NMR analysis of monodisperse w/o/w double emulsions. *Journal of colloid and interface science*, Doi.org/10.1016/j.jcis.2012.07.073.

Maan, A. A., Sahin, S., Mujawar, L., Schroën, K., Boom, R. Effect of surface wettability on microfluidic emulsification. *Submitted for publication*.

Khan, M. K. I., **Maan, A. A.,** Schutyser, M., Schroën, K., Boom, R. Electro spraying of water in oil emulsion for thin film coating. *Submitted for publication*.

Mujawar, L., **Maan, A. A.,** Khan, M. K., Norde, W. W., Van Amerongen, A. Distribution of biomolecules in porous nitrocellulose membrane pads using confocal laser scanning microscopy and high-speed cameras. *Submitted for publication*.



Overview of completed training activities



Discipline specific activities

Courses

Reaction Kinetics in Food Science (VLAG, 2009)

Computational Fluid Dynamics for Chemical Engineers (OSPT, 2009)

Thermodynamics for the Process Technology (OSPT, 2009)

Advanced Food analysis (VLAG, 2010)

Sustainability Analysis in Food Production (VLAG, 2011)

Rheology and structure of food (VLAG, 2012)

Conferences/symposia

Delivery of functionality in complex food systems: Third international symposium (2009, Wageningen, The Netherlands)

5th World Congress on Emulsions (2010, Lyon, France)

6th International Symposium on Food Rheology and Structure (2012, Zurich, Switzerland)

Internal symposium: Food Process Engineering (2009, Wageningen, The Netherlands)

Internal symposium: Food Process Engineering (2010, Wageningen, The Netherlands)

Internal symposium: Food Process Engineering (2012, Wageningen, The Netherlands)

General courses

PhD week (VLAG, 2010)

Information Literacy, including introduction EndNote (WGS, 2009)

Project and time management (WGS, 2010)

Philosophy and ethics of food science and technology (VLAG, 2009)

Optionals

PhD excursion Food Process Engineering (USA, 2010)

PhD excursion Food Process Engineering (Finland, 2012)